AALBORG
UNIVERSITY

STUDENT REPORT

Influence of municipal food waste composition on lipid production of *Cutaneotrichosporon oleaginosus*

Master's thesis in bioengineering

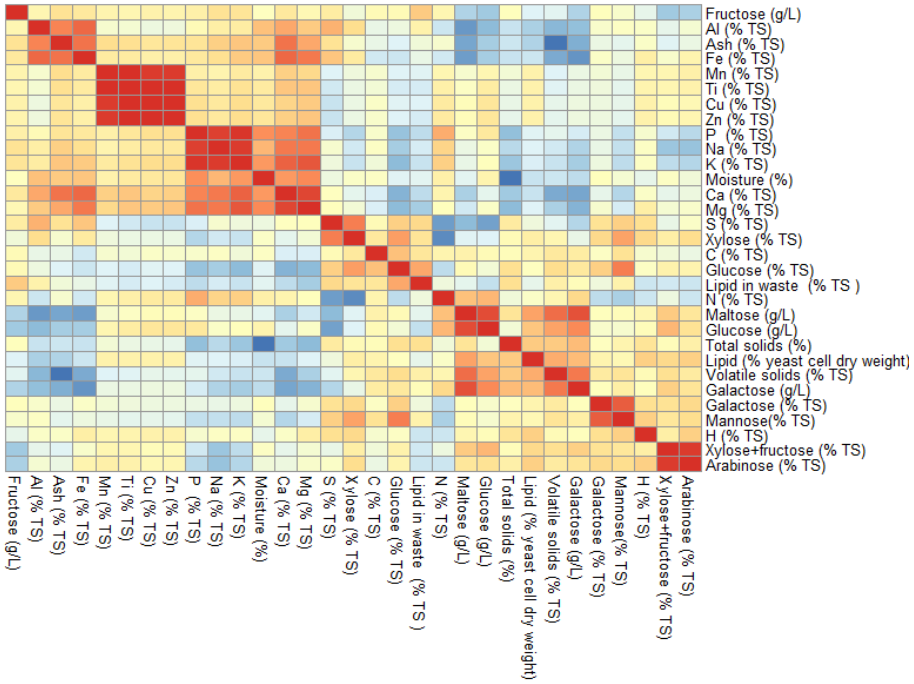

Dalia Basil Farooq Abed Yashou
BIO10-3-F22, Aalborg University Esbjerg

Title page

Title: Influence of municipal food waste composition on lipid production of *Cutaneotrichosporon oleaginosus*

Module name: Master's Thesis

Made by: Group BIO10-3-F22, Aalborg University Esbjerg

Supervisors: Jens Laurids Sørensen and Sergey Kucheryavskiy

Period: 1. September 2021 – 10. June 2022

Page Count (excl. appendices): 61 pages

Keywords: Biofuel, yeast, jet fuel, *Cutaneotrichosporon oleaginosus*, food waste

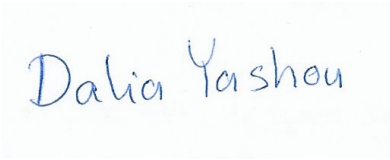

_____

Dalia yashou

AALBORG UNIVERSITY

STUDENT REPORT

Abstract

Around 1.3 billion tonnes of food goes to waste annually. This is a concern for world hunger, resource waste and CO_2 emissions. The Flexi Green Fuels (FGF) project is dedicated to reducing these problems and has the goal to convert municipal solid waste and lignocellulosic waste into valuable biofuels for shipping and aviation by using yeasts, larvae and algae. This master thesis project is a part of the FGF project and has the goal to find the effect of municipal food waste composition on the lipid production in the oleaginous yeast *Cutaneotrichosporon oleaginosus*. Food waste was collected from the food waste handling plant Ragn-Sells once every month for 5 months from November to March. The food waste was analyzed for its heavy metal content, its elemental composition of carbon, hydrogen, nitrogen and sulfur, total carbohydrates and lipid content. Chemometrics methods, principal component analysis (PCA) and partial least squares regression (PLS) were used to explore the behavior of the collected data and to find the correlations between the lipid content accumulated in the yeast and the waste contents. High degrees of correlations (over 0.5) were found between the lipid amount accumulated in the yeast and aluminum, mannose and ash contents in the waste.

Abbreviations

- E, E-waste: Sample collected from Esbjerg Campus, energy department.
- Mix carb. method: The method which analyses the liquid part of the sample for maltose, glucose, galactose and fructose using HPLC.
- SAH: Strong acid hydrolysis
- WAH: Weak acid hydrolysis

Contents

Preface

This master thesis project is written by a master's student in bioengineering (me) and has a duration of one year (60 ECTS). The choice of working with this project was mainly because I love to work with the green transition, making the world a better place for the next generations. The results obtained in this project work will be used in the main project Flexi Green Fuels.

During the project, both experimental work, reporting and data handling methods were used. The process of working on the project was exciting, but also with some challenges. Fortunately, there were people nearby to provide help and support. I will, first of all, express my deepest gratitude to my family for their support throughout the project period and my dog for his unconditional love and emotional support. Special thanks to: my colleague Line Jensen for sharing her knowledge on the subject, the Ph.D. students Malthe Fredsgaard and Laura Hulkko for their assistance, the laboratory technicians Lilian Bondig, Julaine Enas, Linda Madsen and Dorte Spangsmark for their help and assistance in the laboratories, Claus Hansen and the other personnel from Ragn-Sells for helping provide the food waste, Mette Thomsen and Tanmay Chaturvedi for their assistance and advice. Finally but not least, I would like to express my appreciation and gratitude to my supervisors, Sergey Kucheryavskiy for his supervision in the chemometric part, and Jens Laurids Sørensen for his ongoing guidance and support throughout the project period.

1 Introduction

The amount of food produced, that goes to waste, is estimated to be around one-third, globally [1], [2], [3], [4]. This is approximately 1.3 billion tons of food annually and has a value of 680 billion dollars [3]. This is a big world concern, mainly because of world hunger, but also because it is a waste of resources like land, energy, water and not least the production of gas emissions which contribute to the global warming [3]. This project is a part of the Flexi Green Fuels (FGF) project, which is funded by the European Commission to help achieve the European commission's national target of reducing greenhouse gas emissions by 40% compared to the levels of 1990 [5]. The main goal of the FGF project is to convert second-generation waste materials to biofuels for aviation and shipping. A part of the FGF project is improving the conversion of lignin and organic fraction municipal solid waste to lipids by use of yeast, fungi and larvae.

This project has the main goal to find the influence of the food waste composition on the lipid accumulation in the oleaginous yeast *Cutaneotrichosporon oleaginosus* ATCC 20509 (*C. oleaginosus*). The goal will be accomplished through experimental methods and through chemometrics methods to find the correlations between the accumulated lipids in the yeast and the constituents in the waste. The food waste will be collected from two different sources, one is manually made waste from the energy department in AAU Esbjerg Campus and the second type of food waste is collected every month from the food waste handling plant, Ragn-Sells. Section 4 explains Ragn-Sells in greater detail. The influence of the time variation of the collected food waste on the food waste composition will also be investigated.

1.1 Biofuel from lipids

The biofuel that will be produced in the FGF project is Hydro-processed Esters and Fatty Acids Synthetic Paraffinic Kerosene (HEFA-SPK). The process flow diagram of HEFA-SPK, which can also just be called HEFA, can be seen in Figure 1 [6].

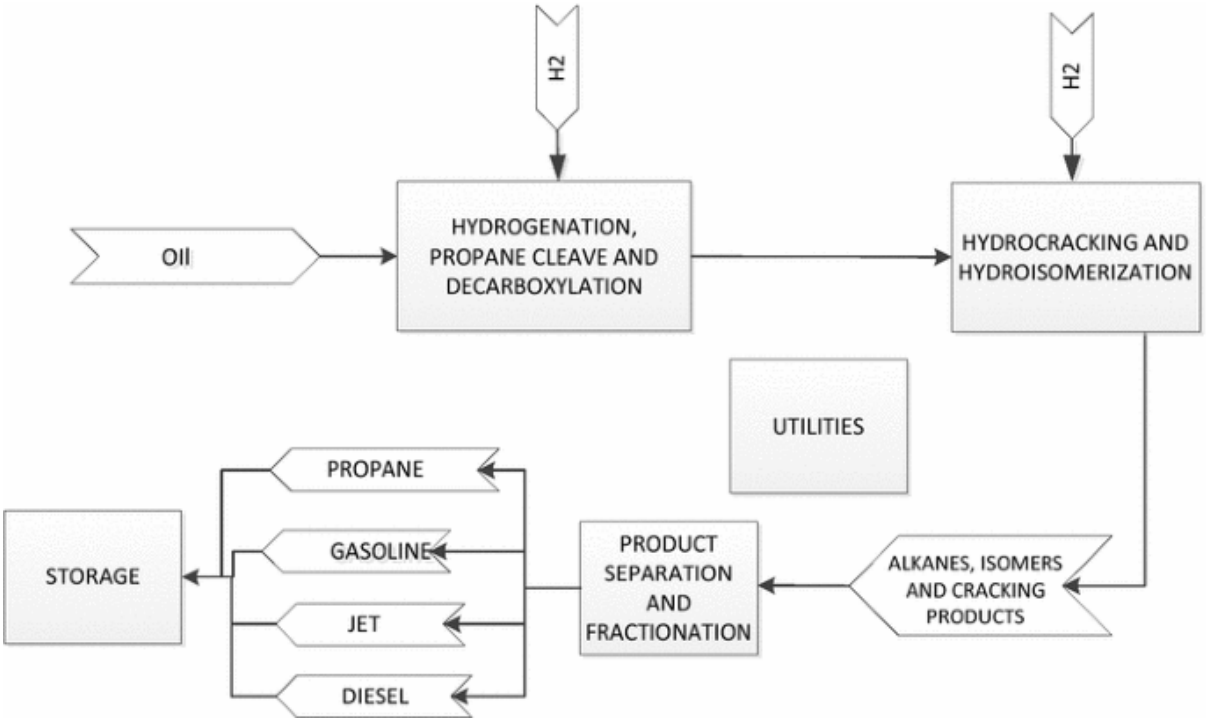

Figure 1. Process flow diagram of HEFA [6].

The HEFA-SPK is approved for use in ASTM (American Society for Testing and Materials) D7566 in 2009, in blends with Jet A-1 and up to 50% of the HEFA-SPK [7], because the paraffinic hydrocarbons don't have all the specifications of jet fuels [8]. The two main processes in converting lipids to HEFA-SPK are hydro-processing and isomerization (first and second blocks in the block diagram, Figure 1). The lipids used for this can be both animal fats and vegetable oils. In hydro-processing, the unsaturated compounds, like aromatics and alkenes are converted into cycloalkanes and paraffins (alkanes) with the use of hydrogen and a catalyst [9], [10], [11], [6]. The first part of the process is hydro-processing, which consists of hydrogenation, propane cleave and decarboxylation [6]. An example of the hydro-genation process can be seen in the study by Fredsgaard et al. [11], where the monounsaturated tri-glyceride triolein (tri-C18:1) is saturated into tristrearin (tri-C18:0) with nickel as catalyst (Equation 1)[11].

Equation 1 , [11], [6]

$$C_nH_{(2n-1-6m)}(COOH)_3 + (3m)H_2 \overset{Ni}{\rightarrow} C_nH_{(2n-1)}(COOH)_3$$

$$triolein + 3H_2 \rightarrow \ tristearin$$

n=number of carbon atoms in the triglyceride aliphatic chain [11].

m= number of double bonds in the aliphatic chains [11].

When adding H_2 to the triglyceride molecules, the glycerol in the triglyceride will be converted to propane. The second step in the first block is cleaving the propane from the triglyceride, producing three free fatty acids.

The hydro-processing also consists of an oxygen removal step, which is the third step in the first block. This step can be done in three ways, which are: decarboxylation, decarbonylation and hydrodeoxygenation. The decarboxylation pathway removes CO_2, the decarbonylation removes CO and hydrooxygenation removes H_2O [6]. After the hydroprocessing treatment, the resulting product is liquid hydrocarbon composed mainly of nC16-nC18 linear paraffins (paraffinic diesel) with a boiling point of 280 °C. This boiling point is higher than the boiling point for the typical jet fuel (150-300°C), and therefore, the hydroisomerization and hydrocracking steps are necessary to lower the boiling point. The hydrocracking saturates the double ring aromatics and raises the smoke point [12]. After the hydro isomerization/hydrocracking step, the linear paraffins (diesel) will be converted into iso-paraffins (kerosene) [9],[11], [6]. The synthetic paraffinic kerosene has a carbon chain ranging from C9-C15 [8]. The last steps are separation and fractionation, where the product from hydro-isomerization/hydrocracking is separated into propane, gasoline, jet and diesel [6].

1.2 Lipid production in oleaginous yeast

Oleaginous yeasts are yeast types that can accumulate high amounts of lipids, they can accumulate lipids in the range of 20 % to 72 % of the yeast's dry cell mass [13],[14],[15]. According to the study by Abeln et al. [16], there are approximately 160 native yeasts out of approx. 1500 species described so far, that can produce more than 20% lipids of the dry cell mass, cultivated in glyceride-rich oil [16], [17]. The number of known oleaginous yeasts however differs in older studies by Garay et al. [18] and Sargeant et al. [19], which give 70 and less than 30 species, respectively [18], [19]. The number of known species of oleaginous yeasts will certainly increase as there is continuous research going on in this area. Among the most studied oleaginous yeasts are *Yarrowia lipolytica, Candida* 107, *Rhodoturla glutinis, Cryptococcus curvatus (C. oleaginosus), Rhodosporidium toruloides* and *Lipomyces lipofer* [13], [14], [15].

Lipid production in oleaginous yeasts is an interesting well-studied topic because of the yeast's high robustness, high lipogenesis capability, the ability of the yeast to use many kinds of substrates and its good potential for the biofuel industry [20],[21],[22]. According to studies by Lamers et al. [13], Rakicka et al. [21], Saini et al. [23], Gong et al. [24] and Yoon et al. [25], the lipid production in oleaginous yeast is affected by oxygenations conditions, carbon/nitrogen ratio, the water content in the sample, enzyme conditions, inhibitors found in the substrate, carbon source, yeast type, temperature and pH

among others. The factors affecting lipid production in oleaginous yeasts will be further studied in this report.

Oleaginous yeasts are excellent lipid producers because of their increased ATP-citrate lyase activity that leads to the formation of acetyl-CoA, which is needed for fatty acid synthesis [26], [27], [28], [29], [30]. Oleaginous yeasts accumulate lipids mostly in the triacylglycerol (TAG) form [31]. Figure 2 shows the lipid biosynthesis of oleaginous yeasts. The formation of acetyl-CoA begins in the cytosol, where glucose is converted to pyruvate through a glycolytic pathway, which is also called glycolysis [28]. The glycolysis extract energy from glucose by cutting it into two molecules, each with three carbon atoms, these carbon atoms are called pyruvates. ATP transfers one phosphate group to glucose, and is released as ADP, this converts glucose to glucose-6-phosphate, making it able to enter the cell through its membrane. Glucose-6-phosphate is converted to fructose-6-phosphate, its isomer. Then ATP transfers one phosphate group to fructose-6-phosphate, making it a fructose-1,6-biphosphate. Fructose-6,6-biphosphate is split into two sugars, each with 3 carbon atoms, dihydroxyacetone phosphate (DHAP), and its isomer, glyceraldehyde-3-phosphate. The DHAP is converted into glyceraldehyde-3-phosphate and then to pyruvate [32]. The pyruvate is transferred to the mitochondria, where it is converted to Acetyl-CoA and oxaloacetic acid (OAA) with help of the pyruvate dehydrogenase, PDH enzyme. The acetyl-CoA is converted to citrate with help of citrate synthase, which comes from the citrate/malate shuttle. Citrate is transformed to its isomer, isocitrate, when it loses one water molecule and gains another one [33]. The nitrogen limitation leads to an increase in the activity of adenosine monophosphate deaminase (AMPD). The AMPD degrades the AMP to supply the cell with nitrogen. The loss of AMP level results in inhibition of isocitrate dehydrogenase (IDH), and accumulation of isocitrate [28]. The isocitrate is converted to citrate, and in this way, there is a continuous supply of citrate in oleaginous yeasts. The citrate is transported to the cytosol via the citrate/malate shuttle cycle, which only happens in oleaginous species. The limitation of nitrogen also leads to high activity of ATP-citrate lyase, which converts the citrate to acetyl-CoA with help of ATP and CoA. The rest of the citrate goes through the shuttle cycle which converts the citrate to oxaloacetic acid and oxaloacetic acid to malate with malate dehydrogenase. The acetyl-CoA is converted to malonyl CoA with acetyl-CoA carboxylase and to acyl-CoA with ketoacyl synthase (KS), ketoreductase (KR), dehydratase (DH) and enoyl reductase (ER). The last step of TAG synthesis takes place in the endoplasmic reticulum, ER, where the acyl-CoA is converted to TAG with the enzymes glycerol-3-phosphate acyltransferase (GPAT) and lysophosphatidic acid acyltransferase (LPAAT), among other enzymes seen in the blue box in Figure 2 [26], [34].

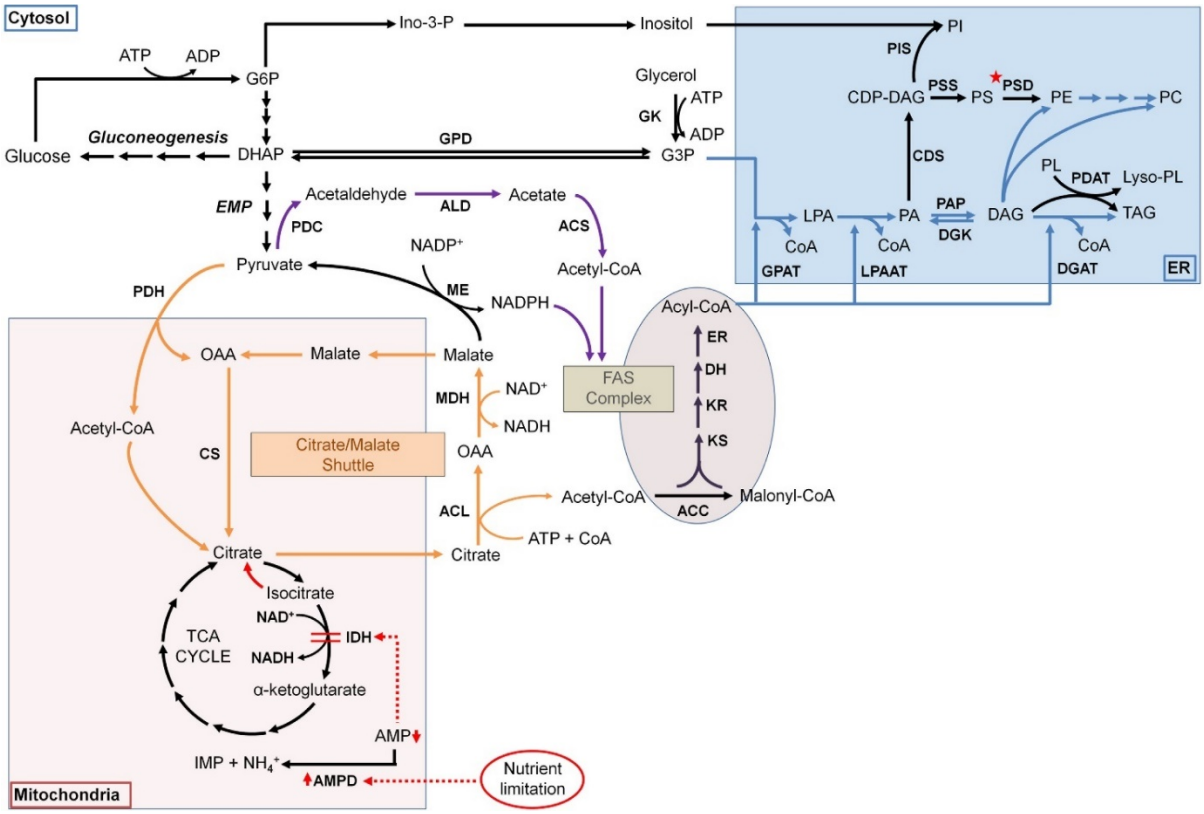

Figure 2 Lipid biosynthesis in oleaginous yeast. The orange lines in the figure are the pathway for the oleaginous yeasts, and the purple lines are the pathway for non-oleaginous yeast. In the cytosol, glucose is converted to pyruvate. In the mitochondria, the pyruvate is converted to citrate, in the cytosol, citrate is converted to acyl-CoA and lastly, in the endoplasmic reticulum, the acyl-CoA is converted to TAG. Abbreviations: ATP: Adenosine triphosphate, ADP: Adenosine di-phosphate, G6P:glucose-6-phosphate, DHAP: dihydroxyacetone phosphate, Ino-3-P: Inositol-6-phosphate,PI: phosphatidylinositol, PIS: phosphatidylinositol synthase, CDP-DAG: Cytidine Diphosphate Diacylglycerol, PSS: phosphatidylserine synthase, PS: phosphatidylserine, PSD: phosphatidylserine decarboxylase, PE: phosphatidylethanolamine, PC: phosphatidylcholine, CDS: CDP-Diacylglycerol Synthases, GPD: glycerol-3-phosphate dehydrogenase, GK: glycerol kinase, GPAT: glycerol-3-phosphate acyltransferase, CoA: Coenzyme A, LPA: lysophosphatidic acid, LPAAT: lysophosphatidic acid acyltransferase, PA: phosphatidic acid, PAP: phosphatidate phosphatase, DGK: diacylglycerol kinase, PL: phospholipid, PDAT: phospholipid diacylglycerol acyltransferase, DGAT: diglyceride acyltransferase, EMP: Embden-Meyerhoff-Parnas Pathway, PDC: pyruvate decarboxylase, ALD: acetaldehyde dehydrogenase, ACS: acetyl-CoA synthetase, NADP+: Nicotinamide adenine dinucleotide phosphate, ME: malic enzyme, FAS: Fatty acid synthase, ACC: acetyl CoA carboxylase, KS: ketoacyl synthase, KR: ketoreductase, DH: dehydratase, ER: enoyl reductase, PDH: pyruvate dehydrogenase, OAA: oxaloacetic acid, CS: citrate synthase, MDH: malate dehydrogenase, ACL: ATP-citrate-lyase, AMPD: adenosine monophosphate deaminase, IDH: isocitrate dehydrogenase. [26] .

1.3 *Cutaneotrichosporon oleaginosus,* ATCC 20509

The yeast that will be used in this project is *Cutaneotrichosporon oleaginosus* ATCC 20509 (*C. oleaginosus)*, which is also known as*, Cryptococcus curvatus, Trichosporon oleaginosus, Apiotrichum*

curvatum and *Candida curvata D* [35]. A microscopic foto of the yeast is seen in Figure 3, it can be seen that the yeast is reproducing by budding and new developing buds are seen [36]. The reason behind the choice of this yeast is the yeast's ability to accumulate high amounts of intercellular lipids. The following Table 1 shows the effect of various parameters on lipid production in *C. oleaginosus* according to studies by Gong et al. [24], Awad et al. [37], Shaigani et al. [38] and Fidio et al. [39].

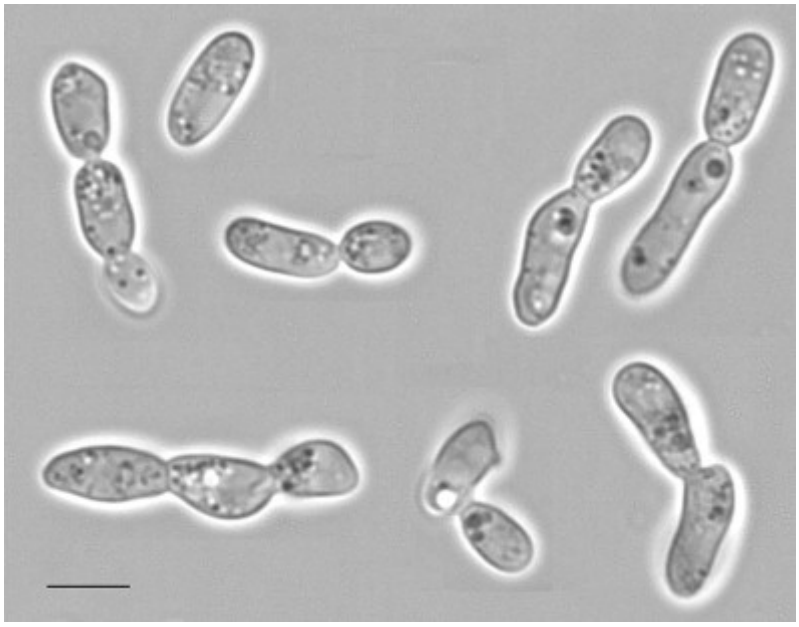

Figure 3. Microscopic foto of C. oleaginosus after 24 h of growth in 5% glucose media [36].

Table 1. Summary of results on lipid accumulation experiments done with C. oleaginosus, MNM=Minimal Nitrogen Media, OPEH= Office Paper Enzymatic Hydrolysates.

Mode of fermentation	Dilution rate	Initial pH	Temperature (°C)	Carbon source and amount (g L^{-1})	Cell mass (g L^{-1})	Lipid content (%)	Lipid yield (g lipid/g sugar)	Reaction time (h)	C/N ratio	source
Batch, stirred tank bioreactor	-	7	30	Acetate, 30	8.1	49.9	0.5	42	50	[24]
Continuous	0.04	7	30	Acetate, 5	1.34 ± 0.03	56.71 ± 2.12	0.18 ± 0.01	-	1.76	[24]
Continuous	0.06	7	30	Acetate, 5	0.84 ± 0.02	50.29 ± 1.43	0.16 ± 0.01	-	1.76	[24]
Continuous	0.08	7	30	Acetate, 5	0.66 ± 0.02	41.17 ± 1.10	0.15± 0.01	-	1.76	[24]
Continuous	0.11	7	30	Acetate, 5	0.36 ± 0.03	31.06 ± 2.49	0.13 ± 0.01	-	1.76	[24]
Continuous	0.14	7	30	Acetate, 5	0.29 ± 0.02	25.50 ± 1.02	0.10 ± 0.01	-	1.76	[24]
Continuous	0.01	7	30	Acetate, 30	5.05 ± 0.13	66.40 ± 0.71	0.12 ± 0.00	-	35.5	[24]

Continuous	0.06	7	30	Acetate, 30	1.60 ± 0.04	39.30 ± 0.66	0.10± 0.01	-	35.5	[24]
Continuous	0.08	7	30	Acetate, 30	1.24 ± 0.05	26.26 ± 1.21	0.07 ±0.01	-	35.5	[24]
Continuous	0.11	7	30	Acetate, 30	0.77 ± 0.03	14.87 ± 0.41	0.03 ±0.01	-	35.5	[24]
Batch	-	-	28	Glucose, 16	15.1 ± 0.60	44.3 ± 2.53	0.41	120	120	[37]
Batch	-	-	28	Galactose, 16	12.4± 1.22	33.36 ± 11.98	0.25	120	120	[37]
Batch	-	-	28	Mannose, 16	13.7± 1.82	52.83 ± 13.82	0.45	120	120	[37]
Batch	-	-	28	Fructose, 16	17 ± 0.77	43.11 ± 11.63	0.45	120	120	[37]
Batch	-	-	28	Sorbitol, 16	4.5 ± 0.45	13.41 ± 2.52	0.03	120	120	[37]
Batch	-	-	28	Xylose, 16	15.3 ± 0.43	36.56 ± 6.57	0.35	120	120	[37]
Batch	-	-	28	Arabinose, 16	8.7 ± 0.75	23.91 ± 6.66	0.13	120	120	[37]
Batch	-	-	28	Maltose, 16	14.5 ± 1.67	41.38 ± 7.73	0.38	120	120	[37]
Batch	-	-	28	Lactose, 16	18.4 ± 2.20	49.74 ± 5.16	0.56	120	120	[37]
Batch	-	-	28	Sucrose, 16	10.3 ± 1.14	27.52 ± 6.60	0.17	120	120	[37]
Batch	-	6.5	28	MNM-Glu.,30	-	56.38	0.19	72	-	[38]
Batch	-	6.5	28	MNM-Glu.,30	-	51.67	0.17	96	-	[38]
Batch	-	6.5	28	MNM-Xyl.,30	-	61.35	0.20	72	-	[38]
Batch	-	6.5	28	MNM-Xyl.,30	-	49.02	0.15	96	-	[38]
Batch	-	5.5	30	OPEH	17.3	52.5	0.20	-	45.9	[39]

From Table 1, the highest lipid amount that was accumulated in *C. oleaginosus* was with 30 g L^{-1} acetate as a carbon source, where the lipid accumulation reached 66.40 % lipid of the cell's dry weight. The mode of the fermentation was continuous with a dilution rate[1] of 0.01. The lipid yield and C/N ratios were 0.12 g g^{-1} and 35.5, respectively. For the continuous fermentation mode, both the nitrogen-limited, and nitrogen-rich media had promising results on the lipid yield and accumulation, but the lipid yield was better with the nitrogen-rich media. The different carbon sources also had an effect, on the lipid yield, where the highest lipid yield was 0.56 g g^{-1} achieved with the lactose as carbon source followed by mannose, fructose, and glucose. As glucose is the cheapest type of sugar, and the difference between the lipid yield of glucose and lactose is not that big (0.14 g g^{-1}), glucose will be a better choice to be used in the lipid fermentation with *C. oleaginosus* [40]. The cultivation time is seen to influence the lipid yield, where cultivation at 72 h resulted in higher lipid yield than 96 h, but obviously, the higher cultivation time gave higher lipid accumulation. Doing the lipid fermentation with yeast on

[1] Media flowing in the vessel per. hour / culture volume

a big scale, one should reach the highest possible lipid yield, to have minimal costs with the lowest possible amount of sugars. The pH and temperature for all experiments were between 5.5-7 and 28-30, respectively. The study by Fidio et al. [39] showed that *C. oleaginosus* can also accumulate lipids by using wastepaper hydrolysates as substrate [39], which means that the *C. oleaginosus* is a very promising microorganism for the green transition and converting waste materials into valuable lipids.

Studies by Hofmeyer et al. [41] and Fuchs et al. [42] showed that *C. oleaginosus* contains coding sequences for enzymes that can degrade cellulose, lignocellulose and monomeric sugars. There are no studies yet that fully describe the enzymes and their amount inside this yeast, but only that the enzymes are there, and there is potential for developing the yeast for lipid accumulation by further studying its genomic structure. This is the reason behind the yeast's ability to accumulate high amounts of intercellular lipids, but obviously, the amount of these enzymes is not big enough to omit the enzymatic hydrolysis process before/ together with the fermentation.

1.4 Lipid profile of *Cutaneotrichosporon oleaginosus*

The lipid profile of the lipids produced by *C. oleaginosus* according to studies by Gong et al. [24], Awad et al. [37] and Shaigani et al. [38] can be seen in Figure 4. The lipid profile of jet fuels contains C8-C16 carbon atoms, but those atoms with higher carbon chains can also be used to jet fuel production by cracking, and the smaller carbon chains fatty acids can be used for gasoline [43].

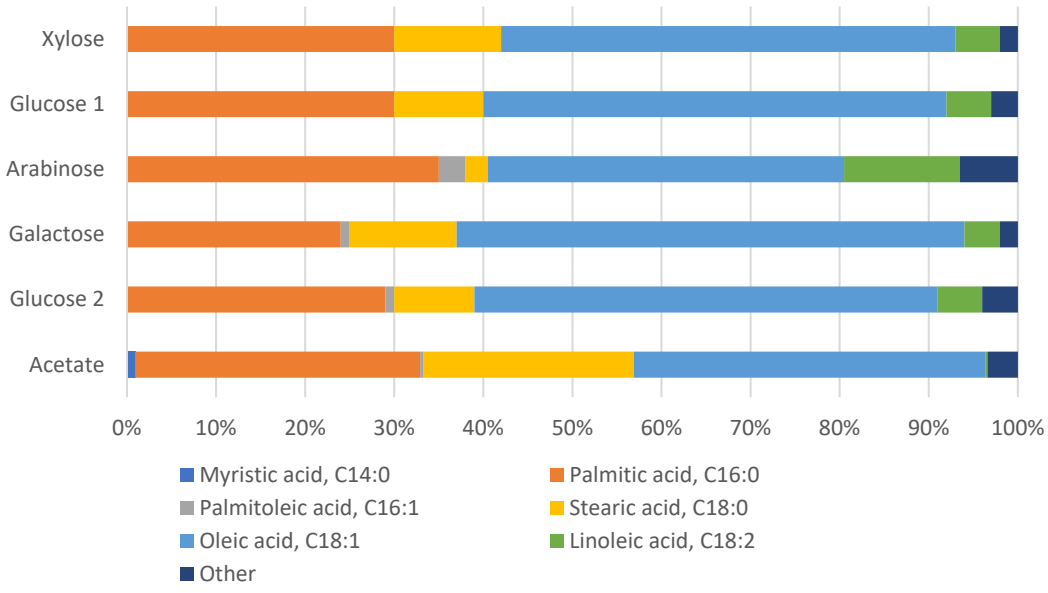

Figure 4. Lipid profiles for lipids from C. oleaginosus, glucose 1 and 2 are from two different sources [24], [37], [38].

From the lipid profile stacked bar chart above, it is seen that the carbon source can affect the distribution of the different fatty acids. Galactose as a carbon source lead to the highest amount of oleic acids (57%) and acetate as a carbon source resulted in the highest amount of stearic acid (23.6%). When using arabinose, the palmitic acid was the highest with about 35 % compared to the other sugars used.

A study by Yang et al. [44] showed that the C/N ratio affected the FAME production in *Yarrowia lipolytica*, a high C/N ratio for yeast cultivation resulted in 5 % FAME production whereas a low C/N resulted in 3 % FAME and a low C/N ratio with nitrogen depletion, that is, no nitrogen was added, resulted in 7 % FAME [44]. Assuming that all oleaginous yeasts behave similarly, a nitrogen depletion will have a positive effect on the lipid production in *C. oleaginosus*. The lipid profile was also affected when using a nitrogen depleted media, where the C18-1 amount was more than doubled with the nitrogen depleted media than it was with both high and low C/N ratio media. However, the nitrogen-depleted media did not result in satisfying amounts of C16 and C18 compared with both the high and low C/N ratios, which were more than doubled using media with added nitrogen [44].

2 Literature study of food waste characterization and analysis

As mentioned earlier, food waste is a major concern, and every single human being can do an effort to reduce food waste globally. 1.3 billion tonnes of food is wasted per year, globally, that is, one-third of the food produced [45]. 6% of the global greenhouse gas emissions come from food losses and food waste, and the main reason behind this is the methane gas that is produced when the food waste is decomposed [46], [47]. About 56 % of the food waste ends up in landfills in the USA, where it rots and emits methane gas [48], [49]. In Denmark in 2019, about 1.7 million tonnes of municipal waste is recycled and almost the same amount is sent to incineration and landfills, and food waste accounts for about 7% of the total recycled municipal waste [50]. Denmark has only recently applied the sorting of food waste method in the households, therefore, no exact numbers of the recycled food waste are found.

Characterization and analysis of food waste are important to be done before managing and treating the waste and using it for conversion to valuable products like biofuels and biogas. As food waste varies geographically and seasonally, the potential of the outcome of food waste conversion can vary. In this section, the food waste characterization methods will be described briefly, and the results of the characterization will be shown.

The studies by Wavrer [51] and Haro et al. [52] worked with the characterization of municipal solid waste (MCW) using the MODECOM method. MODECOM is a French abbreviation for “Method for

Characterization of Domestic Waste". MODECOM is a guide to organizing and analyzing the MCW. The MODECOM method consists of five major parts (Figure 5). The first part is a preliminary inquiry to collect the data required to organize the analysis. The organization could be to divide the samples into geographic zones or population districts among others. The second part is to select which collection vehicles the sample should be taken from, from each of the selected sections from the first step. The third step is to take samples from the selected collection vehicles from the second step. The fourth step is sorting the waste. The fifth and last part of the MODECOM is the laboratory analyses to determine the moisture content, heavy metals content, organic matter content and loss of ignition [51]. The results of the two studies can be seen in Table 2.

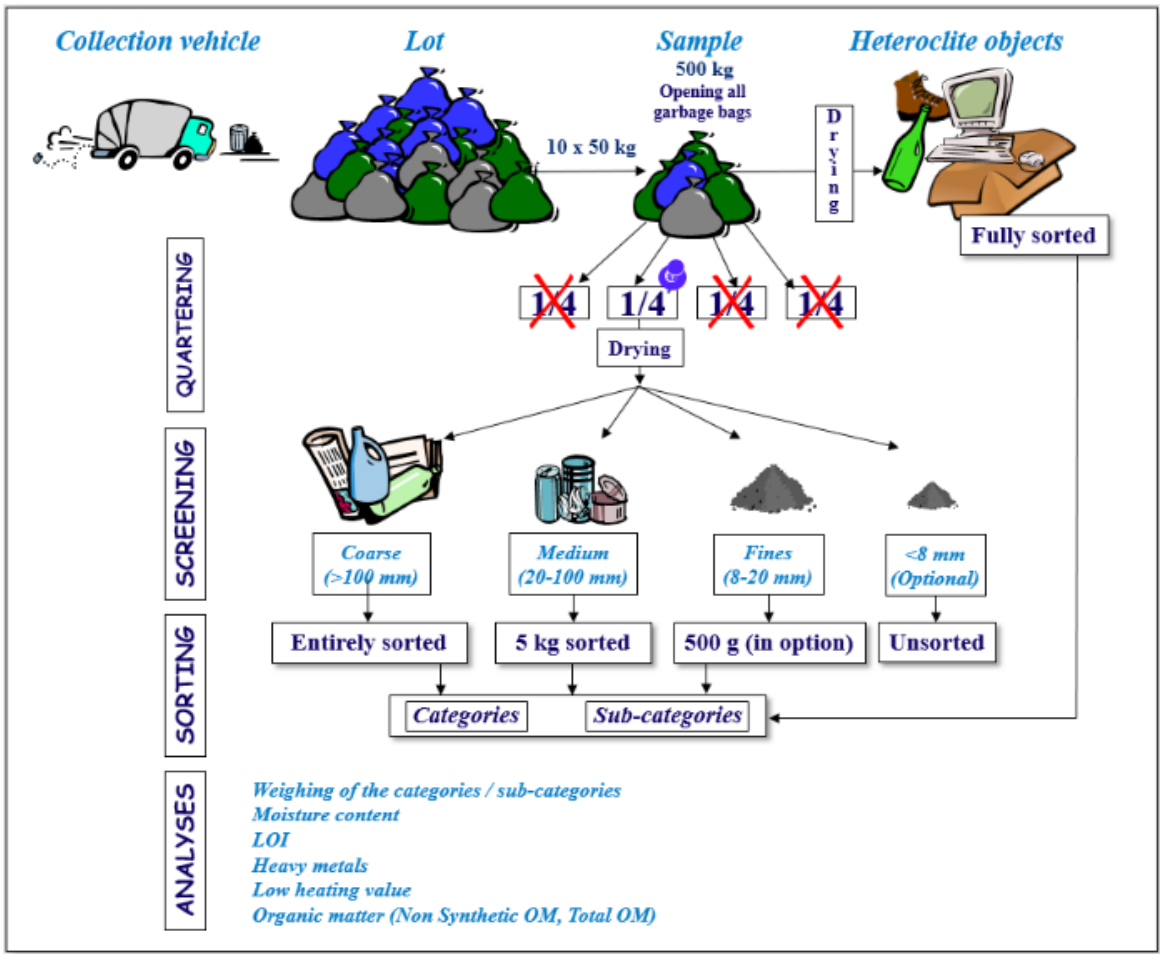

Figure 5. MODECOM method illustration. The shown parts of the method are from the third to fifth major steps, including substeps. Starting from the upper left part of the figure: Collection and dividing the lots, sampling, screening, sorting and analysis [51].

Table 2. NCC= nonclassified combustibles, NCI= nonclassified incombustible, numbers are given in % of waste weight, moisture content was analyzed separately (the numbers in each row will result in 100% without the moisture content).

	Fermentable waste (dry %)	Paper	Cardboard	Composites	Textiles	Sanitary textiles	Plastics	NCC	Glass	Metals	NCI	Special wastes	Fine materials (<20 mm)	Moisture	Source
France	8.79	9.71	8.84	2.43	4.78	9.35	22.79	6.3	5.61	5.64	0.58	0	15.20	-	[53]
Burkina Faso, rainy season	23.86	1.65	4.49	1.53	5.41	1.69	11.13	3.46	1.14	2.89	4.27	0.22	38.27	56.69	[52]
Burkina Faso, dry season	19.94	2.37	5.19	2.28	4.32	1.94	12.1	2.81	3	1.71	5.12	1.14	38.08	37.69	[52]

From the table above, it is seen that the composition of waste varies significantly in France and Ouagadou (the capital of Burkina Faso, a country in West Africa). The composition of waste in the rainy season and dry season in Ouagadou varies also. We can conclude from the two studies, that the waste composition will most likely vary from season to season and from country to country. The fermentable waste fraction is bigger in the rainy season than in the dry season, and the moisture content is higher in the rainy season.

Studies by Zhang et al. [54], Nwobi [55] and Ho et al. [56] worked with the characterization and analysis of food waste composition. The study by Zhang et al. [54] analyzed the composition of food waste entering the source segregated streams in selected regions in Italy, UK, Portugal and Finland. The goal of this study was to obtain knowledge of the properties of food waste and the effect of the different food waste compositions as feedstock for anaerobic digestion. The same goal was given in the study by Nwobi [55], but here the analysis was done in the Emirates, Abu Dhabi. The waste stream from the study by Zhang et al. [54] was categorized in the organic fraction of municipal solid waste, source segregated organic waste and food waste from households, among others. In the study by Ho et al. [56], the chemical composition of food waste in China was analyzed from three different sources, household kitchen waste (HH), wet market food waste (WM) and Chinese restaurant food waste (CR). In both studies by Zhang et al. [54] and Nwobi [55], the food waste samples were analyzed physio-chemically

by analyzing the pH, volatile solids (VS), total solids (TS), total organic carbon (TOC), calorific value (CV) total Kjeldahl nitrogen (TKN), protein, lipid, total potassium, total phosphorus and elemental composition [54]. The results can be seen in Figure 6 and Figure 7. In the study by Ho et al., only VS, pH, TK, lipids, crude protein and C contents were analyzed.

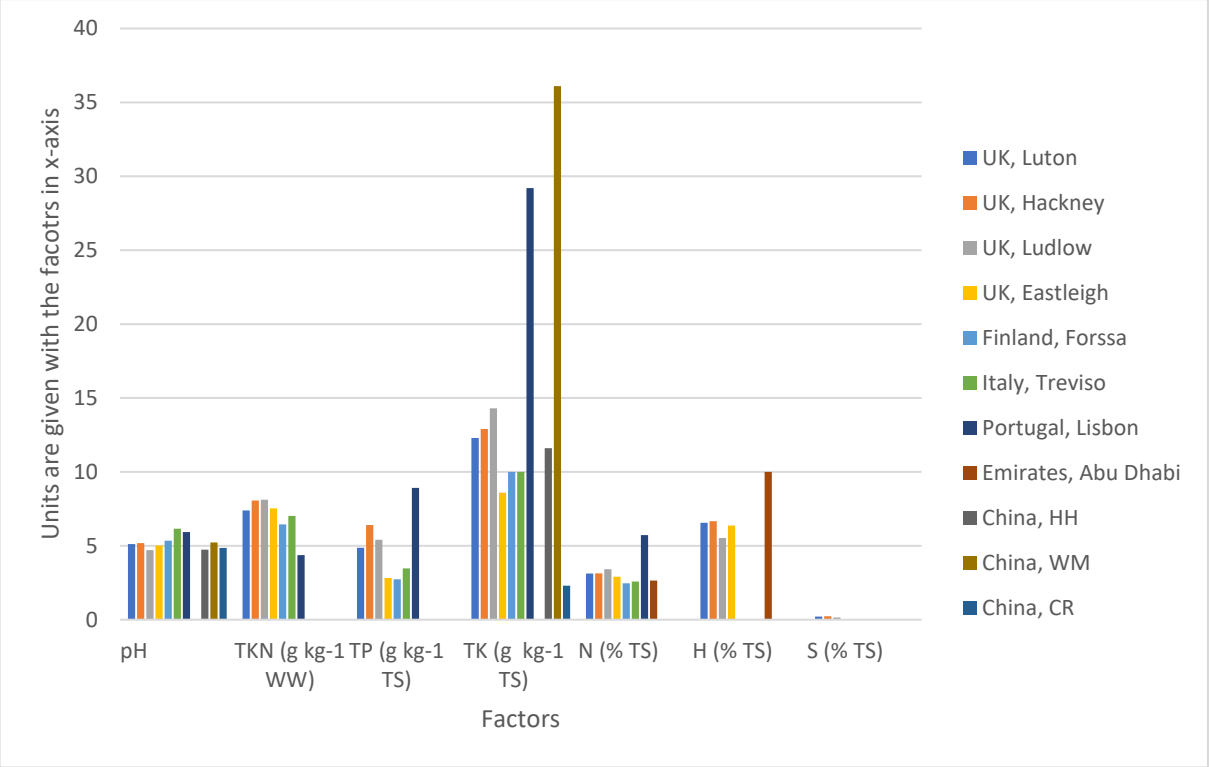

Figure 6. Results of the studies by Nwobi, Zhang et al. and Ho et al., WW= wet weight, TS= total solids, TKN= total Kjeldahl nitrogen, TP= total phosphorus, TK= total potassium. Empty columns means particular measurements were not conducted [54], [55],[56].

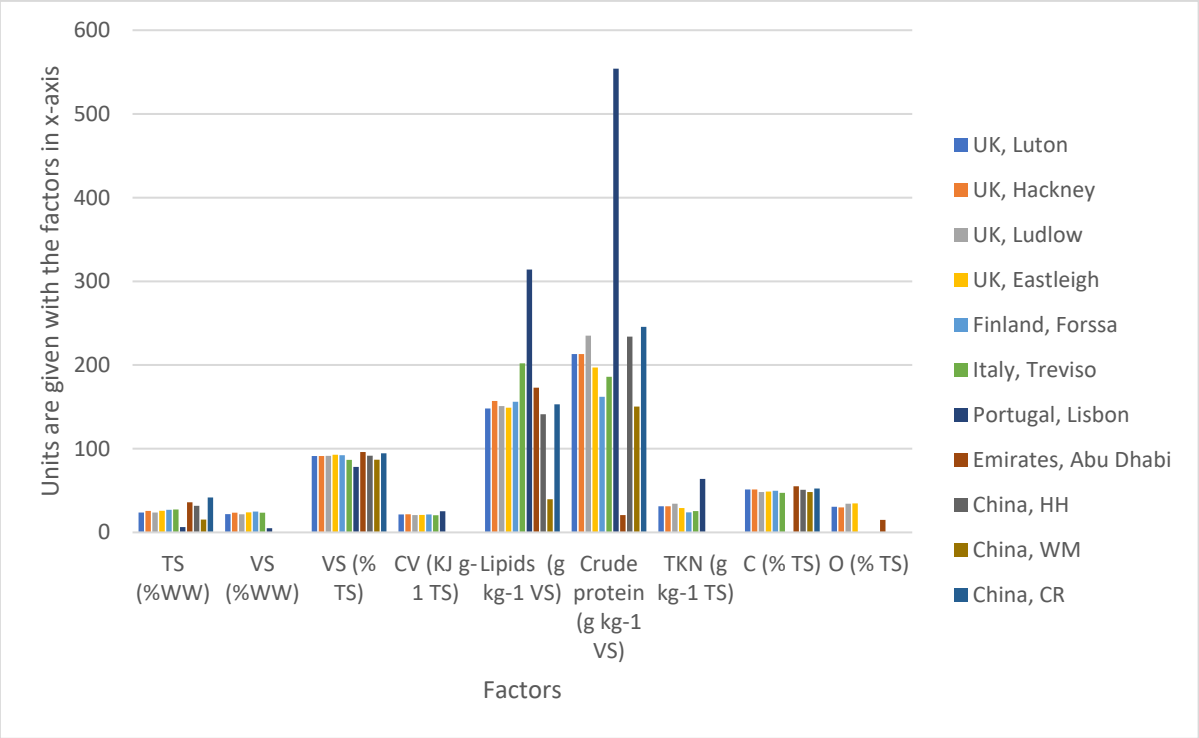

Figure 7. Results of the studies by Nwobi, Ho et al. and Zhang et al. WW= wet weight, TS= total solids, TOC= total organic carbon, TKN= total Kjeldahl nitrogen, CV= calorific value. Empty columns mean particular measurements were not conducted [54], [55], [56].

From Figure 6 and Figure 7 it is seen that some components of the sample from Portugal, Lisbon, have significantly higher values than the other samples. That is because the sample from Lisbon is collected from the digestion feed from an anaerobic digestion plant, and some contents from the food waste are excluded before reaching the digestion feed. The other samples are from the source segregated raw food waste, but some samples contained non-food waste, like paper and garden waste, but such kinds of waste do not count as contamination. Items like glass, plastic and metals are counted as contamination, and the contamination part of samples from the UK, Finland, Portugal and Emirates does not exceed 6%, whereas the sample from Italy contains up to 20% of contamination, which can affect the values for the physio chemical characteristics [54].

Comparing the data from Emirates by Nwobi [55] and the data from China by Ho et al. [56], with the other data by Zhang et al. [54], it can be seen that the most values for Emirates and China lies in the same range as the other values, except the hydrogen amount, which is a bit higher for the Emirates sample and the amount of crude protein, which is very low comparing to the samples from other counties. The lipid amount is noticeable lower for the Chinese wet market, as it is the food waste from fish and meat stores, and these usually don't contain high amounts of lipids. It can also be concluded that

food waste from different sources contains different amounts of content. As all three studies had similar results, it can be assumed that all results are reliable.

Studies by Flyhammar et al. [57],[58],[59], Chang et al. [60], Zennaro et al. [61], Ho et al. [56] and Pollak et al. [62] showed that metals are found in the MCW and can exist as additives, compounds in different structures or as elemental forms [57]. Table 3 shows the metal ions content found in these different studies.

Table 3. Concentrations of metals found in MSW in different sources, HH= Household kitchen waste, WM= wet market food waste, CR= Chinese restaurant. Empty cells mean particular content is not given in the study, but are certainly found in the wastes in small amounts.

Metal ions	Fresh MSW (% DW)	Fresh MSW (% DW)	OFMSW (% DW) range	Food waste (% DW) range	HH, (% DW)	WM, (% DW)	CR, (% DW)
Fe	1.2413	-	-	-	-	-	-
Mn	0.0816	-	-	-	-	-	-
Zn	0.2677	0.1336	0.0014 – 0.0032	0.0006-0.0112	-	-	-
Cu	0.0139	0.04	0.00011 – 0.001	0.001-0.0025	-	-	-
Pb	0.0216	0.075	ND-0.00043	0.000042-0.002	-	-	-
Cr	0.0016	0.025	ND-0.00068	0.00016-0.0018	-	-	-
Ni	0.0025	0.008	0.00003 – 0.00089	0.00016-0.003	-	-	-
Cd	0.0006	0.00083	0.000005 – 0.00005	0.000006-0.00014	-	-	-
Ca	1.4995	-	-	-	1.09	0.98	0.70
P	0.0964	-	-	-	-	-	-
S	0.0698	-	-	-	-	-	-
Na	-	-	-	-	0.58	0.42	0.41
Mg	-	-	-	-	0.18	0.36	0.14
Country & source	Sweden, [58]	Sweden, [59]	China, [60]	Italy, Austria [61], [62]	China, [56]	China, [56]	China, [56]

A study by Rajakumar et al. [63] investigated the effect of cadmium (Cd) on the lipid metabolism in *S. cerevisiae* and showed that it alters the lipid production as it has a toxic effect on the yeast cell. The study showed that Zinc (Zn) has similar physical and chemical properties as Cd, and hence when yeast is exposed to Cd, it can lead to Zn deficiency, and disturbances in Zn balance can alter the lipid metabolism. Both accumulation and depletion of Zn are toxic for yeast cells [63]. Normally, yeasts require 0.1 to 0.2 mg/l of Zn ions for successful fermentation, and the yeast can be inhibited by Zn concentrations higher than 0.6 mg/l[64]. The Zn level is maintained by efflux and influx mechanisms. Zn transporters (Zrt1p and Zrt2P) are located in the plasma membrane of the yeast cells, and these are activated by the Zn transcription factor ZAP1 (Figure 8). Cd can also be uptaken into the cell by Zrt1P if Zn concentrations are limited in the cell. The Zrt1p transporter can also avoid the overload of Cd. When Zn is depleted, the ZAP1 is activated and regulates the phospholipid metabolism, and phosphatidylethanolamine (PE) and phosphatidylinositol (PI) are changed, which can potentially cause lipid accumulation and generation of reactive oxygen species ROS (Figure 8). The generation of ROS can result in changes in the cell's antioxidant defenses, and this can cause oxidative stress. Exposing cells to oxidative stress can lead to damage of lipids, proteins and DNA as well as mitochondrial cell damage and apoptosis [63], [65], [66].

A study by Iwanyshyn et al. [67] showed that depletion of Zn resulted in a 66% decrease in the amount of PE and 29% decrease in PI. When the yeast cells were exposed to Cd, the Zn levels were reduced in *S. cerevisiae*, indicating that Zn and Cd have a similar effect on the cell [63].

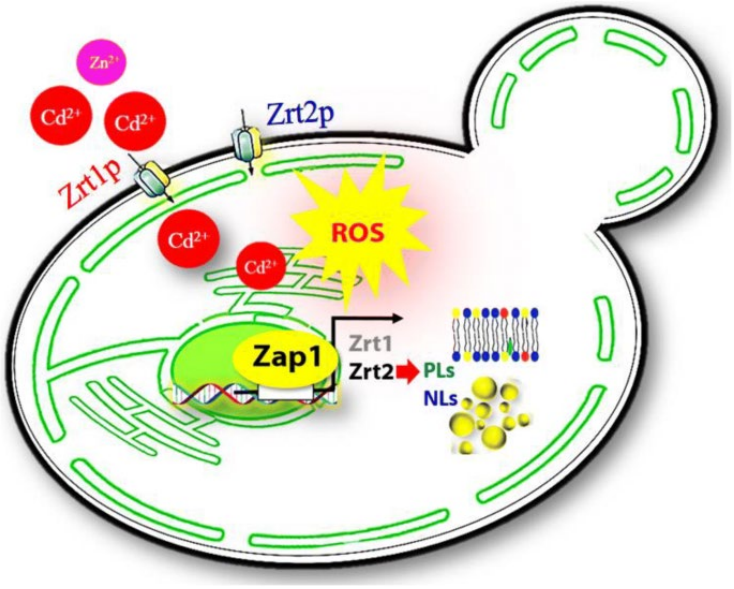

Figure 8. Uptake of Cd by Zn transporters (Zrt1p and Zrt2P) in the yeast cell, PLs=Neutral lipids, NLs=Polar lipids, Zap1=Zn transcription factor [63].

Metal ions such as Fe, Cu, Zn, Mn and Ca can also have a toxic effect on the yeast [63]. A study by Yang et al. [68] showed that the following metals are also toxic to the yeast cells, ranked in decreasing order of toxicity: Hg>Ag>Au>Cu, Ni, Co, Zn. *S. cerevisiae* yeast cells exposed to 0.1325 µM Hg ions decreased their viability by 20% compared to those which was not exposed to Hg and when the amount of Hg ions added to the cells increased to 0.625 µM, the yeast cells were not growing. Ag ions had a similar effect on the yeast cells, where exposing the yeast to 5 µM Ag ions led to the loss of 25 % of the viability of the cells [68].

2.1 Carbohydrate's impact on the lipid accumulation in yeast

Many studies showed that the nitrogen, carbon and oxygen content in the fermentation media affected the lipid production by oleaginous yeasts [21],[55],[69],[70],[71].

Different types of yeast behave differently when fermented with different types of sugars, and obviously, the lipid amount accumulated by the yeast will also have different quantities. In the following part of the report, the effect of the different types of sugars on lipid accumulation by various yeast strains will be investigated briefly. In Figure 9 then the comparison is seen and the data are taken from studies by Sha [72] and Awad et al. [73]. From Figure 9 it can be seen that the highest lipid accumulation was achieved with *C. oleaginosus,* where both glucose and xylose fermentation media gave high amounts of lipid accumulation. When mannose was used as a substrate, the lipid accumulation was

lower. The data obtained from the studies indicate that the type of sugar has an effect on the amount of lipid accumulation in yeasts.

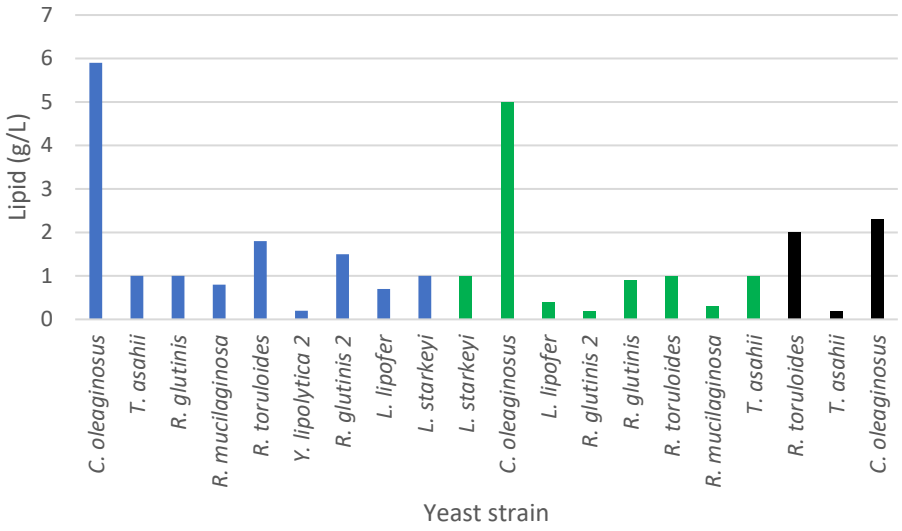

Figure 9. Comparison of different sugars on lipid accumulation in several yeast strains. The blue, green and black colors indicate the substrate, blue= glucose, green= xylose and black= mannose. A fermentation time of 96 h was used for all experiments [72], [73].

2.2 Carbon and nitrogen impact on lipid production in yeasts

Studies by Lopes et al. [74] and Ye et al. [75] showed that the C/N ratio affects the lipid production in yeast. Table 4 shows the results obtained by those studies. Both studies used the yeast *Rhodotorula toruloides* but each study used a different strain. It is seen that the highest lipid content achieved was 60 % for the continuous mode and a C/N ratio of 120 with xylose as a carbon source. A similar lipid amount was achieved using the batch mode, where the lipid amount achieved was 59 %, but the C/N ratio was 200 and the carbon source was sucrose. It can be concluded from these two studies, that a higher C/N ratio will result in higher lipid accumulation in yeasts.

Table 4. Effect of different C/N ratios on the lipid production in oleaginous yeast.

Mode of fermentation	Yeast type	Carbon source	Nitrogen Source	C/N ratio	Lipid (% dry weight)	Source
Turbidostat continuous	*Rhodotorula toruloides* CCT 0783	Acetic acid	Ammonium sulfate	80	38	[74]
Turbidostat continuous	*Rhodotorula toruloides* CCT 0783	Glycerol	Ammonium sulfate	80	37	[74]

Turbidostat continuous	*Rhodotorula toruloides* CCT 0783	Xylose	Ammonium sulfate	80	30	[74]
Turbidostat continuous	*Rhodotorula toruloides* CCT 0783	Acetic acid	Ammonium sulfate	100	39	[74]
Turbidostat continuous	*Rhodotorula toruloides* CCT 0783	Glycerol	Ammonium sulfate	100	52	[74]
Turbidostat continuous	*Rhodotorula toruloides* CCT 0783	Xylose	Ammonium sulfate	100	50	[74]
Turbidostat continuous	*Rhodotorula toruloides* CCT 0783	Acetic acid	Ammonium sulfate	120	53	[74]
Turbidostat continuous	*Rhodotorula toruloides* CCT 0783	Glycerol	Ammonium sulfate	120	41	[74]
Turbidostat continuous	*Rhodotorula toruloides* CCT 0783	Xylose	Ammonium sulfate	120	60	[74]
Batch	*Rhodosporidium toruloides* (R-ZL2)	Sucrose	Ammonium sulfate	40	20	[75]
Batch	*Rhodosporidium toruloides* (R-ZL2)	Sucrose	Ammonium sulfate	80	24	[75]
Batch	*Rhodosporidium toruloides* (R-ZL2)	Sucrose	Ammonium sulfate	160	38	[75]
Batch	*Rhodosporidium toruloides* (R-ZL2)	Sucrose	Ammonium sulfate	200	59	[75]

2.3 pH impact on lipid production in yeasts

A study by Johnson et al.[76] showed that the pH affects the lipid accumulation in oleaginous yeasts. The pH range that was tested in the study was 3-6. A pH of 4 was the most favorable with 66% lipids (% w/w of biomass) and the pH that gave the lowest lipid accumulation was 3, where the lipid content was only 12 % w/w of biomass [76]. Most of the studies done in this research area use pH 4-6, as this range is shown to be most optimal [13],[24],[76],[77], however, yeast strains that can grow on low pH are more interesting because the slightly acidic environment can reduce contaminations significantly in big scale production [13].

The knowledge obtained from this literature study provided the knowledge needed to determine which parameters are to be analyzed in the organic waste material. Most of the metals will be analyzed in ICP, these include Cd, Cu, Zn, Fe, Ca and Mn, moreover, K and P will also be analyzed in the ICP-OES. Additionally, total carbohydrates, carbon, nitrogen, hydrogen, sulfur and lipids will also be analyzed.

2.4 Enzymatic degradation of food waste

Enzymes can be used for the valorization of food waste (Figure 10). Figure 10 shows the use of enzymes used for the conversion of food waste into valuable chemicals, biofuels and biodiesel [78]. For example, lipase enzymes can be used for the transesterification of frying oil into biofuels, lubricants and surfactants [1].

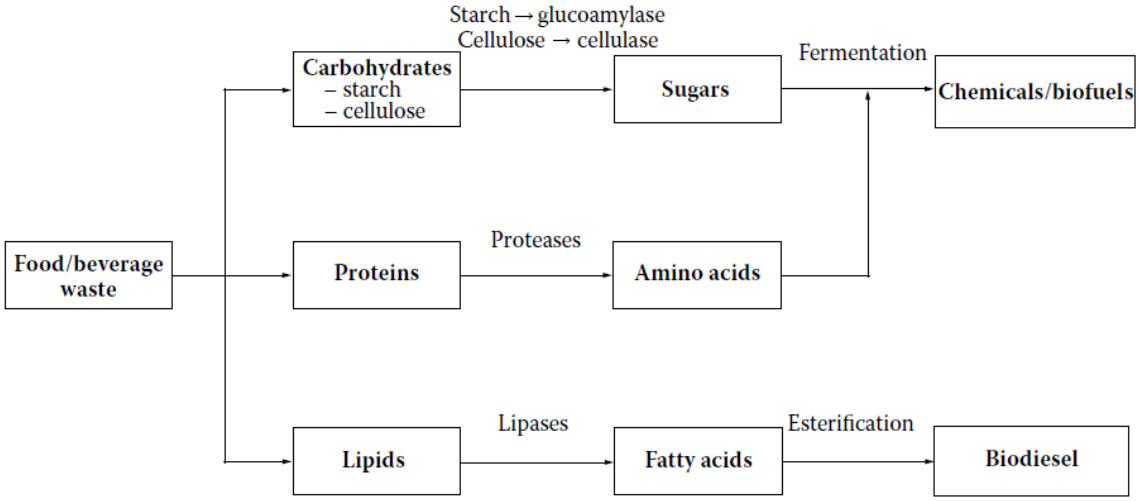

Figure 10. The use of enzymes for the valorization of food waste. Carbohydrates use glucoamylase and cellulase to convert to sugars. Proteins use proteases to convert to amino acids and lipid uses lipases to convert to fatty acids. Sugars and amino acids can be chemicals and biofuels, and fatty acids can be converted to biodiesel [78].

2.4.1 Starch degradation

The glucoamylases, which are also called amylases, catalyze the hydrolysis of α-(1,6) glucosidic bonds and α-(1,4) glycosidic bonds on starch, giving glucose as a product as seen in Figure 11. The starch can be amylose, which is a linear chain of glucose molecules linked together by α-(1,4) glycosidic bonds, or amylopectin, which is a branched polymer of glucose linked by 1,4- and 1,6-glycosidic bonds [79], [80], [81]. Glucoamylases are found in animals, plants and microorganisms, but industrially, the glucoamylase is produced from filamentous fungi such as *Aspergillus* and *Rhizopus* through submerged fermentation [82], [83].

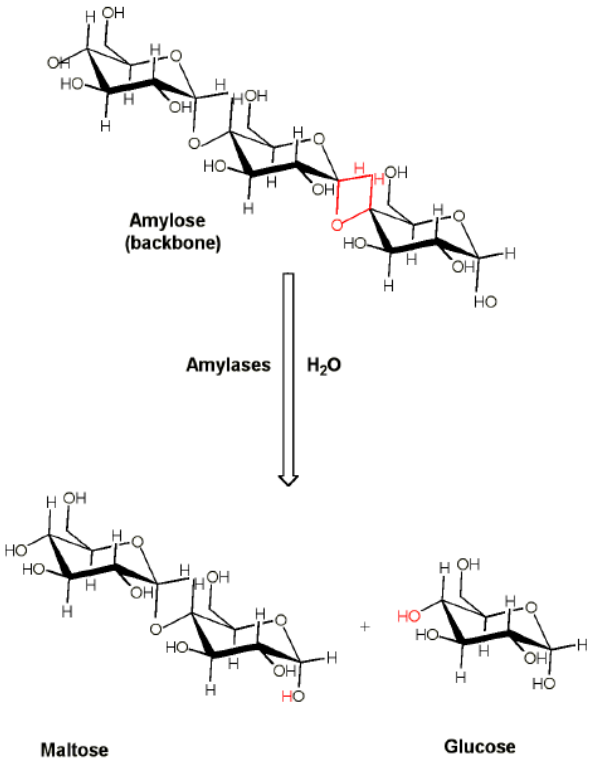

Figure 11. Hydrolysis of amylose into maltose and glucose [81].

2.4.2 Cellulose degradation

Cellulases are a group of enzymes consisting of three enzymes, endo-(1,4)-β-D-glucanases, exo-(1,4)-β-D-glucanases, and β-glucosidases. The cellulases hydrolyze β-(1,4)-glucan bonds in cellulose producing glucose. The endocellualse hydrolyze the crystal cellulose to cellulose, glucan chains in various lengths, by attacking O-glycosidic bonds. The exocellulase hydrolyses cellulose to β-cellobiose and the β-glucosidases hydrolyses the cellobiose disaccharides to glucose (Figure 12) [84], [85]. Cellulases are produced by animals, plants, fungi, protozoans and bacteria. From the bacteria, *E. coli*, *Acidothermus* and *Bacillus subtills*, are cellulase producers, among many others. Among fungi, the most studied organisms that produce cellulases are *Penicillium, Fusarium, Aspergillus* and *Trichoderma,* especially *Penicillium* and *Aspergillus* can produce high levels of extracellular cellulases [83], [86], [87].

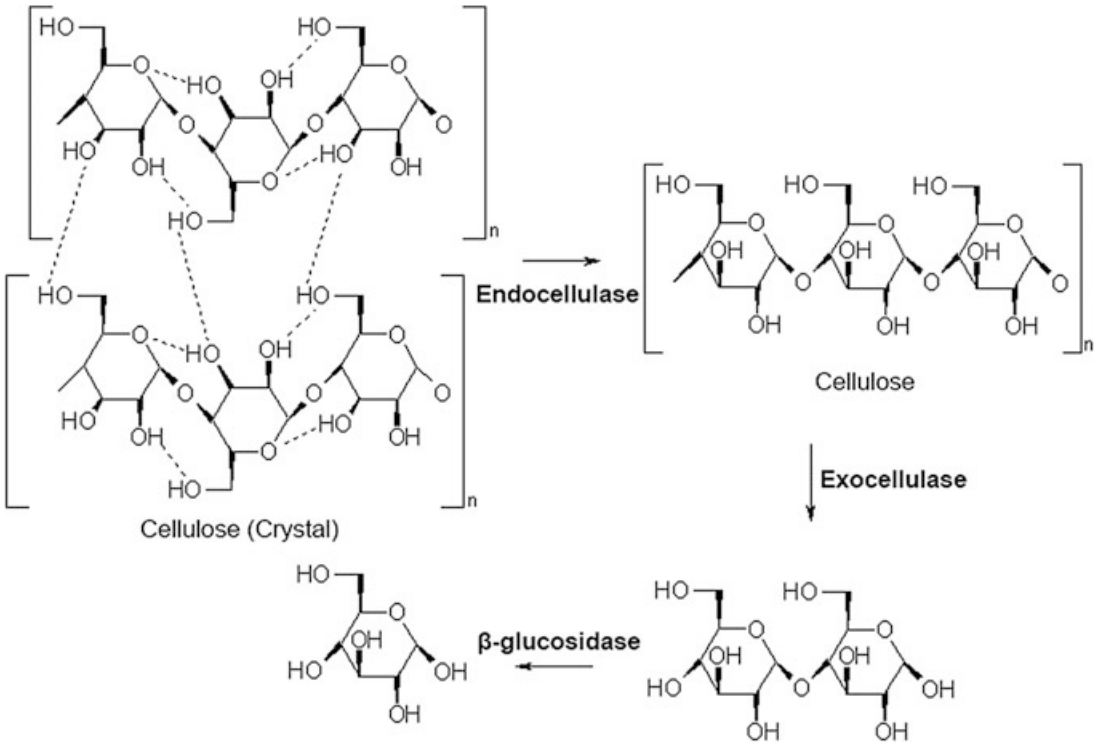

Figure 12. Hydrolysis of cellulose [84].

2.4.3 Protein degradation

Proteases, also called proteinases, can hydrolyze the peptide bonds in proteins and result in amino acids or smaller peptides (Figure 13) [88],[89], [90]. Proteases are produced in almost every living organism including plants, animals and microbes. The most commercially used organism for the production of proteases is the bacteria *Bacillus sp*. [91], [92].

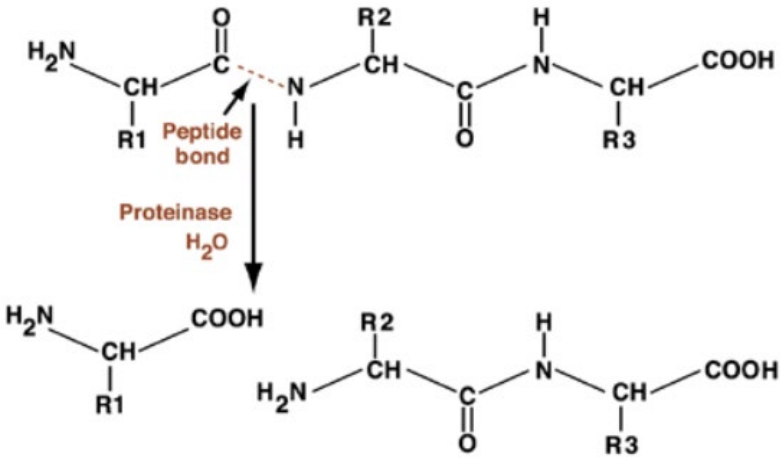

Figure 13. The upper structure shows a protein. The protease (proteinase) enzyme degrades the peptide bond resulting in smaller protein fragments (peptides) or single amino acids [88].

2.4.4 Hemicellulose degradation

Hemicellulases are a group of enzymes that are used to hydrolyze hemicelluloses. Hemicelluloses are together with celluloses, the most important renewable energy sources. Hemicelluloses are complex polysaccharides that can be found in plant fibers and consist of mixed pentoses or hexoses together with uronic acids [93], [94],[95]. Hemicellulases are generally produced inside saprophytic microbes, which grow on dead organic materials. Thermophilic bacteria- and fungi, are excellent producers of hemicellulases, as they can tolerate extreme culture conditions, like temperature and pH. Examples of hemicellulose producers are *Bacillus, Paenibacillus, Thermobacillus xylanilyticus* and *Thermomyces lanuginosus* [96], [97].

The most important hemicellulolytic enzymes are endoxylanases, and their function is to hydrolyze glycosidic bonds of xylan resulting in shorter xylooligosaccharides. Xylosidases are hemicellulases that hydrolyze beta-1,4-type bonds in xylooligosaccharides, e.g., xylobiose, giving xylose as a product. Arabinofuranosidase releases L-arabinofuranose from xylan (Figure 14). Beta-mannases have the function to hydrolyze hemicelluloses which are composed of mannans resulting in mannologomers. Mannose can be released from mannologomers by beta-mannosidases [93], [94], [95].

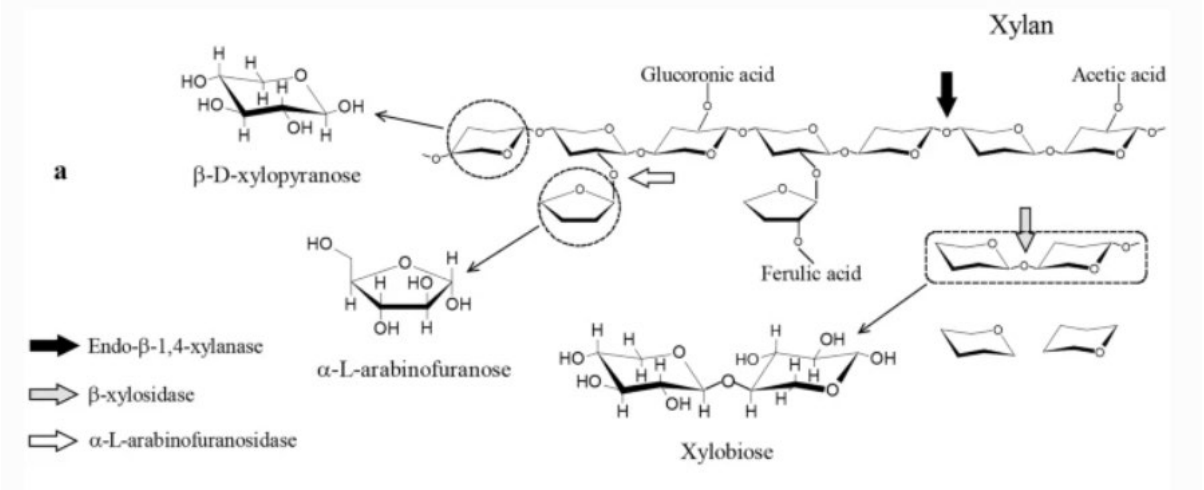

Figure 14. Hemicellulolytic enzymes hydrolyze xylan [93].

2.4.5 Pectin degradation

Pectate lyases, also known as pectate transeliminases, are enzymes that are used to degrade the plant cell wall, and they are produced by pathogenic organisms, but are also found in plants and animals [98], [99],[100], [101]. The backbone of a pectin polysaccharide is made of α-1,4 linked polygalactosyluronic acid residues with rhamnosyl residues and galactosyluronic acids [100]. Pectate lyases use the β-elimination mechanism to degrade pectin (Figure 15). The β-elimination mechanism is the cleavage of the β(1–4) linkage between galacturonosyl residues by pectate lyases, resulting in double bonds oligogalacturonates [100],[99].

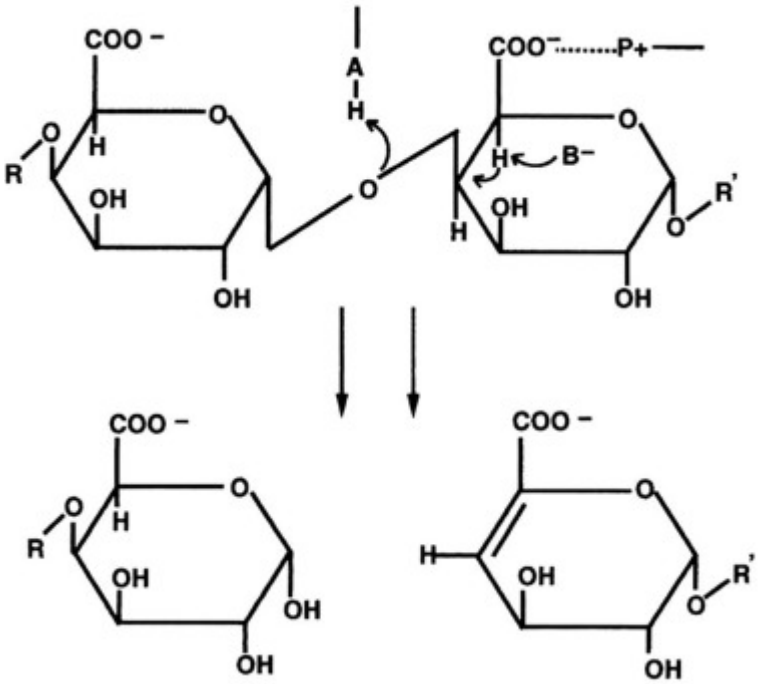

Figure 15. Pectate lyases cleave the β(1–4) linkage in 1,4-polygalacturonic acid [99].

3 Simultaneous saccharification and fermentation (SSF)

Simultaneous saccharification and fermentation (SSF) can be used to convert lignocellulosic waste materials and organic waste to fermentable sugars and then to valuable products by microorganisms. The products of microorganisms can be ethanol, amino acids, lipids and many others. An example is paper sludge which can be converted to ethanol by the use of the cellulose content in the paper [22], [102], [103].

In the SSF process, enzymatic hydrolysis and fermentation are performed at the same time. This process can be used instead of the conventional two-step process, where the enzymatic hydrolysis and fermentation processes are made separately. Studies by Nwobi et al. [104], Olofsson et al. [105], Gong et al. [106] and Mihajlovski et al. [107] showed that the SSF process has some advantages over the separate hydrolysis and fermentation processes. The advantages can be reducing of the inhibition effect of glucose on the yeast and thereby increasing the overall lipid yield, reducing of cellulase inhibition by the end product, decreasing the contamination risk by doing it in the same reactor, reduced cost and reduced process time [104], [105], [106], [107].

The simultaneous saccharification and enhanced lipid production (SSELP) process is a kind of SSF, where the aim of it is to produce lipids by microorganisms. A study by Gong et al. [106] compared the SSELP with SHELP (separate hydrolysis and enhanced lipid production) processes by *Cryptococcus*

curvatus for optimization of lipid production. *Cryptococcus curvatus* is used as it is a very effective yeast type at accumulating lipids. Different parameters were tested, and results showed that increasing the initial pH from 4.4 to 5.2 decreased the cellulose conversion from 85.5% to 84.1% and increased the lipid content from 5.5 g/L to 6.5 g/L. A pH of 5.2 was the most optimal for the SSELP. The optimal dosage for cellulase and cellobiase per gram of cellulose were 7.5 FPU and 15 CBU, respectively. The optimal temperature is challenging to choose when working with SSF processes because the fermentation and saccharification have different temperature optima. Normally, oleaginous yeasts have optimal growth at 30 °C, and enzymatic saccharification temperature optimum is around 50 °C, but *C. curvatus* had temperature optima at 37 °C in the SSELP process, this is because no auxiliary nutrients were added to the fermentation process, and thus no inhibition of cell propagation happened [106]. The results of this study are seen in Table 5.

The study by Mihajlovski et al. [107] compared the separate hydrolysis and fermentation (SHF) with Fed-batch SSF, and the fed-batch SSF was more efficient and economically feasible than batch SSF and SHF [107]. The fermentation media included alkaline pretreated corn cobs and growth media (phosphate buffer, trace elements and nutrient solution. The SSF conditions and results are seen in Table 5.

Table 5. A summary of SSF experiments compared to SHF, the substrate loading is the concentration of the substrate (pretreated corn cobs) in the fermentation media.

Fermentation type	Yeast strain	Substrate	Temperature	Substrate loading	Enzyme loading	Lipid yield, g lipid/ 100 g sugar)	Source
Batch SSF	*Trichosporon oleaginosus*	Pretreated corn cobs	30	15 %	5 FPU g^{-1} glucan	8.01	[107]
Batch SSF	*Trichosporon oleaginosus*	Pretreated corn cobs	30	20 %	5 FPU g^{-1} glucan	6.26	[107]
Fed-batch SSF	*Trichosporon oleaginosus*	Pretreated corn cobs	30	15 %	5 FPU g^{-1} glucan	12.58	[107]
Fed-batch SSF	*Trichosporon oleaginosus*	Pretreated corn cobs	30	20 %	5 FPU g^{-1} glucan	13.37	[107]
Fed-batch SSF	*Trichosporon oleaginosus*	Pretreated corn cobs	30	20 %	30 FPU g^{-1} glucan	13.40	[107]
SHF	*Trichosporon oleaginosus*	Pretreated corn cobs	Enz. h. 50 Cultivation: 30	15 %	10.5 FPU g^{-1} glucan	7.22	[107]
SSELP	*Cryptococcus curvatus*	Corn stover	37	-	4 FPU, 8 CBU, 5 mg xylanase	6 g/L	[106]

SHELP	*Cryptococcus curvatus*	Corn stover	-	-	10 FPU, 20 CBU, 10 mg xylanase	43.4 and 7.2 g/L	[106]

The table shown above summarizes the results of the comparison between SHF and SSF processes from two studies. It is seen that the SSF performs better in terms of lipid accumulation. The SHELP process written in the last row gives a higher lipid yield than the SSELP from the same study, but it is because the enzyme loading is much higher there, so the SSELP performs better.

4 Ragn-Sells

Ragn-Sells is a food waste handling plant in Holsted, Jutland, Denmark. Figure 16 shows how Ragn-Sells handles food waste. They receive food waste from 7 municipalities, including Esbjerg municipality and they also receive food waste from stores and restaurants. The food waste is received in plastic bags. Big things are taken out from the waste. Then the food waste is taken out from the bags and blended. The plastic bags are separated as well as Metals. The plastic is shredded, washed and delivered for reuse. The metals are delivered for reuse as well. The food waste is blended with water. Glass and stones are sorted from the food waste and delivered to be re-used as well. The plastic that remained in the biomass is removed and delivered for combustion, and the food waste is delivered to a biogas plant as biomass [108].

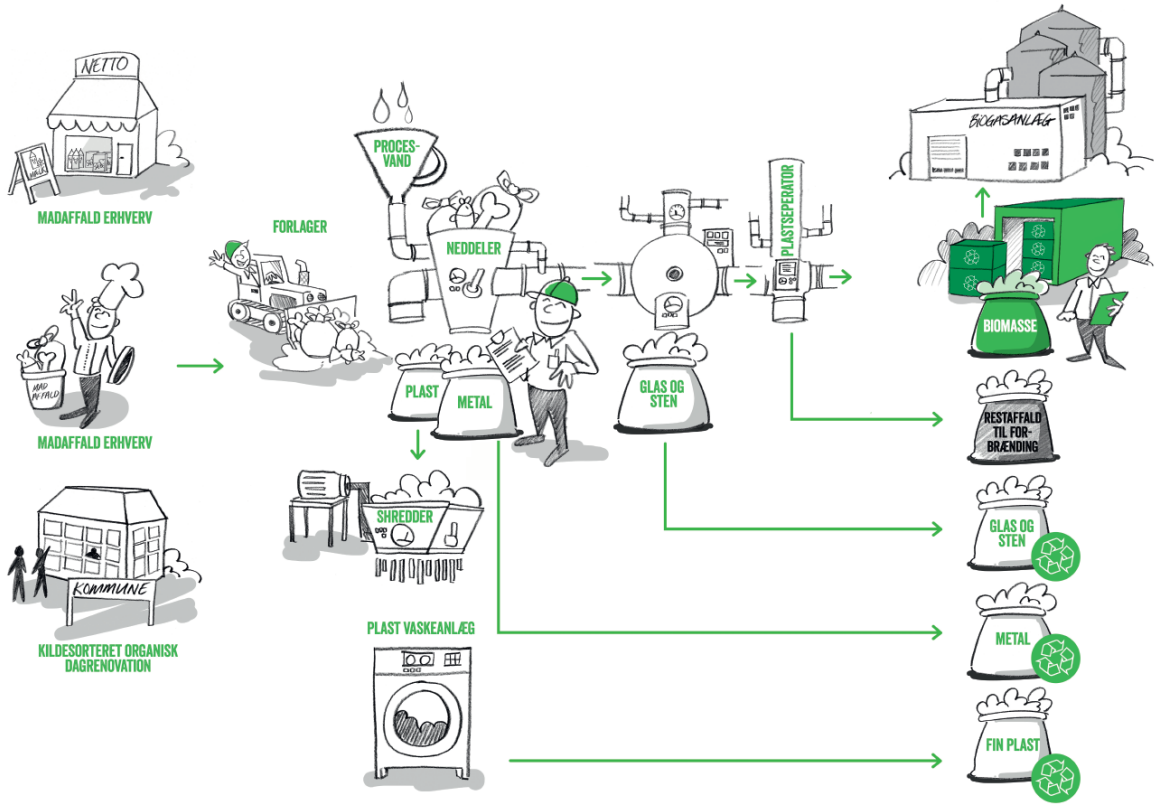

Figure 16. Ragn-Sells food waste handling steps [108].

5 Materials and methods

Two types of food waste samples were used. One from the AAU Esbjerg Campus energy section, which is manually made food waste. The second waste type is from Ragn-Sells waste handling plant in Holsted. Only one waste sample of about 2 kg, from the energy department, was used, and five samples of 4 kg each were collected each month (November 2021-March 2022) from Ragn-Sells. Section 4 includes a description of the Ragn-Sells plant. Before starting the analytical methods, the samples were dried in the oven at 105 ° C for 24 h and homogenized using a hand mortar and/or food processor. All the dried samples were kept in a desiccator until use.

5.1 Determination of total solids and ash in OFMSW

As biomass samples contain varying amounts of moisture which changes rapidly, the results of all the chemical analyses of biomass are based on the biomass's dry weight. The first analysis performed on the OFMSW is therefore the determination of total solids, moisture and ash content [81].

This is done by weighing some of the waste in a crucible and drying it at 105 °C in approx. 24 hours and weighing the crucibles again, when cooled to room temperature in a desiccator [81]. This analysis was conducted in triplicate.

The total solids and the moisture content are calculated from the equations below [81]:

$$\%\, Total\ Solids = \frac{Weight_{\,dry\ crucible\ +dry\ sample} - Weight_{\,dry\ crucible}}{weight_{\,fresh\ sample}} * 100$$

$$\%\, Moisture = 100 - \left(\frac{Weight_{dry\ crucible\ +dry\ sample} - Weight_{dry\ crucible}}{weight_{fresh\ sample}} * 100\right)$$

The inorganic material of the biomass is measured as the ash remained after heating to 550 °C in a muffle furnace. This analysis is also done in triplicate. Three dried crucibles were weighed, and 0.5-2 g of dried and granulated OFMSW were added to each crucible and weighed. The crucibles were heated in the muffle furnace at 550 °C for two hours. When cooled down to under 100 °C, the furnace was opened and crucibles were placed in a desiccator until cooled to room temperature and weighed again. The total ash percent is calculated from the equation below [82]:

$$\%\, Ash = \frac{Weight_{crucible+sample\ after\ heating\ to\ 550\,^{\circ}C} - Weight_{empty\ crucible}}{Weight_{sample}} * 100$$

5.2 Determination of heavy metals

ICP-OES (inductively coupled plasma-optical emission spectrometry) was used to determine the composition of elements in dissolved samples. The element ions that are being measured are Al, Sb, As, Ba, Cd, Co, Cr, Cu, Fe, K, Mg, Mn, Mo, Na, Ni, Pb, Ag, Se, Ti, Zn, P, Sr, V, Tl and Ca. This analysis was also done in triplicate. Samples were dissolved before analyzing in ICP-OES. 1 g of the homogenized dried sample was weighed in each of three autoclave bottles and 20 mL of 7M nitric acid was added. The bottles were autoclaved for 30 minutes at 120 °C. After cooling down to room temperature, the samples are filtered through filter papers (VMR European Cat. No. 516-0285) with 8-12 µm hole size and transferred to a 50 mL volumetric flask and diluted with distilled water up to 50 mL. Samples were then analyzed using the PerkinElmer ICP-OES with a multi-element method that can analyze 27 metals including P and Sr. Every sample was analyzed in triplicates and the average result of these was used for further data handling. Some of the samples were further diluted 10 times and analyzed again because the concentration of these without further dilution was higher than the calibrated metal concentrations.

5.3 Carbon, hydrogen, nitrogen and sulfur elemental analysis

The CHNS elemental analyzer (Pekin Elmer 2400 series CHNS/O) can analyze the carbon, hydrogen, nitrogen and sulfur content in samples. The sample was analyzed as a dried sample where 2-10 mg sample is weighed on small tin capsules and analyzed on the elemental analyzer.

The basic principle behind the elemental analyzer is that, under the combustion process, at about 1000 °C, carbon is converted to carbon dioxide, hydrogen is converted to water, nitrogen to nitrogen gas or nitrogen oxides and sulfur is converted to sulfur dioxide. The machine needs a continuous flow of helium, nitrogen and oxygen gasses. The combustion products are then detected by the apparatus [83].

5.3.1 Protein calculations

The protein content will be calculated based on the nitrogen content. To do this, a nitrogen-to-protein conversion factor (NPCF) is needed. The NPCF which is used, is 6.25, as it is assumed that all proteins have a 16% content of nitrogen. The number is definitely not exact, but approximated [109], [110].

The used formula for the nitrogen to protein conversion is:

$$N \cdot NPCF = P$$

Where N= nitrogen content (%) in the dried sample

NPCF= nitrogen to protein conversion factor, 6.25

P= Protein content (%) in the dried sample.

5.4 Total carbohydrate determination

For the carbohydrate determination, three methods can be used, strong acid hydrolysis, weak acid hydrolysis and sugar determination using HPLC. The goal of the strong acid and weak acid hydrolysis methods is the same, but the procedure is different. In the first sample (sample E), all three methods were used, but as the weak acid hydrolysis had issues running on the HPLC, it was neglected, and only the two other methods were performed for the rest of the samples.

For the strong acid hydrolysis, 0.16 g dry biomass is weighed in 6, 60 mL glass tubes and 1.5 mL 72% H_2SO_4 was added to the tubes and 2 reference tubes. The tubes were incubated in a water bath at 30 °C for 60 minutes. Then the tubes were placed in an ice bath and 42 mL Millipore water was added to each tube. 1 mL SPIKE 1 sugar was added to 2 of the samples and 1 mL of SPIKE 2 sugars were added to 2 of the samples. The SPIKE 1 is a 30 g/L sugar solution that contains 3 g of D-xylose, 3 g of L-

arabinose and 3.30 g of D-glucose-monohydrate diluted with water to 100 mL. SPIKE 2 is also a 30 g/L sugar solution that contains 3 g of D-xylose, 3 g of galactose, 3 g of mannose and 3.30 g of D-glucose-monohydrate, also diluted with water to 100 mL. The tubes were autoclaved at 121 °C for 60 minutes to let the waste sample release its content of sugars. When samples were cooled to room temperature, they were filtered in two ways. The first two samples were filtered with vacuum suction through pre-weighed dry ashed crucible (crucibles were in a muffle furnace for 4 hours and then stored in a desiccator until use) and the rest of the samples were filtered with a paper filter (8-12 µm). After filtering, samples were stored in falcon tubes and put in a freezer until the next step. The next step is divided into two parts, sample preparations for spike 1 and spike 2. For the SPIKE 1, 0.50 g $Ba(OH)_2.8H_2O$ is weighed in 15 mL falcon tubes and 5 mL hydrolysate was added. Tubes were vortex mixed and centrifuged at 4000 rpm for 5 minutes. The pH should be 2-3, if not, drops of either 0.1 M H_2SO_4 or 1 M NaOH were added. 1.5 mL supernatant was filtered into the HPLC vials and analyzed with an Aminex HPX-87H column [84].

For the SPIKE 2, 0.40 g $CaCO_3$ was weighed in 50 mL falcon tubes and 5 mL hydrolysate was added. After 5 minutes, tubes were mixed by inversion, this was repeated until no foams were observed. The tubes were centrifuged at 4000 rpm for 5 minutes. 0.2 g Ion exchanger (Dowex MR-3 (Sigma-Aldrich)) were weighed in 15 mL falcon tubes and washed with water twice. The ion exchanger is used to remove cat- and anions from the sample. 2 mL Hydrolysates from the 50 mL centrifuged falcon tubes were added to the ion exchanger and pH was corrected to be around 5.5, as earlier mentioned. 1 mL supernatant was filtered to HPLC vials and analyzed in lead column BioRad Aminex 87P [84].

The concentration of sugars is calculated as g/100 g of dry matter and entered in the two formulas below to find the corrected amount of sugar [84]. R_f is the retention factor for each sugar, that is, the distance traveled by the sugar compound divided by the distance traveled by the solvent [85].

$$R_f = \frac{C_{h+s\ (measured)}}{C_{s(added)} + C_{h(measured)}}$$

$C_{h+s\ (measured)}$: Sugar in acid hydrolysate with standard addition (g/100 g DM)

$C_{s(added)}$: Sugar standard added (g/100 g DM)

$C_{h(measured)}$: Sugar in acid hydrolysate without standard addition (g/100 g DM)

$$C_{corr} = \frac{C_{h(measured)}}{R_f}$$

C_{corr}: Corrected amount of sugar

To calculate the Klason lignin, the crucibles with filtrate were ashed at 550 °C for 3 hours and left in a desiccator to cool to room temperature and weighed again [84].

5.4.1 Carbohydrate determination by weak acid hydrolysis

This analysis has the same goal as the strong acid hydrolysis, to determine the total carbohydrate content in the sample, but its process is shorter. This analysis is also done in triplicate. 1 mg of dried sample is weighed in each of three 50 mL volumetric flasks, and the exact weight is noted, and the flasks were filled with demineralized water up to 50 mL. Then, 10 mL of waste juice was added to each of the 6 glass tubes. 10 mL of 8% H_2SO_4 was added to the 6 tubes with waste juice and 3 reference tubes. SPIKE 1 was added to 3 of the tubes with the sample and one of the reference tubes. The glass tubes were autoclaved and filtered into 9 HPLC vials and 9 50 mL falcon tubes and stored in the freezer until analysis [86].

5.4.2 Direct sugar determination by HPLC

The sugar content of maltose, glucose, galactose and fructose were analyzed using the HPLC, lead column BioRad Aminex 87P. The preparation of this analysis was to centrifuge the food waste media in a mini centrifuge, then take the liquid part and filter it with 0.22 µm syringe filters into HPLC vials. Samples were analyzed and the results obtained only tell about the sugar content in the liquid part of the sample.

5.5 Optimization of fermentation and lipid extraction

Several experiments will be done before the SSF, to be sure that the yeast will work efficiently and produce the highest lipid amount possible on the waste media. The most effective method of lipid extraction will be determined also. All experiments in this section were done in triplicates and the shaking incubator used for the fermentation was set to 150 RPM and 30 °C. All fermentations were dried and lipids were extracted with soxhlet extraction.

5.5.1 Growing yeast on YPD media

The first fermentation experiment that was done, had the goal to check the activity of the yeast and to see if it can accumulate lipids. The yeast was activated by streaking it on new YPD agar plates and incubating it at 30 °C for 48 h. After 48 h, one yeast colony was put together with 35 mL liquid YPD medium containing 20g/L peptone, 10g/L yeast extract and 20g/L glucose in 50 mL centrifuge tubes

and incubated at 30 °C for 48 h in a shaking incubator with 150 rpm. One centrifuge tube was done for each fermentation flask. The substrate used here was 50 mL liquid YPD media with 8% glucose, which is more sugar than the conventional YPD media, which only contains 2% glucose. The extra sugar was added to give the yeast the best circumstances to grow and accumulate lipids. The Erlenmeyer flasks were incubated in a shaking incubator for 7 days.

5.5.2 Fermentation without enzymes

The next experiment was to make the fermentation without the enzymatic hydrolysis step, to see if the enzymes are actually needed. 50 mL of waste was blended in an Erlenmeyer flask with precultured yeast, that is the prepared yeast explained in section 5.5.1 and incubated in a shaking incubator for 5 days.

5.5.3 Enzymatic Hydrolysis

To check the enzymatic behavior, that is, if the enzymes can convert the starch in the waste to fermentable sugars. Waste and enzymes were blended in Erlenmeyer flasks and incubated at 30° C for 7 days. The sugar content was measured with HPLC at the start and end of the experiment.

The enzymes used here and in all the SSFs made in this project is an enzyme mix containing cellulase (320 µL), amylase (320 µL), protease (65 µL), hemicellulase (65 µL) and pectate lyase (65 µL). This will be referred to as the enzyme mix further in the report.

5.5.4 Lipid extraction methods

Three lipid extraction methods were tried to choose the one that results in the biggest amount of lipids. The first was the conventional soxhlet method, the second was soxtherm and the third was the Ultrasonic Assisted Extraction (UAE) method.

The soxtherm innovation is 4 times faster than the traditional technique and can extract 4 samples at one time [111]. 150 mL of hexane was used for each extraction beaker and the program was set to run for 1,5 h. This extraction process is very similar to that of the conventional extraction method.

The Ultrasonic Assisted Extraction method was done using the Q700 Sonicator with power up to 700 W. Hexane was used as the solvent. Hexane and the dried sample were put together in a beaker. The ultrasound probe was directly immersed into the beaker. When the low-frequency and high-power ultrasound waves are in contact with the sample, the waves create cycles with both high- and low pressure, and because of the alternating high and low-pressure cycles, acoustic (ultrasonic) cavitation

happens. The acoustic cavitation results in high temperatures, pressures and shear forces, which leads to the formation of vacation bubbles. The bubbles create collisions between the particles inside the media, and the yeast cells disrupt, releasing the lipids [112], [113]. The temperature was checked with a thermometer during the extraction process, and should not exceed the boiling point of hexane (69 °C). The extraction was run twice, each run lasted 30 min. and the break between the two runs was about 20 minutes and was necessary to cool down the device.

5.6 Simultaneous saccharification and fermentation (SSF)

The yeast that was used is *C. oleaginosus* ATCC 20509. The waste media were autoclaved, and the waste media from the energy department were blended with water so the ratio of waste/water was 50/50. The waste from Ragn-Sells was not added water, because it already had about 14% dry mass, which is half the dry mass of the waste from the energy department. The yeast was activated as described in section 5.5.1. After two days of incubation of the yeast in liquid YPD media, the SSF experiments were started by mixing 50 mL of the autoclaved waste media in 250 mL Erlenmeyer flasks, with the enzymes and yeast. The yeast tubes were centrifuged at 4000 rpm for 5 minutes and the liquid YPD media was poured out and the yeast cells were resuspended with 1 mL of autoclaved water and added to the fermentation flasks. The flasks were incubated in a shaking incubator for 7 days at 30 °C and 150 rpm.

5.7 Lipid extraction

For the lipid extraction, the Soxhlet extraction method was used. Lipid extraction was done for both the dried waste sample and the dried fermentation broth, to calculate how many lipids the yeast produces.

For the dried waste sample, 5 g of dried sample was weighed in an extraction thimble which was dried and kept in a desiccator. The round bottom bottles were also weighed. 200 mL hexane was added to each round bottom bottle and the extraction was run for four hours starting from the boiling time. After the extraction, hexane was removed with a rotating evaporator and stored in the bottle for reuse. The lipid extraction for the waste was done in triplicate. For the dried fermentation broth, the lipid extraction was done once for each fermentation broth.

5.8 FAME analysis

The composition of the lipids, both the waste lipid and lipids produced by the yeast after SSF, was determined using the FAME (fatty acid methyl ester) analysis. In this method, the triglycerides,

phospholipids and free fatty acids were converted to fatty acid methyl esters (FAME) and the fatty acid methyl esters were analyzed with GC-MS.

The preparation of the sample was begun by adding 1 mL of 0.5 M methanolic sodium hydroxide to transesterfy the glycerol-bound fatty acids to methyl esters. The tubes were heated for 5 minutes at 90 ºC. 1 mL of boron trifluoride-reagent and 0.5 mL hydroquinone-solution were added to the tubes to methylate hydrolytic free fatty acids. The tubes were heated again, and 4 mL saturated sodium chloride solution and 3 mL n-heptane were added to the tubes. After a few minutes, face separation happened, and about 1.5 mL of the top phase was transferred to GC-MS vials and analyzed.

5.9 Principal Component analysis

Principal Component Analysis (PCA) was used to explore the data. For the PCA, data was constructed as a matrix with rows and columns, where the rows contain the samples and the columns are the variables analyzed. The idea of the PCA is to get imaginary variables (latent variables) that describe the variation of the data by reducing the data dimensionality without reducing the quality. If we don't make PCA and we have 32 variables, then we have 32(32-1)/2=496 combinations of variables, and it's almost impossible to compare this number of variable combinations. In PCA, data is split into structure and noise, where the structure is the data we capture and analyze, and the noise is the less important data that will remain unexplained, and it's only a small part of all the data. The latent variables which will be found, are variables that describe most of the variance, that is, the first latent variable will describe the biggest data spread, and the next latent variable will be orthogonal to the first one, and capture the second biggest variation of the data.

To detect systematic patterns in the sample variation and relate the patterns to specific variables and their interactions, scores and loadings plots were produced when doing the PCA. The loadings plot shows the correlation between the variables, and the scores plot illustrates how the samples are related to each other. Variables, that are close to each other are positively correlated to each other, and variables that are opposite to each other, have negative correlations. The importance of the variables on the principal components is seen in the distance to the origin, if we have the first principal component as the y-axis and the second principal component as the x-axis, then the variables lying away from the origin close to the x-axis have high influence on the first principal component. Variables lying close to the origin, have no or very little influence on the principal component.

Preparation of the data

The data were prepared on a data sheet with 14 rows (samples) and 32 columns (variables).

For the chemometrics data, the total solids and moisture content for the E-sample were changed, because in the SSF, the E-waste media was kind of solid, and 50 % of water was added to the waste media, before autoclaving. For the December waste, there is only one measurement in the data for the PCA, because of the lack of waste for SSF, but all the measurements for the sample were done for three subsamples, except for SSF which only was done for one December sample, in triplicate.

As the different variables have different units, and it is not realistic to compare variables with different units, then we need to standardize the variables.

5.10 Linear regression analysis

The linear regression method, partial least squares regression (PLS) will be used to find the potential effects of variables on the lipid accumulation in yeast. The idea of the PLS is similar to that of PCA where data are decomposed with the use of latent variables. For the PLS model, predictors and response values are used. The predictors are all the variables excluding "Lipid accumulated in yeast" and the response values are the variable which will be analyzed, lipid accumulated in yeast. For the PLS model, a predicted vs. measured plot will be produced, and it shows how comparable the calibration line (predicted vs. measured data) is to the cross-validation (cv). The cross-validation tells about how good the predictions are, if the cv line follows the calibration line, then the predictions are pretty good. The summary of the PLS model shows four important values for the calibration curve, which are the coefficient of determination (R^2), root mean squared error (RMSE), Slope and Bias. The R^2 value is how much y-variance the model explains and takes into account both systematic and random errors. If we have no errors, the R^2 value will be 1. The root mean squared error (RMSE) estimates both systematic and random errors and should be as close to 0 as possible. The slope for the calibration line tells if there is a systematic error in the predictions, the slope for the calibration line should be as close to one as possible if the predictions are good. These systematic errors depend mainly on the measured y value (reference). Another type of systematic error is Bias, and this is the value for the average error of predictions.

6 Results & discussion

The following section shows the results obtained by the analysis done in the project. All measurements were done in triplicate unless otherwise stated. Error bars are shown for each sample and demonstrate the standard deviation of three measurements.

6.1 Total solids, moisture and ash content

The total solids and moisture content was found using the drying method, for all the samples. The data obtained from this experiment are seen in the column chart below (Figure 17).

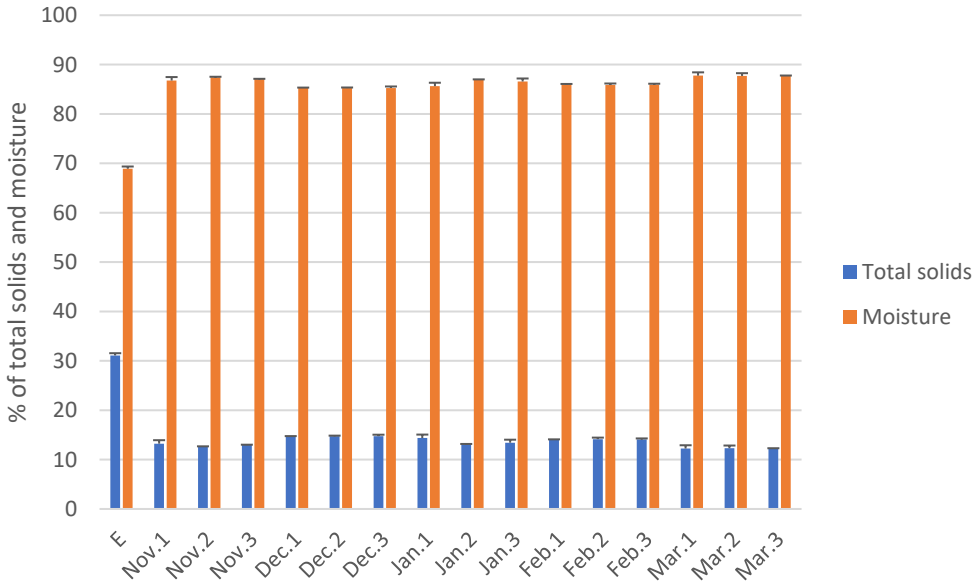

Figure 17. Total solids and moisture content with error bars indicating standard deviations.

The total solids percentage is between 10 and 15% for the samples from Ragn-Sells, and for the sample from the energy section(E-waste), the total solids constituted 30%. The moisture content was between 85 and 90 % for the Ragn-Sells waste, and around 70% for the E-waste. The waste's total solids/moisture for the different months from Ragn-Sells were very close to each other, and the pre-treatment done for the waste hides the weather effect on the moisture content of the food waste. It can also clearly be seen visually, cf. Figure 18 and Figure 19, that the food waste from RagnSells contains more moisture. From the literature review (Figure 7 and Table 2), the moisture content varies between 37 and 56 % and the total solids lie between 6-44%. The total solids from this analysis lie within the range found in the literature study, whereas the moisture content is found to be higher. The moisture content of the food waste varies a lot, because it is pretreated before analyzing (blended, shredded, water added, etc.), and the treatment process varies from one another.

Figure 18. Food waste from energy department.

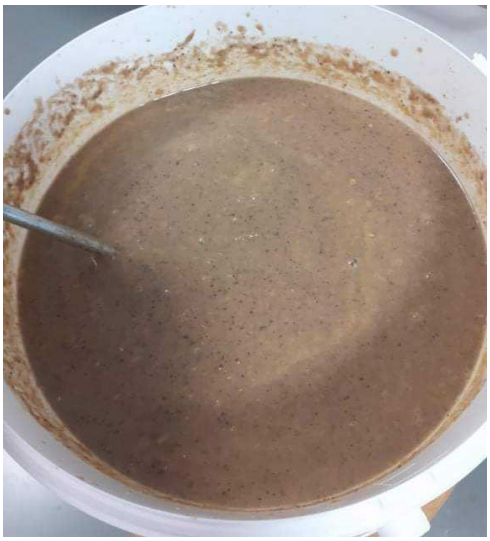

Figure 19. Food waste from RagnSells

The ashing analysis was done using the muffle furnace. The results obtained are seen in Figure 20. The ash content is between 4-9% of the dried samples and the volatile solids (VS) are between 90-98 % of the total solids (TS). Comparing the obtained data with the data from the literature study (cf. Figure 7), where the VS was in the range of 78-96% from the TS, both the data obtained in this study and the data obtained by the other studies, are close to each other. When obtained data from own analysis are close to the data obtained by others, one can suppose that the analysis is correctly conducted.

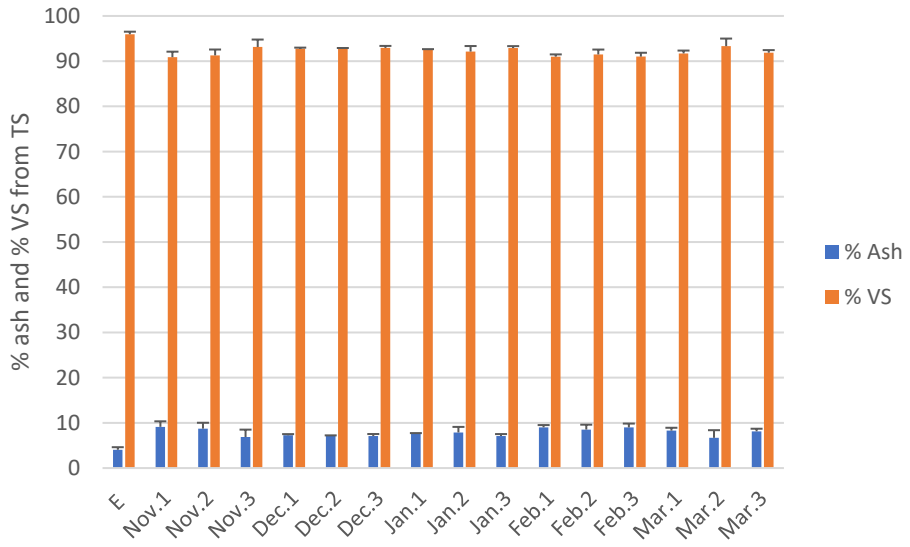

Figure 20. Results for the ashing analysis.

6.2 Content of metal ions in food waste samples

The heavy metal ions content together with phosphorus content were analyzed using the ICP-OES. The results obtained from the ICP-OES analysis were converted from mg/L to % of DW and are visualized in Figure 21. Concentrations less than 0.01 mg/g or 0.001 % DW were excluded from the results.

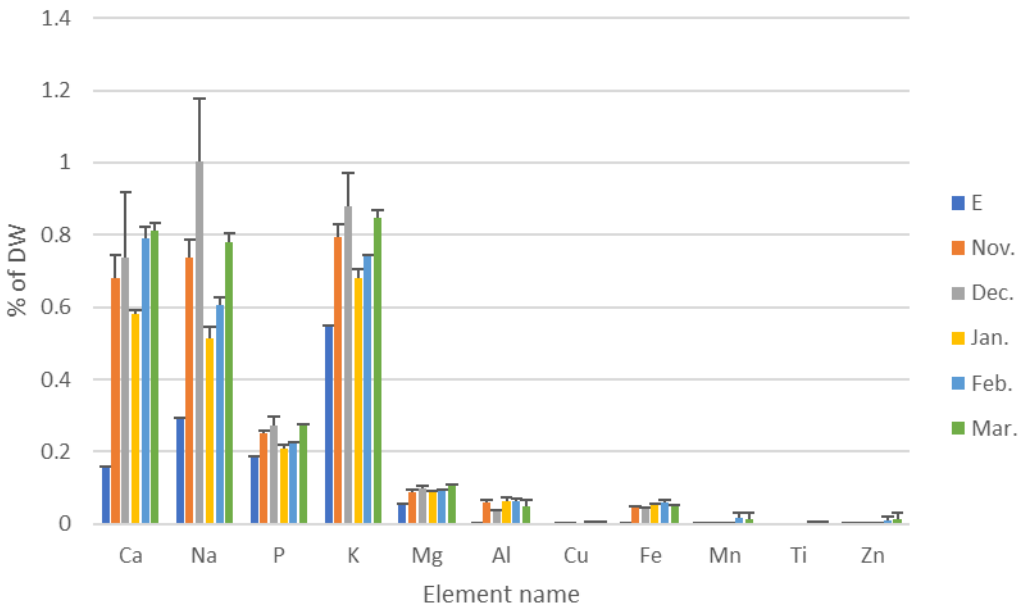

Figure 21. ICP-OES results with standard deviations.

The results obtained from the ICP-OES analysis show that the concentrations of the metals and Phosphorus are close to each other for the waste from Ragn-Sells and lower for the E-waste compared to Ragn-Sells waste. The Ca content is in the range of 0.15-0.8 % DW, and in the literature study it is between 0.7-1.5 %, which is higher than the obtained average. The phosphorus content lies in the range between 0.2-0.3 % of DW which is 2-3 g/kg TS. This is close to the result from the literature study, cf. Figure 6, which is 2.5-9 g/kg TS. The natrium amount lies in the range 0.2-1 % and 0.4-0.6 % for the experimental analysis and the literature study, respectively, which gives a similar overall Na range. The potassium content lies in the range between 0.5-0.9 % of the DW (5-9 g/kg TS) and has a similar content of 8-15 g/kg TS in the literature review. The potassium content of the waste from Portugal (Figure 6) is however much higher because the waste was pre-treated and was ready for anaerobic digestion. The other metal's contents are less than 1 % and comparable to those from Table 3 which are between 0-1.5% of the DW samples.

As mentioned in the literature study, Zn can have a toxic effect on the yeast, if it exceeds 0.6 mg/L or if it is depleted (section 2), hence it can also lead to a decrease in lipid accumulation. The Zn content has a range of 0.001 -0.1 % DW, and by calculating that to mg/L (appendix 9.1) it gives a range of 1.4 -14 mg/L and this can give the yeast a toxic effect (section 2). The high standard deviations, for example, the one seen on Na for dec. waste can be due to uncertainties in the experimental execution, i.e., a little more or less water than needed was added in the volumetric flask to dilute the nitric acid.

6.3 Carbon, hydrogen, nitrogen and sulfur contents in food waste

The carbon, hydrogen, nitrogen and sulfur (CHNS) contents in the waste were determined for the food waste samples using the elemental analyzer. The results of the CHNS elemental analysis can be seen in Figure 22.

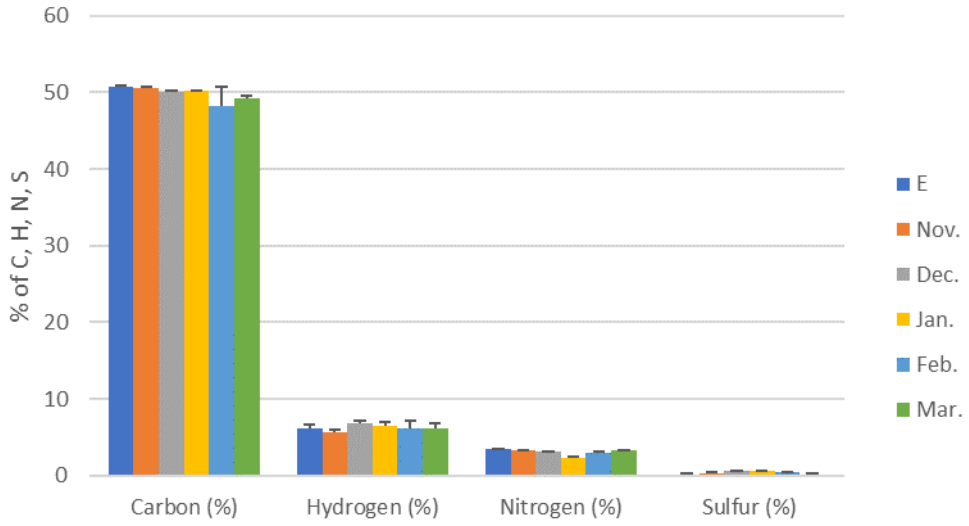

Figure 22. Results for the elementary analysis.

From the bar chart above, it is conspicuous that all the samples have a very similar amount of carbon, hydrogen, nitrogen and sulfur. The error bars which show the standard deviations are also very low, indicating that the obtained results are reliable. From the literature study in Figure 6, the nitrogen, hydrogen and sulfur contents in the waste are 2.5-6 %, 0-10% and 0-1 % respectively, whereas the carbon content (Figure 7), has a range between 45-44% of the DW. The corresponding content of carbon, hydrogen, nitrogen and sulfur, in the collected waste, cf. Figure 22, are 48-51%, 5-7%, 2-4% and 0-1%, respectively. Both data, the ones from the literature study and the ones from the conducted experiment, are similar.

According to Figure 22, the C/N ratio is 50/5=10/1. The C/N ratio in the literature study in Table 1 that resulted in the highest amount of accumulated lipids in *C. oleaginosus* was 35.5 (Table 1), which means that the C/N ratio of 10 for this current study´s experiment is not optimal. The C/N ratio in the SSF experiments will not have the exact same C/N ratio as the dried waste but will be similar to it, as the water also contains small quantities of nitrogen. Adjusting the C/N ratio is one of the most important parameters when the goal is lipid accumulation in yeasts. This can be done by adding a carbon source or a nitrogen source. As mentioned in section 2.2, a higher C/N ratio will result in a higher lipid accumulation, and hence, a carbon source may be added. The carbon source can be acetate, as it showed to result in a high amount (23.6%) of stearic acid (C18:0) which is useful for jet fuel production (section 1.4).

The protein content was calculated from the achieved nitrogen content. Results can be seen in Figure 23.

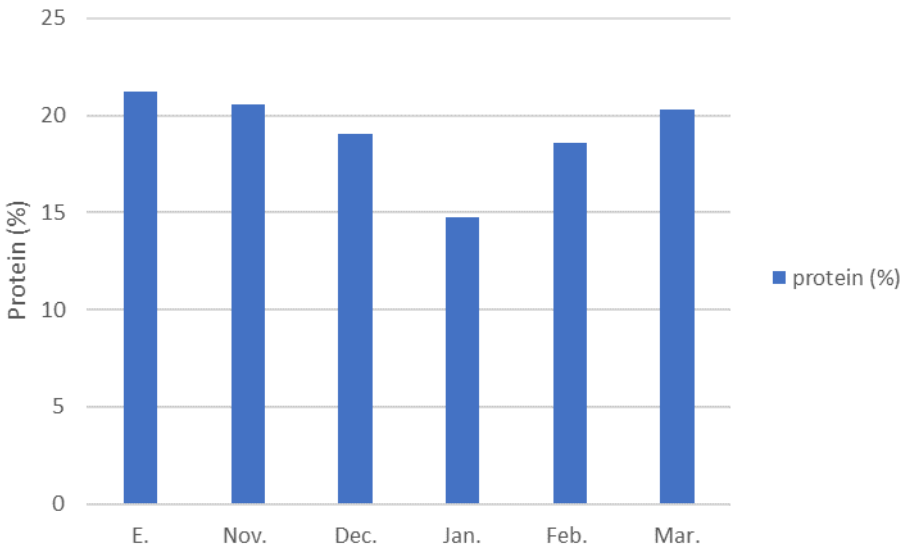

Figure 23. Protein content, given as % protein of DW sample.

The protein content is between 14-21% of the DW (Figure 23), and in the literature study, it has an average of 150-200 g kg^{-1} VS. The waste from Emirates had a much lower degree of crude protein and the waste from the digester in Lisbon had a higher content at about 500 g kg^{-1} VS. Converting the value 14-21% of DW, to g kg^{-1} VS, gives 133-199.5 g kg^{-1} VS, based on the calculations below, where 0.95 is the amount of VS per 1 unit TS. Both the calculated protein content and the one based on the literature review are comparable.

$$14\% \cdot 10\frac{g}{kg} \cdot 0.95 = 133 \text{ g kg}^{-1} \text{ VS}$$

$$21\% \cdot 10\frac{g}{kg} \cdot 0.95 = 199.5\ \mathrm{g\ kg^{-1}\ VS}$$

This method of calculating the protein content may not be the most accurate, as it assumes that all proteins contain 16% of nitrogen [109], and this is certainly not true, but it is the most simple method that doesn't contain as many possibilities for analytical errors as the Total Kjeldahl Nitrogen analysis.

6.4 Results for total carbohydrates

The total carbohydrates for all the samples were measured using the HPLC with two methods, strong acid hydrolysis (SAH) and mixed carb. method. The third method was weak acid hydrolysis (WAH), which was only used for the E-sample. The results in this part are divided into four parts, the first part is the comparison of the weak acid hydrolysis and strong acid hydrolysis for the E-sample. The second part is the SAH with SPIKE 1, and the third part will explain the SAH with SPIKE 2. The last results shown in this part are for the mixed carb. method.

Figure 24 presents the results of SAH and WAH for the E. waste sample, both with SPIKE 1 sugar. A t-test (appendices 9.2) was done to be sure that the visual difference can be seen statistically. There is a significant difference in the glucose amount and the total amount, and this may be due to inaccuracy in the methods, or non-homogeneity in the sample.

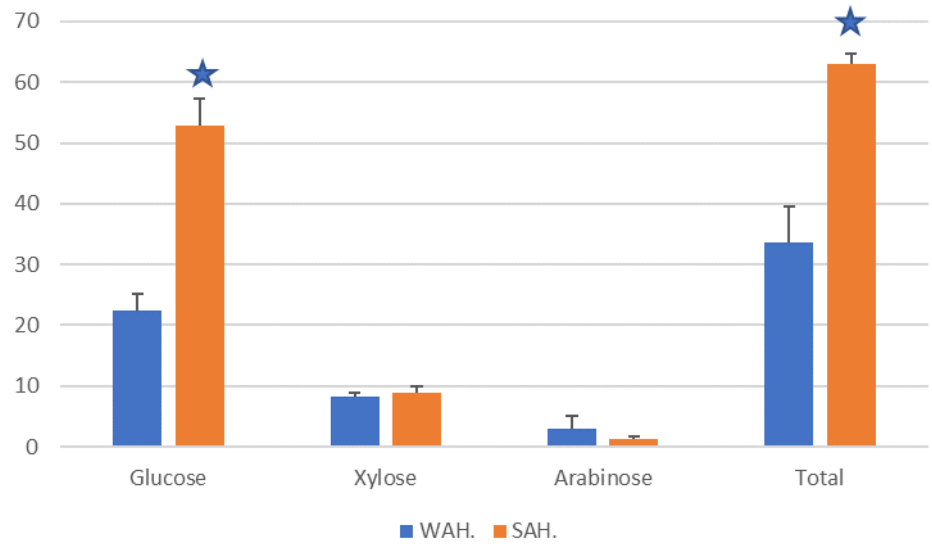

Figure 24. Comparison of the results of weak acid hydrolysis (WAH) and Strong acid hydrolysis (SAH) for the E. waste. A column marked with a star means that it has a significant difference from its corresponding column for the WAH. It is seen that there is a significant difference between the two methods regarding the glucose amount and the total sugar amount.

The strong acid hydrolysis (SAH) was done in two methods, and for each method, SPIKE 1 or SPIKE 2 sugar solutions, were used, as described in the Materials and methods section. The difference between

SPIKE 1 and SPIKE 2 sugars is that SPIKE 1 contains glucose, xylose and arabinose and we can measure those sugars in HPLC when using SPIKE 1. Whereas when using the sugar solution SPIKE 2, one can measure glucose, xylose, galactose and mannose. It can be seen in Figure 25 and Figure 26 that the results deviate from SPIKE 1 method to SPIKE 2 method, for example, the glucose amount for Dec. 1 sample is around 70 g/100 g DM in SPIKE 1 and 25 g/100 g DM. As seen in all the results for SAH, the glucose amount is higher than xylose, arabinose, fructose, galactose and mannose. Some of the results, for example, the December samples in Figure 25 contain 50-70% glucose of the DM, and that is too much when compared to Table 2, where the highest amount of fermentable waste is around 23 % of the DM. Although the results for the SPIKE 2 have more uncertainties, and higher standard deviations, than SPIKE 1 results, the results for SPIKE 2 look more reliable, as it is closer to those from the literature study. Thus, for the chemometrics part of the project, the glucose will be used for SPIKE 2 method, whereas xylose+fructose and arabinose will be taken from the SPIKE 1, and xylose, galactose and mannose will be taken from SPIKE 2.

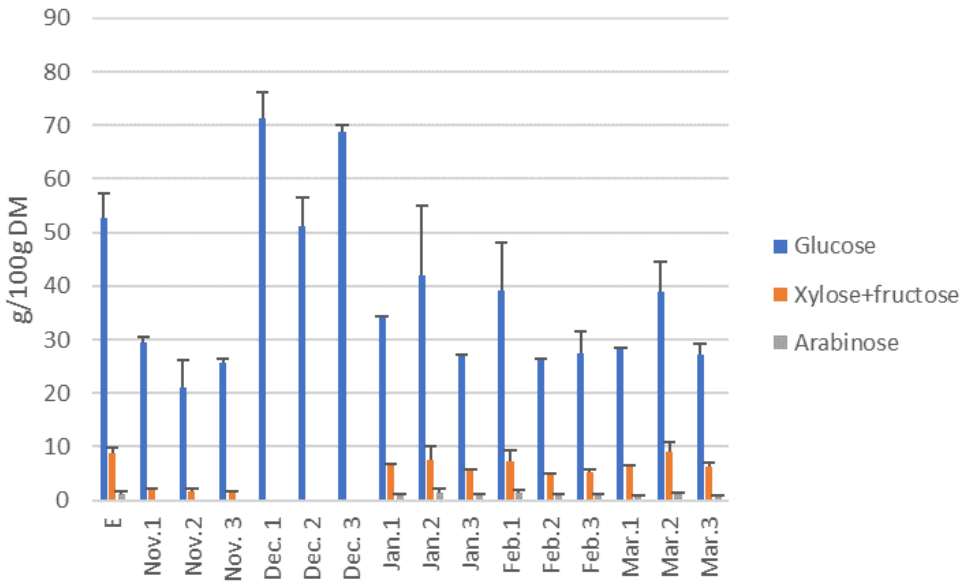

Figure 25. Strong acid hydrolysis results, SPIKE 1

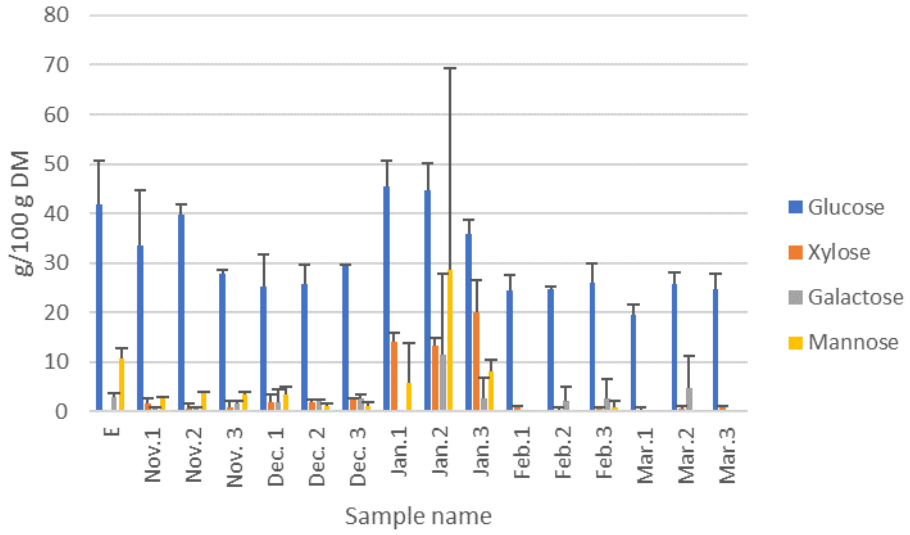

Figure 26. Strong acid hydrolysis results, SPIKE 2

The mixed carb. analysis was also conducted using the HPLC, but no pre-treatments were needed here, only to filter the supernatant from the food waste, and analyze it. The results (Figure 27), show a high amount of fructose, followed by maltose and glucose, whereas the galactose amount is only in the range of 0-1 g/L. The sugar amounts found in the supernatant are different from the sugar amounts found in the dried mass, and therefore, both the results for the supernatant and the dry mass will be used further in the chemometrics part.

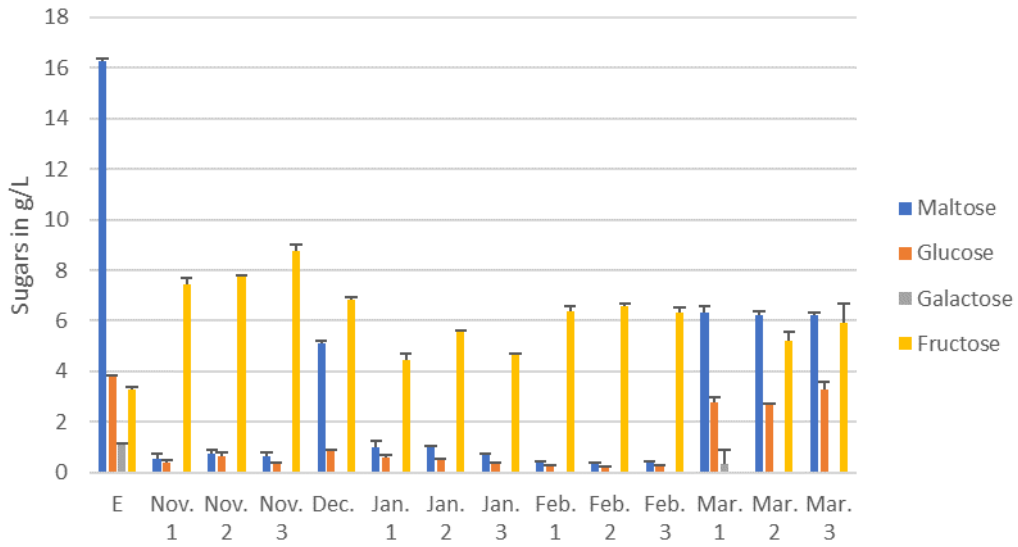

Figure 27. Sugar analysis with mixed carb. method.

The Klason lignin experiment, which was done for the first 3 collected samples, showed that no Klason lignin is found in the biomass.

The big difference in the SPIKE 1 and SPIKE 2 results and the high standard deviations may be due to the handling of many samples simultaneously. The samples should be placed in an ice bath directly after the water bath, and after that, water should be added. The process of taking to samples from the water bath to the ice bath and adding the water, can't be done fast enough when dealing with over 20 samples at the same time. To overcome this limitation, fewer samples can be analyzed at the same time, or more hands can help. Other uncertainties may be in the weighing of the dried samples and the measurement of the amount of added acid and water. The SPIKE 1 and SPIKE 2 methods, were analyzed with two different HPLC machines, this can also be the reason for the differences between SPIKE 1 and SPIKE 2 results. The limitation in the mixed carb. method is that when the waste is not very homogeneous, the supernatant samples can have a difference in the sugar content. For both the E-waste and Ragn-Sells waste, the samples were not very homogenous, as they contained visible pieces of food debris in the waste, for example, tomatoes pieces or slimy remnants, and when only 2 mL supernatant is needed for the mix carb. analysis, variations in the sugar contents can occur. To overcome this limitation, the waste can be blended in a blender before use.

6.5 Optimization of lipid production

Five experiments for the optimization of the fermentation and the lipid extraction were done, before starting the fermentation with *C. oleaginous*. The first experiment was to grow the yeast only on liquid YPD media, to see if it can accumulate lipids. The result for the lipid accumulation for the yeast grown on YPD media showed an average of 12.97 % lipids with a standard deviation of 3.6. The high standard deviation can be due to different levels in the yeast activity, that is the lipid accumulation ability and cell growth level, and/ or because no two yeast colonies have the exact same amount of yeast cells. As the yeast does accumulate lipids, the other optimization experiments can be performed.

The second experiment was to check if the yeast can grow on the waste only, without prior enzymatic hydrolysis. In Figure 28, it is seen that there is no difference in the lipid content before the fermentation with the yeast and after. A t-test (Appendix 9.3) is made to be sure that there is no significant difference between the two sets of measurements, and the p-value for the t-test showed 0.95, that is, there is no a significant difference, which means that the yeast can not accumulate lipids based only on the food waste as substrate. Therefore, enzymes will be added and SSF will be done instead.

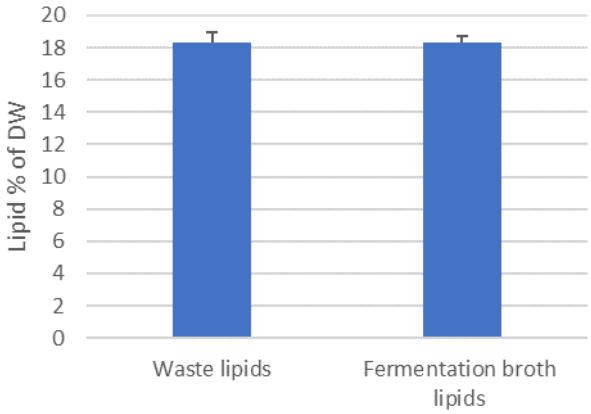

Figure 28. Lipid content in the yeast before and after the fermentation for 5 days.

The third experiment was to make enzymatic hydrolysis on the waste to see if the enzymes can convert the starch in the waste to fermentable sugars. The results for the waste and enzyme media (Figure 29) were promising and showed a clearly higher percentage of sugars when enzymes were mixed with the waste media. From this experiment, it can be concluded that the enzymes are doing their work by converting starch to glucose, and the enzymes can be used for the SSF.

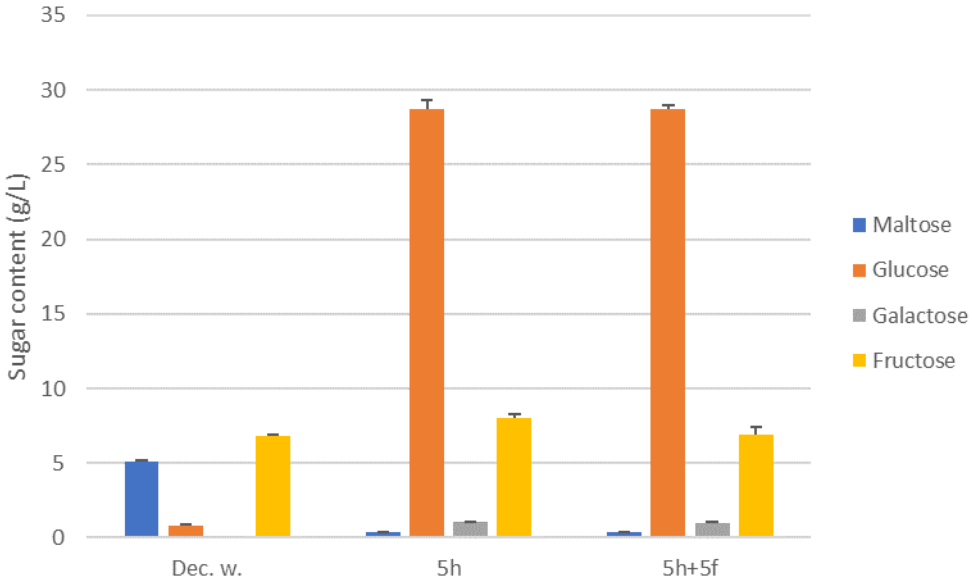

Figure 29. Sugar content before enzymatic hydrolysis for December waste and after 5 days of enzymatic hydrolysis.

The fourth and last optimization experiments are the optimizations for the lipid extraction method. All the lipid extractions here were done for the December sample waste. From Figure 30 it can be seen that the extraction with the conventional soxhlet extraction method gave a higher lipid content than the soxtherm and UAE. ANOVA (Appendix 9.4) is used to check if there is a significant difference

between the three methods, and the p-value for the ANOVA test showed 0.00177, which means, that at least one group has a significantly different mean value than the two others. To find out which one of the methods has a significant difference, the Tukey test is performed (Table 6 and Appendix 9.4) The Tukey test showed that there is a significant difference when comparing soxhlet with UAE and soxtherm. It can then be concluded that the conventional soxhlet is better in extracting lipids, and therefore will be used further in the project work.

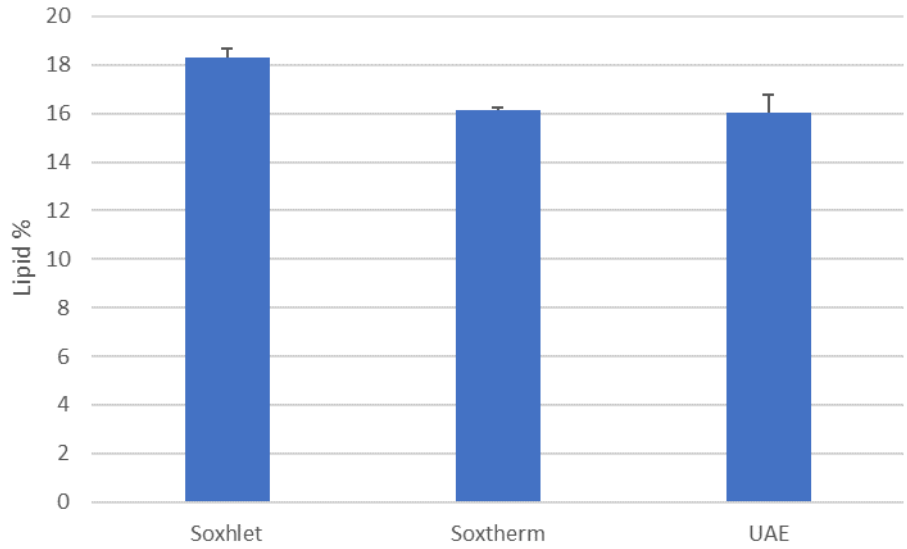

Figure 30. Lipid extraction with soxhlet, soxtherm and UAE methods, the same waste sample was used for all three methods.

Table 6. P-values for the Tukey-test

Groups	P-value
Soxtherm - Soxhlet	0.0033
UAE-Soxhlet	0.0028
UAE-Soxtherm	0.9836

The three extraction methods can be optimized further to decrease the cost, increase productivity and make the processes more time-efficient. The conventional soxhlet method can be experimented with running for less time than 4 hours, or with other solvents than hexane. Other solvents can also be tried with the soxtherm and UAE methods. The soxtherm program settings/durations can be changed and investigated further, as no previous studies investigated the difference in the amount of extracted lipids when the program settings were changed.

It is worth mentioning that the yeast, that has been stored in the fridge long time (more than one week), was contaminated, and had problems with accumulating lipids when fermented in waste media, but could accumulate lipids with no problems when fermented in YPD media. So, to be sure that

the yeast is not contaminated, the yeast should be streaked in the agar directly from the frozen yeast, because the ones stored in the fridge may be easier contaminated. It is also better to streak new plates each time the yeast is needed, and not just incubate the same old plate in the incubator for activation.

The enzyme amounts used for the SSF can potentially be optimized by using fewer amounts of enzymes or just avoiding using some of them, and controlling the sugar amounts achieved when changing the enzymes doses, if, for example, the sugar amount is the same after enzymatic hydrolysis with and without the use of protease, it can just be omitted. No previous studies investigated the effect of proteases, pectate lyases and hemicellulases on the food waste enzymatic hydrolysis, but the amylases and cellulases were shown to convert starch and cellulose into simple sugars [114], [115].

6.6 Lipid content before and after the SSF

The lipid amount accumulated in the yeast *C. oleaginosus* was achieved by extracting the lipids from the dried waste and extracting the lipids after drying the SSF product. It is seen as the difference between the orange and blue columns in Figure 31. All the values for lipid amount after SSF are significantly higher than the lipid amount in waste, except for two, Jan. 1 and Jan. 2 samples, which have p-values of 0.06 and 0.12 for the t-test. The results for the t-test are seen in appendix 9.5. The columns for lipid after SSF, which are significantly higher than its corresponded waste column, are marked with a star. The highest lipid amount accumulated is about 10% and the lowest value is 3 % lipids of the yeast cell's dry weight, which is lower than the amount obtained in the literature study, cf. Table 1, where the accumulation percentage was 61% of the cell's dry weight, using batch mode. The most important factor, that affects the lipid accumulation in yeasts, is the substrate, and the substrate of clear nutrients (sugar) will obviously give higher lipid accumulation than the food waste substrate. From Table 5 it is seen that the highest lipid yield achieved with SSF and 15% substrate, is 8.01 g/100 g sugar, that is 1.2015 g lipid /100 g DM and this result is more comparable with the results achieved in Figure 31.

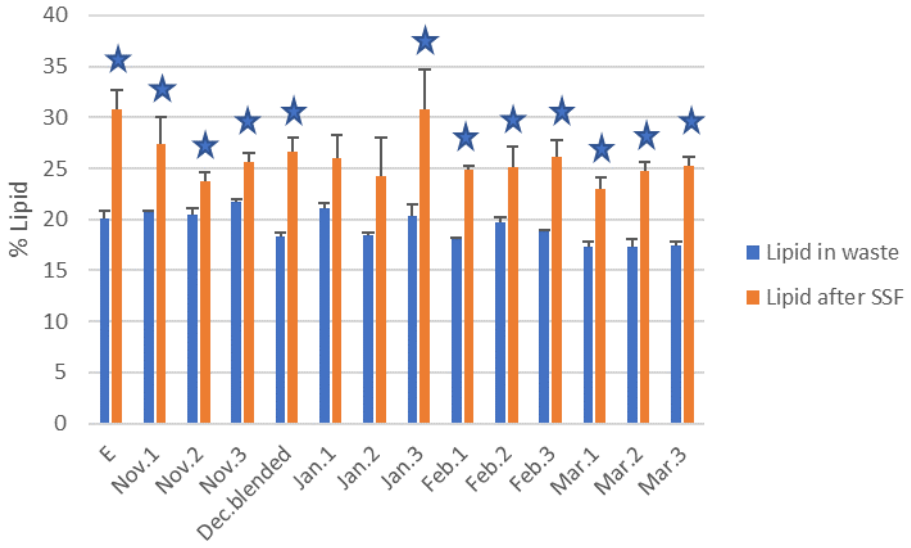

Figure 31. The difference in lipid % from the dried food waste and dried SSF product, columns with a ★ means they are significantly higher than the starting material.

One method that can be optimized here is the crushing of the dried SSF. The crushing by a hand mortar may not be as effective as the crushing by electric mortar, therefore, one uncertainty in the obtained lipid from the SSF product can be due to the crushing method.

Another uncertainty in the lipid extraction method is the evaporation of the hexane afterward. It was discovered that when letting the rotary evaporator run for more time than necessary, when all the hexane was evaporated, water droplets could be seen in the extracted oil.

6.7 Characterization of lipid profiles

The lipid profiles for the lipids obtained from the extraction were analyzed using the GC-MS, to see if there are any differences in the lipid profile for the dried waste lipid and the SSF product lipid. Figure 32 shows the lipid profile obtained for all the oil samples extracted from the waste and from the SSF product. Chromatograms for the lipid profiles of both the waste and SSF products can be seen in Appendix 9.6. For the waste lipids, the highest amount of fatty acids are found in the oleic acid form (C18:1), the second-highest is the myristic acid (C16:0), followed by linoleic acid (C18:2) and stearic acid (C18:0).

It can be seen from the overall view, that C16 increases after the SSF, and so do the C18 and C18:2. The lipid profile for lipids from different fermentation products, obtained in the literature study, Figure 4, contains high values of C18:1 and C16 compared to the other FAMEs, which is also the case in Figure 32. The lipid profile for all the waste samples looks similar, while the SSF lipid profiles have some deviations. That can, as mentioned earlier, be due to the yeast's quality and its reproduction methods.

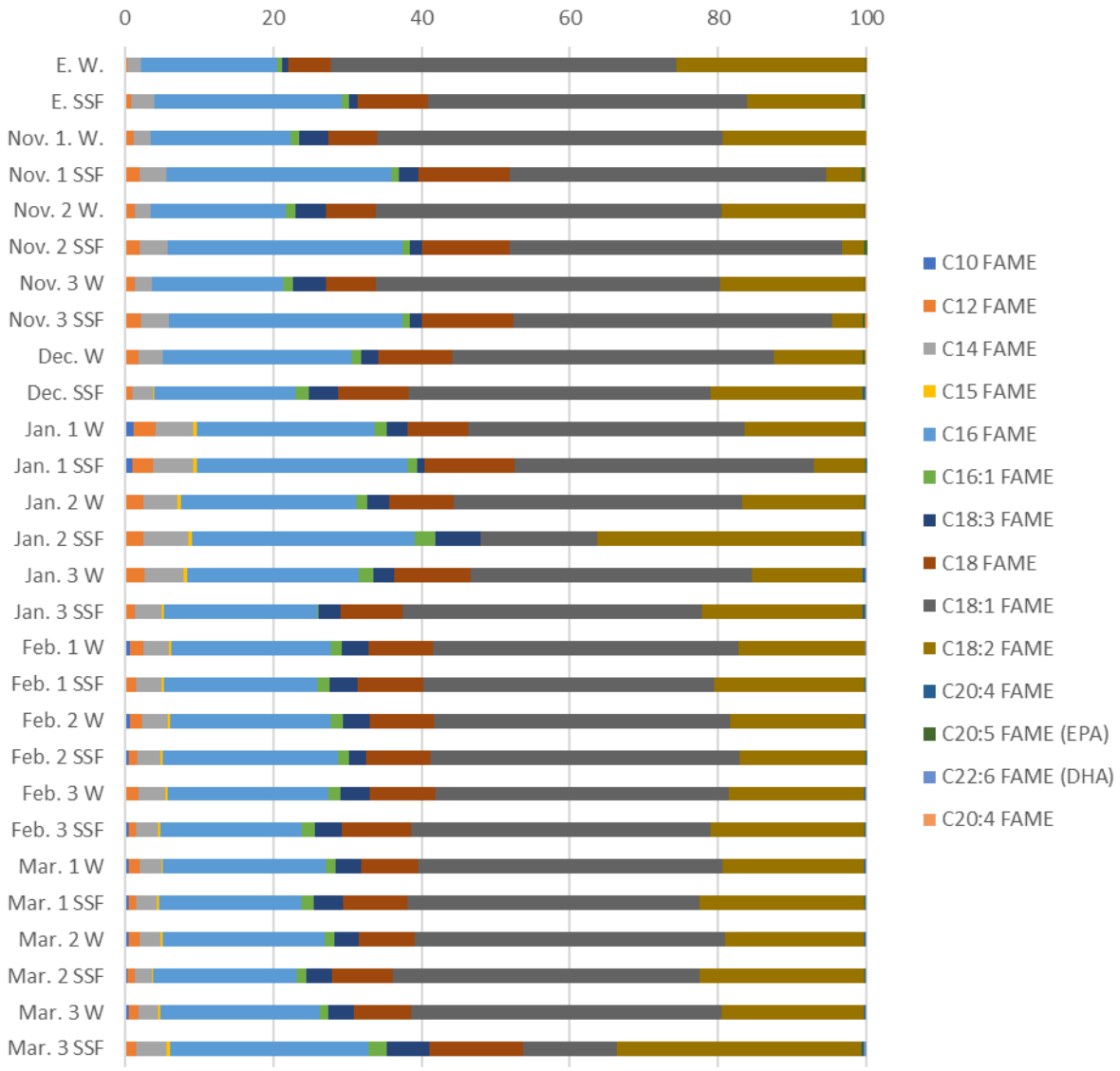

Figure 32. Lipid profile for lipids extracted from the dried waste (W) samples and dried SSF.

As the HEFA-SPK biofuels use the hydrogenation method to convert the unsaturated fatty acids to saturated fatty acids (section 1.1), the increase in the saturated C16 and C18 after the SSF, would be excellent for the HEFA-SPK process to reduce the hydrogenation step in the hydroprocessing. As mentioned in the literature study, the C/N ratio affects the lipid profile, therefore, measuring and adjusting the C/N ratios will help achieve high amounts of the preferrable saturated fatty acid (section 1.4). In Figure 4, the lipid profiles for the *C. oleaginosus* had the highest amount of C18 when fermented in media with acetate, therefore one can choose acetate instead of other carbon sources if the goal is bigger amounts of saturated fatty acids.

6.8 Exploratory analysis

After analyzing the waste material for its contents and completing the SSF and lipid extractions for the samples, the next step was data analysis, where the major goal was to find the correlations between the amount of lipid accumulated in the yeast and the amount of the different waste constituents. The data analysis consists of exploratory and regression methods. For the exploratory analysis, Principal Component Analysis (PCA) was applied.

As seen in Figure 33, the first principal component explains 32.58% of the total variations of data values and the second component explains 21.05 % of the variations. Variables, that are close to each other in the loading plot, are positively correlated, for example, Ca (%), Mg(%), and the moisture content make a cluster, and P(%), Mn (%), Ti(%), Cu(%) and Zn(%) also make a cluster and are positively correlated to each other. It's seen in the loadings plot, that the moisture content and the arabinose content have a negative correlation. S(%) has a negative correlation to N(%) and glucose (g/L) and this is illustrated in Figure 34. The amount of lipid in the waste has a negative correlation with Fe and the lipid accumulated in the yeast has a negative correlation with glucose (%TS), Mannose (%TS), lipid in waste, P(%) and Mn(%). The variables that have the most influence on principal component 1 are Ca (%), Mg (%), and K (%) contents, these are also the variables that mostly affect the variation between samples. For the second principal component, the most important variables are S (%), maltose (g/L), glucose (g/L), and N (%).

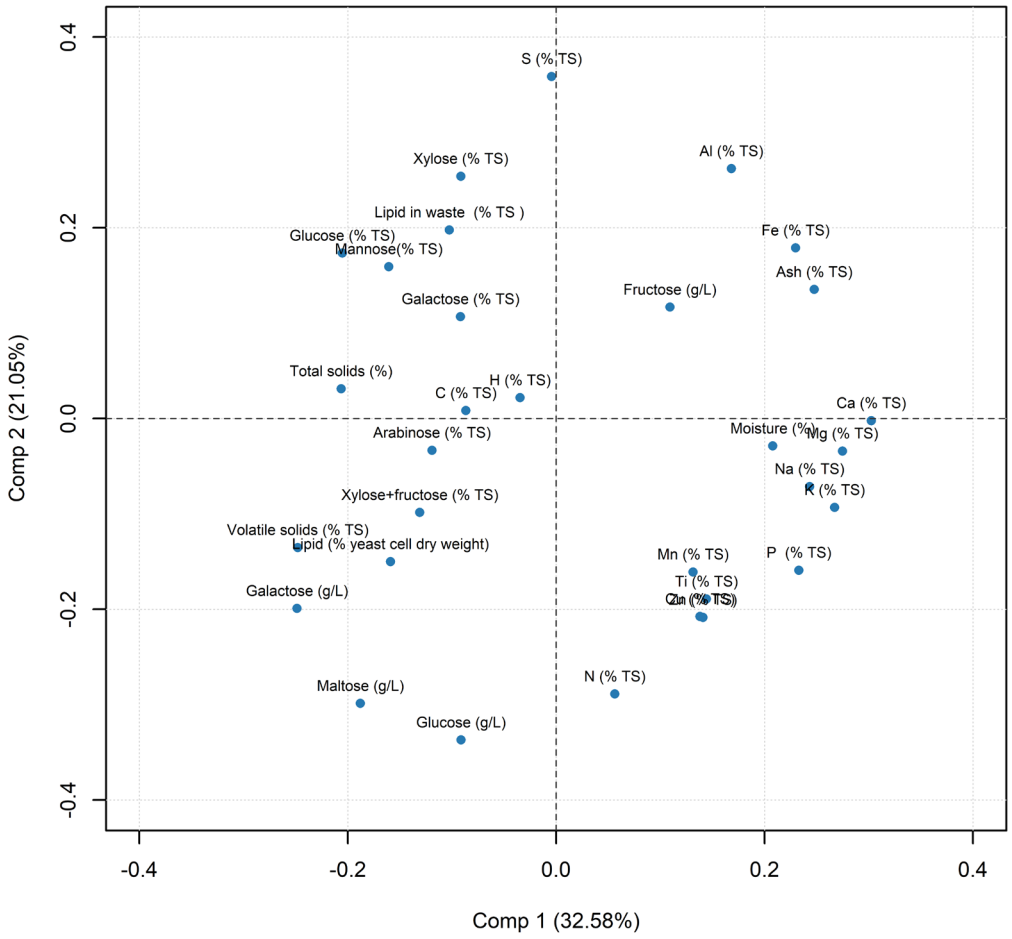

Figure 33. Loadings plot showing the correlations of variables.

The scores plot for the PCA is seen in Figure 35 to the left, and it shows that samples from the same collection month are somehow correlated to each other, and E-sample deviates from the others, as it is from another main source. It is clearly seen that the E-sample affects the first principal component the most and also affects the second principal component, together with Mar. 3 sample. To see how much the loadings plots and scores plot differ without E-sample, the PCA is made only for the RagnSells samples, cf. Figure 35 and Figure 36. The amounts of explanations of variations in the samples for the first two principal components, PC1 and PC2, are 33.33 % and 16.64%, respectively. That is <1 % higher than the first component for PCA for all the samples together, and PC2 explains <5 % less for the PCA without E-sample than the PCA for all samples. When comparing the loadings plots in Figure 36 and Figure 33, it can be seen that there are many differences in the distribution of the variables and thus these two loadings plots are not comparable. The scores plot (Figure 35) shows a more widespread distribution without E-sample. The differences between the two PCA models mean that doing a PCA

with samples from more than one or two sources, will result in a more general waste component model, and not only related to one or two waste sources.

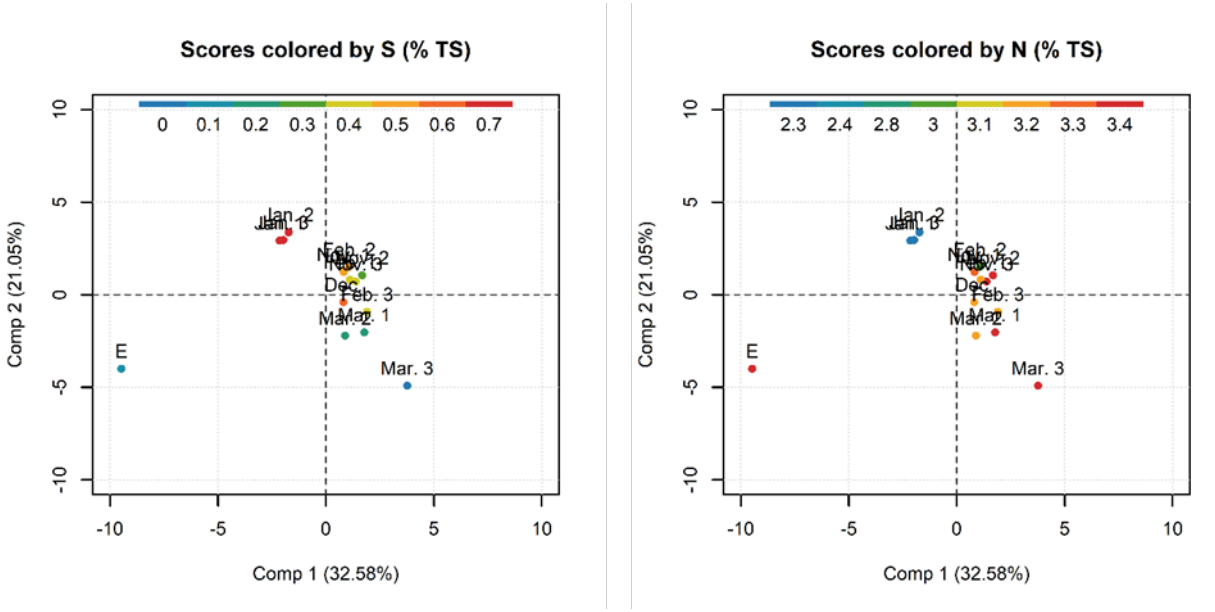

Figure 34. Scores plot for PCA, colored by S and N (% TS). Figures that are zoomed, so the exact sample names are seen, can be seen in appendix 9.7.

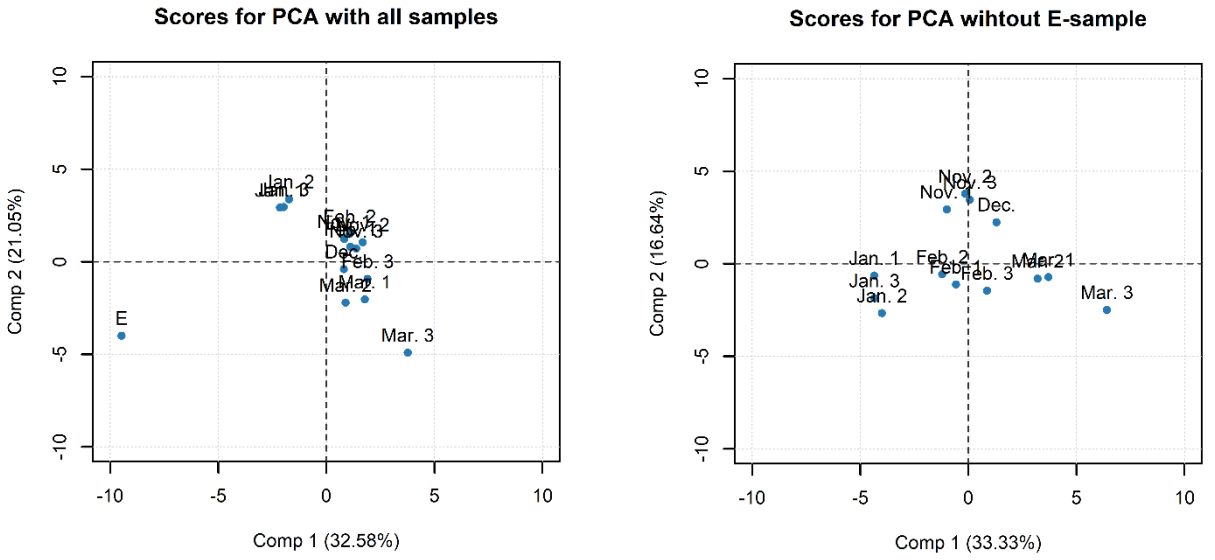

Figure 35. Scores plots for PCA, with and without E-sample.

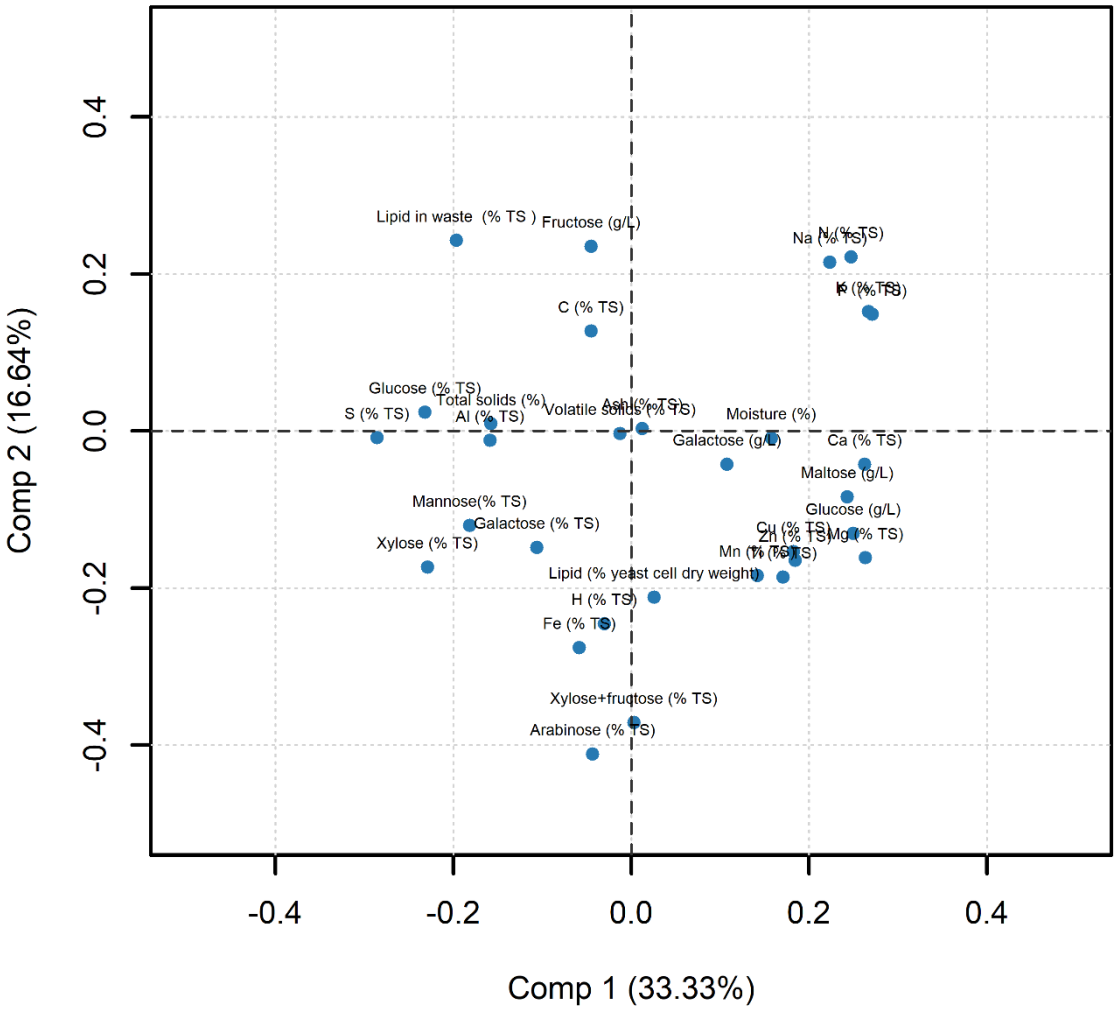

Figure 36. Loadings plot for PCA without E-sample. A zoomed edition of this plot can be seen in appendix 9.7.

After looking at the PC1 and PC2, it will be looked at PC3, and see how much variance it explains and if it explains some important correlations. Figure 37 shows the loading plot for PC1 and PC3. The PC3 explains 13.59 % of the variance and the biggest correlation was seen regarding PC3 is between arabinose and lipid in waste and between arabinose and N (% TS). The scores plots (Figure 38) show the scores for PC1 and PC3 colored by lipid in waste and arabinose content, respectively, it is seen that they are negatively correlated, but not highly correlated, as the colors in the middle of the plots are almost the same in both plots. The important variable, lipid accumulated in yeast, is positively correlated with xylose, galactose and mannose and negatively correlated with Fe and Mg. The H and N amounts are also negatively correlated, and that is peculiar as the N and H amounts from the elementary analysis do not seem to correlate in Figure 22. Obviously, the correlation is not that big due to the

relatively small explanation percentage by PC3. The fourth principal component explains only 9.1% of the variance, and will not be analyzed.

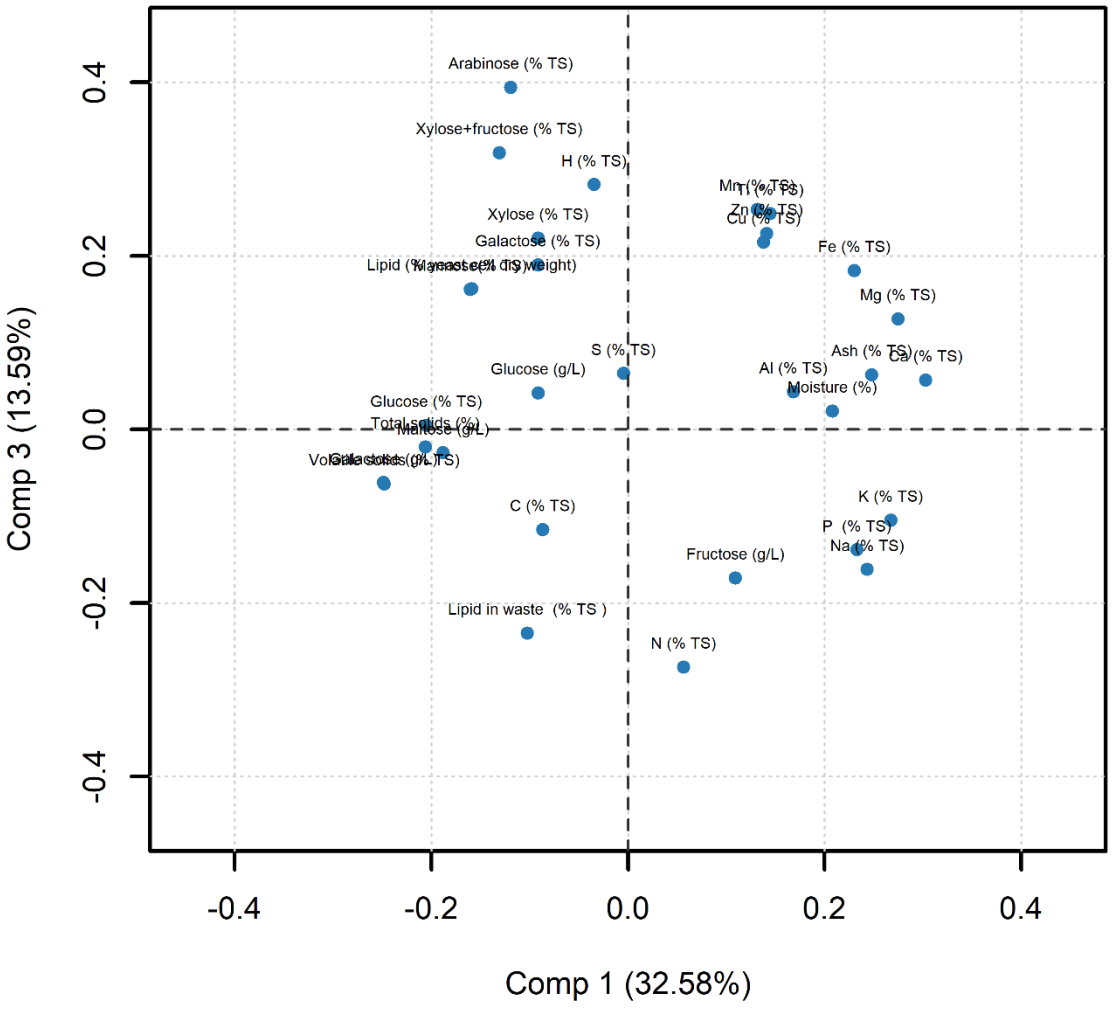

Figure 37. Loadings for PC1 and PC3. A zoomed version of the plot can be seen in appendix 9.7

.

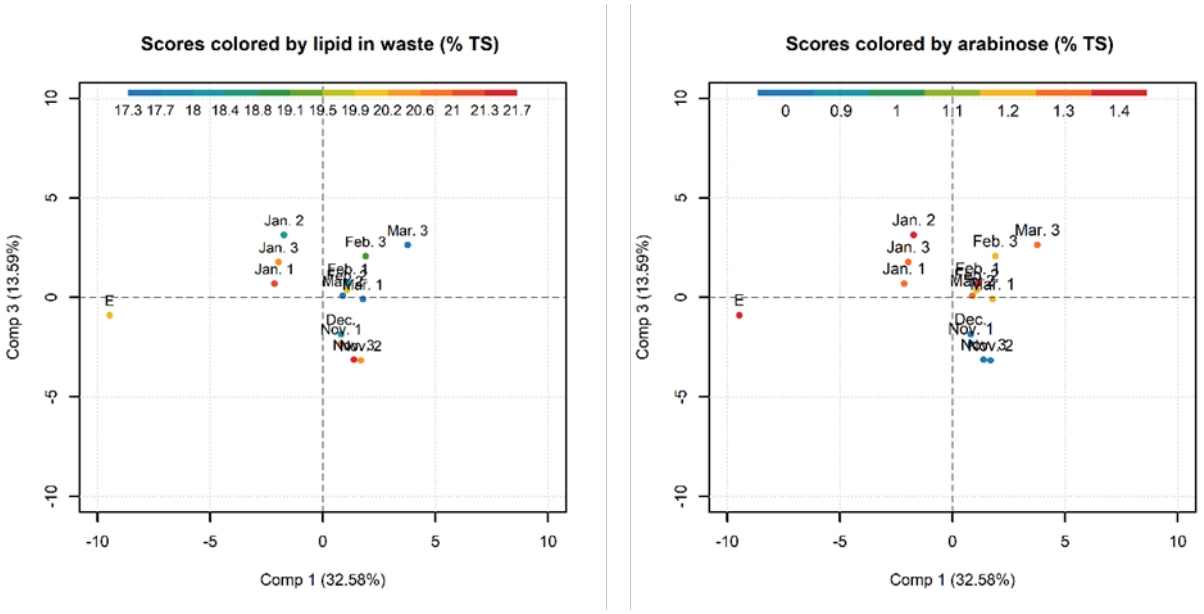

Figure 38. Scores for PC1 and PC3, colored by lipid in waste and arabinose (% TS).

To detect outliers, residuals plots are made (Figure 39), together with critical limits. As seen in Figure 39, no outliers are detected, only one extreme value for the PCA model with one principal component, and thus, no data are needed to be removed.

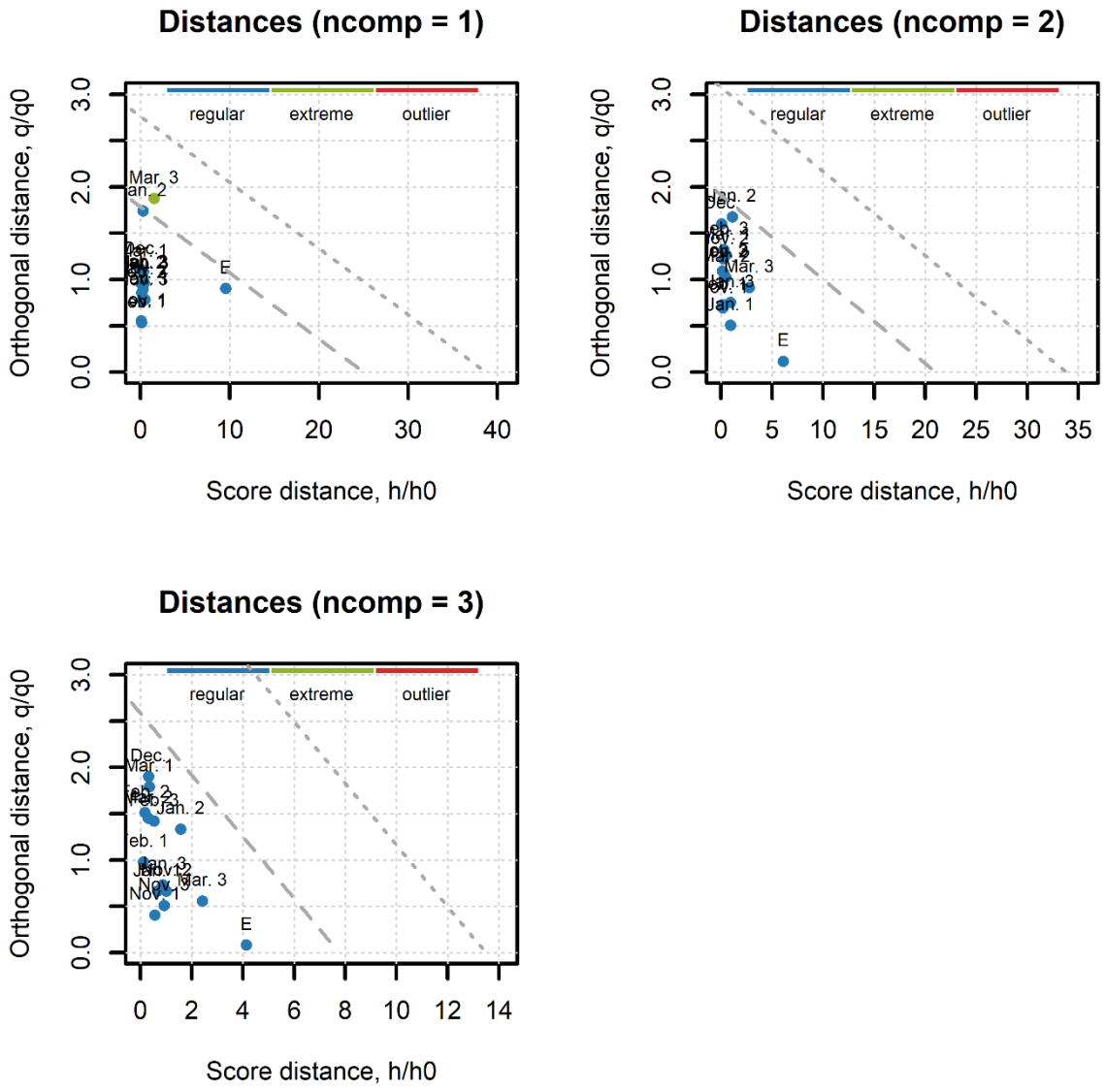

Figure 39. Residuals plot with critical limits for PC1, PC2 and PC3. A more detailed explanation for the Residuals plot can be seen in appendix 9.8.

The last thing in the exploratory data analysis is showing the correlation matrix, a heat map, to visualize how the variables correlate to each other. Figure 40 shows the correlation matrix. It is seen that the variables that correlate mostly with lipid accumulated in yeast are maltose (g/L), volatile solids (% TS) and galactose (g/L), but all these have correlation values of about 0.5, which means, that they correlate, but are not very highly correlated. A nice red cluster is seen in the correlation matrix between Mn (%), Ti (%), Cu (%) and Zn (%), meaning that these variables highly and positively correlate with each other. P, Na and K are also highly correlated with each other, and it is noteworthy because all the three elements serve as essential nutrients for living organisms. Maltose (g/L) and glucose(g/L) have a high positive correlation and most of the sugars (maltose (g/L), glucose (g/L) and galactose (g/L)) have a

positive correlation to the lipid content in the yeast. The galactose (g/L) has a higher correlation to the lipid amount in yeast than the galactose (%TS) and this can be because the galactose in the dried waste is dissolved in the waste supernatant.

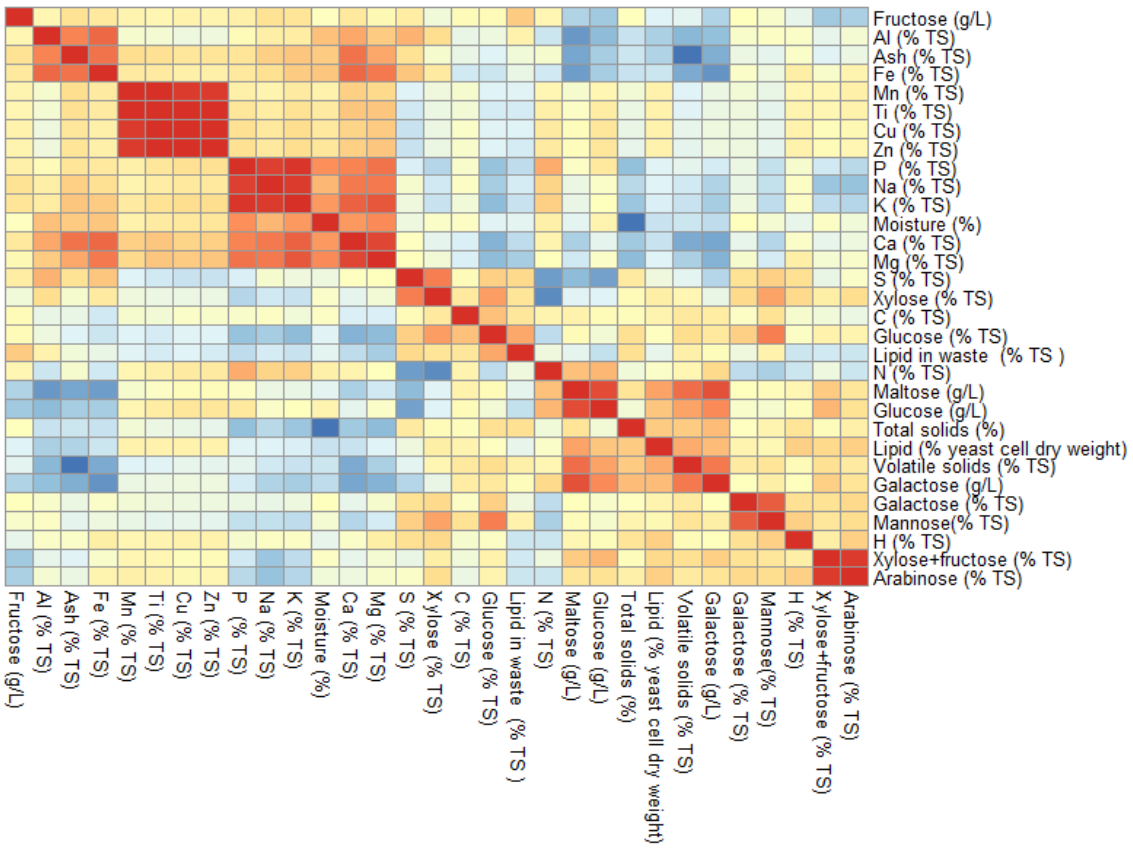

Figure 40. Correlation matrix heat map. The color gradient goes from blue to red, where blue means a strongly negative correlation and red means a strong positive correlation, the yellow color means there are no correlations.

6.9 Effect of the variables on the lipid amount accumulated in yeast

After the observation of the data and variables, now it will be looked at the effect of variables on the lipid accumulation in yeast. To do this, Partial least squares regression, PLS regression, will be done. The PLS model will be done for the predictions of lipid accumulated in yeast.

A precited vs. measured plot is seen in Figure 41 and it is seen that the calibration line and the cross-validation line are not comparable, as the calibration line doesn't follow the cv line, and the points lie very randomly in the plot, far away from the lines, thus, according to this plot, there is no big correlation between the lipid in yeast and the other variables.

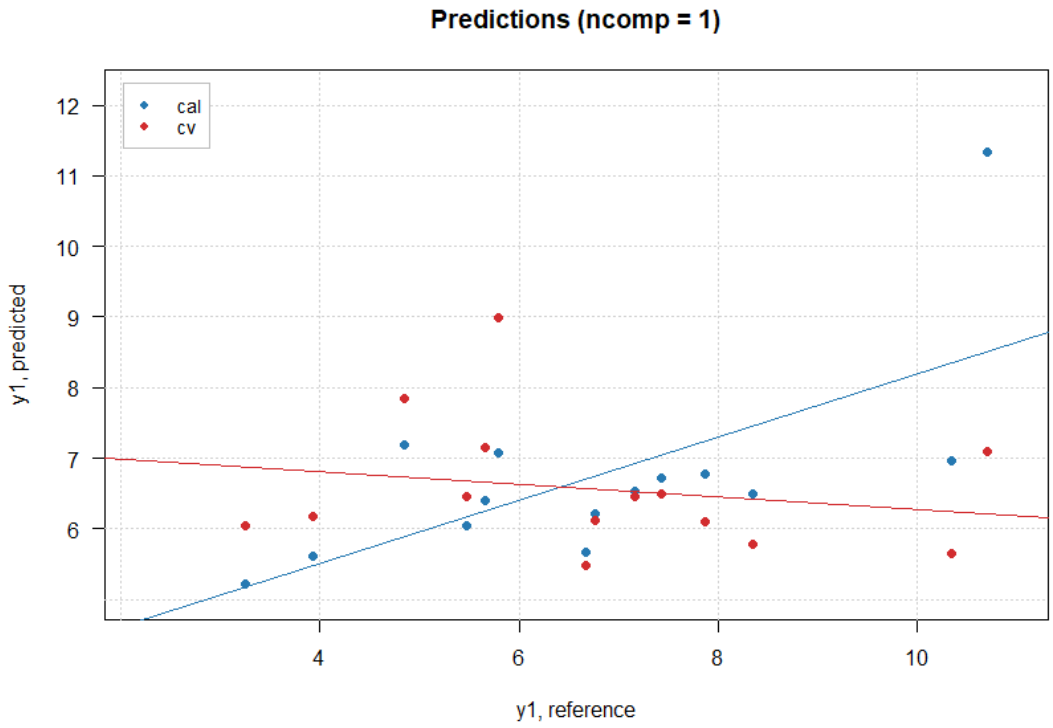

Figure 41. Predicted vs. measured plot. Cal= calibration values, cv= cross validation

Looking at the summary for the PLS model (Table 7) it is seen that the slope for the predicted vs. measured line is 0.449, which means that there is a systematic error. The Bias is 0.167 and the value also tells that we have errors in the predictions. The R^2 value is 0.449 for the calibration line and -0.374 for the cv, indicating that the predictions contain many errors. The RMSE for the calibration line is 1.544. All the statistics indicate errors in the model, and this can be due to the small sample size or just because no big correlation is found between lipid accumulation in yeast and the other variables.

Table 7. Summary for PLS model.

	R^2	RMSE	Slope	Bias
Cal	0.449	1.544	0.449	0.00
Cv	-0.374	2.439	-0.088	0.1669

The last part of the chemometrics data analysis is to see which variables have the highest correlation with lipid accumulated in yeast. A correlation matrix is constructed and the variables that affect the lipid accumulation the most are given in Table 8. Although the correlation values are above 0.5 (plus and minus), the correlations are not that high. The correlation table is supported by correlation plots (Figure 42). It is clearly seen in the plots that one sample is lying outside the others, this is the E-sample, and without it, the correlations levels would have been lower.

Table 8. Highest correlation values with lipid accumulated in yeast.

	Ash (%)	VS (% TS)	Al (% TS)	Maltose (g/L)
Correlation	-0.531	0.531	-0.548	0.577

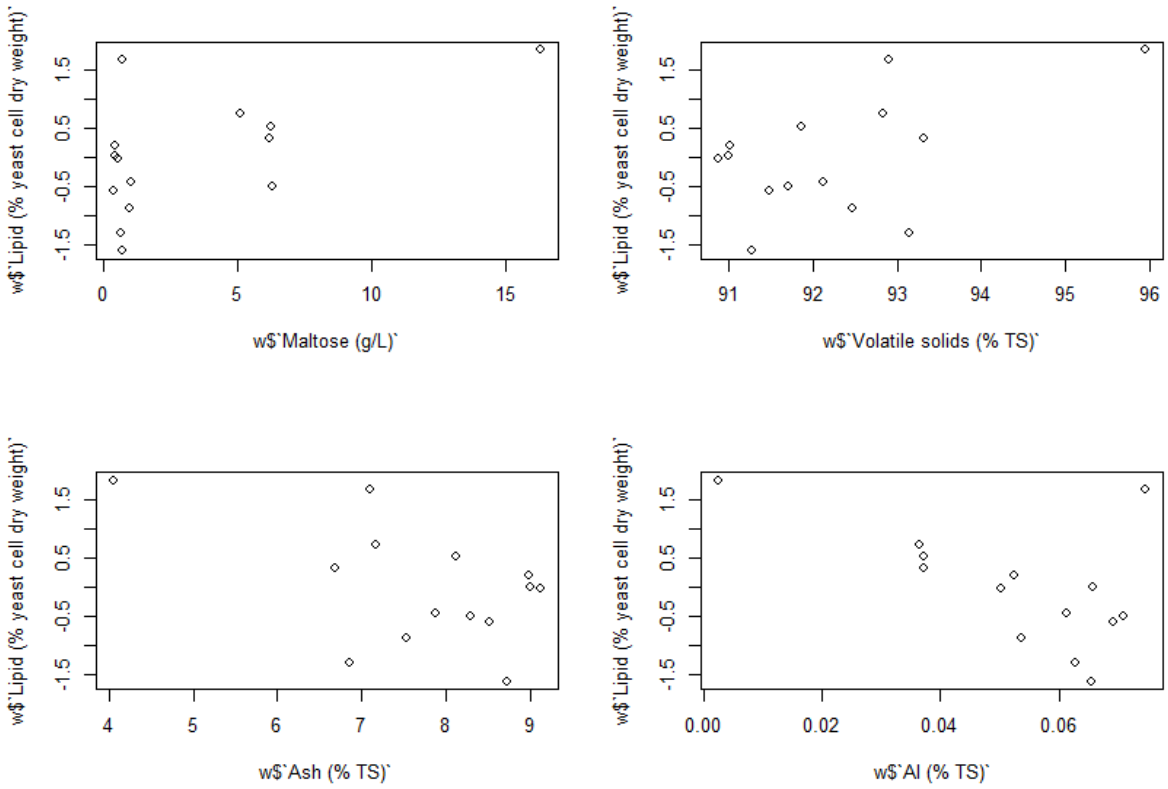

Figure 42. Correlations between lipid % in yeast, and maltose (g/L), V (% TS), Ash (% TS) and Al (% TS)

To conclude on the statistics part, it was seen that the contents in the food waste, that mostly affect the lipid accumulation in yeast, are Maltose, VS, Ash and Al contents. The ash and volatile solids are two contrary variables. The correlation values are about 0.5, and this is not very high (just at the start level of a high correlation), but most important, it can tell, that there is a little correlation. If more samples were collected and analyzed, and from more sources, the correlations would most likely be higher. Al (%TS) has a negative correlation to lipid accumulation, and this means, it can have a toxic effect. Maltose has a positive correlation to lipid accumulation, and this is very logical. The Zn content did not show any effect on the lipid accumulation in yeast, although it has a concentration range of 1.4 -14 mg/L waste and could have a toxic and inhibitory effect (section 6.2).

7 Conclusion

The main goal of the project was to find the effect of the composition of the food waste on the lipid production in the oleaginous yeast *C. oleaginosus*. To achieve this goal, the composition of food waste from two different sources, synthetic food waste from campus Esbjerg and food waste from the food waste handling plant, Ragn-Sells, were analyzed. Food waste was collected from Ragn-Sells each month from November 2021 to March 2022 to investigate the time variation in the composition. The time variation of the collected food waste did not affect the food waste composition. The food waste was analyzed for its contents of total solids, ash, heavy metals, phosphorus, carbon, hydrogen, nitrogen, sulfur, total carbohydrates, lipids and lipid profiles. Simultaneous saccharification and fermentation (SSF) were done for the food waste to investigate the amounts of lipids produced inside the yeast cell. The lipid amounts for the different waste months and E-waste were similar and ranged from 3-10 % of the yeast cell dry weight, the two highest lipid accumulations were 10 % of the yeast DW and were found in the E-waste and Jan.3 samples.

To find how the waste components affect the lipid accumulation, two chemometrics analyses were used, Principal Component Analysis (PCA) and partial least squares (PLS) regression. The PCA was used to explore the data and find special trends. The PLS was used to find the correlations of the variables on the lipid accumulated in yeast. It was found that maltose, ash and Al contents in the waste had some correlations to the lipid amounts in the yeast. The correlation values are not more than 5, meaning that it is not a big correlation, but a correlation with some uncertainties. The uncertainty in the chemometrics methods is that it needs much data to work best, and the data set collected from this project, was not big enough. The contents in the food waste were very similar, which resulted in similar lipid accumulation in yeast, thus there were no high correlations.

8 Perspective

The future work on this project can be to get more food waste samples from more sources, or different countries, and do a more comprehensive characterization of it. The obtained correlations for the aluminum and maltose contents with the lipid accumulation can be investigated further by adding or removing these contents to see how the lipid production in yeast behaves. As aluminum has a negative correlation to the lipid accumulated in the yeast (section 6.9), the removal of the aluminum may be interesting to investigate.

The SSF can be optimized so the exact C/N ratio is measured and regulated for the benefit of lipid production. Getting a higher C/N ratio by adding acetate to the waste media can also be investigated, as the acetate can easily be converted to acetyl-CoA and fermentation with only acetate as a carbon source showed a very promising amount of lipid accumulation of 66 % (Table 1). The yeast *C. oleaginosus* or other yeast strains can be manipulated genetically to produce more lipids and possibly also to produce lipids without the addition of enzymes.

As the maltose had a positive effect on the lipid accumulation, the waste from breweries can be blended with the food waste to improve the lipid accumulation in the yeast, as the brewery waste contains high amounts of maltose from the malt used in the brewing process.

The content of Zn ions in the waste had a range of 1.4-14 mg/L and higher Zn content than 0.6 mg/L can have a toxic effect on the yeast (section 2), thus, removing some of the Zn ions from the SSF, could possibly lead to higher lipid accumulation and would be interesting to study.

9 Appendix

9.1 Converting g Zn /100 g DW waste to mg Zn/L waste (for section 6.2)

There are 0.001 to 0.01 g Zn per 100 g DW waste.

In every liter of fresh waste, there are approx. 14 % dry matter, that give 140 g dry waste in 1 L of fresh waste.

$$\frac{0.001\ g\ Zn}{100\ g\ DW} = \frac{x}{140\ g\ DW} \rightarrow x = 0.0014\ \frac{g\ zink}{L.waste} \rightarrow 1.4\ \frac{mg\ Zn}{L.waste}$$

$$\frac{0.01\ g\ Zn}{100\ g\ DW} = \frac{x}{140\ g\ DW} \rightarrow x = 0.014\ \frac{g\ zink}{L.waste} \rightarrow 14\ \frac{mg\ Zn}{L.waste}$$

9.2 T-test for section 6.4

```
data:  WAHGLU and SAHGLU
t = -8.5435, df = 1.4625, p-value = 0.03184
alternative hypothesis: true difference in means is not equal to 0
95 percent confidence interval:
 -52.47272  -8.18698
sample estimates:
mean of x mean of y
 22.43000  52.75985
```

Figure 43. T-test for the difference between SAH and WAH for glucose, both analyses were done to the E-waste.

```
data:  WAHXYL and SAHXYL
t = -0.90839, df = 1.2117, p-value = 0.5081
alternative hypothesis: true difference in means is not equal to 0
95 percent confidence interval:
 -7.210936  5.817602
sample estimates:
mean of x mean of y
 8.193333  8.890000
```

Figure 44. T-test for the difference between SAH and WAH for xylose, both analyses were done on the E-waste.

```
data:  WAHARA and SAHARA
t = 1.1606, df = 2.2557, p-value = 0.3539
alternative hypothesis: true difference in means is not equal to 0
95 percent confidence interval:
 -2.814392  5.227725
sample estimates:
mean of x mean of y
 2.496667  1.290000
```

Figure 45. T-test for the difference between SAH and WAH for arabinose, both analyses were done on the E-waste.

```
data:  WAHTOT1 and SAHTOT1
t = -5.9338, df = 1.8745, p-value = 0.03164
alternative hypothesis: true difference in means is not equal to 0
95 percent confidence interval:
 -52.885666  -6.747668
sample estimates:
mean of x mean of y
 33.12333  62.94000
```

Figure 46. T-test for the difference between SAH and WAH for the total sugar amount (glucose, arabinose and xylose).

9.3 T-test for section 6.5

```
data:  decwaste and dec5daysferm
t = -0.068623, df = 3.2547, p-value = 0.9493
alternative hypothesis: true difference in means is not equal to 0
95 percent confidence interval:
 -1.356810  1.297023
sample estimates:
mean of x mean of y
 18.28839  18.31828
```

9.4 ANOVA and TUEKY test

Table 9. ANOVA test

```
            Df Sum Sq Mean Sq F value  Pr(>F)
ind          2  9.687   4.843    21.8 0.00177 **
Residuals    6  1.333   0.222
```

Table 10. TUKEY test

```
                          diff       lwr        upr     p adj
soxtherm1-soxhlet1 -2.16666667 -3.347646 -0.9856873 0.0032461
UAE1-soxhlet1      -2.23333333 -3.414313 -1.0523540 0.0027791
UAE1-soxtherm1     -0.06666667 -1.247646  1.1143127 0.9836422
```

9.5 t-test significance values

	waste	SSF	t.test p-values
E1	20.95933	30.21845	0.01612
E2	19.81383	29.21348	
E3	19.46809	32.92308	
nov1.1	20.68966	29.84293	0.04585
nov1.2	20.81081	27.71084	
nov1.3	20.77295	24.73498	
nov.2.1	20.83333	24.65753	0.008506
nov.2.2	19.8	23.61905	
nov.2.3	20.81129	22.92052	
nov.3.1	21.48594	25.7485	0.01012
nov. 3.2	22.03791	26.47059	
nov. 3.3	21.66667	24.74227	
dec. 1	17.55556	27.95341	0.001591
dec. 2	19.40928	26.67814	
dec. 3	18.24645	25.26132	
jan. 1.1	20.71429	28.22878	0.05946
jan. 1.2	21.08963	25.9962	

jan. 1.3	21.62162	23.73832	
jan. 2.1	18.67704	20.80153	0.1192
jan. 2.2	18.12865	23.54086	
jan. 2.3	18.52552	28.36439	
jan. 3.1	21.54472	27.28905	0.03572
jan. 3.2	20.37618	30	
jan. 3.3	19.29825	34.97164	
feb. 1.1	17.93103	25.11346	0.0005219
feb. 1.2	18.02657	24.30669	
feb. 1.3	18.22742	25.04119	
feb. 2.1	20.30948	24.2268	0.03067
feb. 2.2	19.53125	23.91304	
feb. 2.3	19.25344	27.37896	
feb. 3.1	18.9011	24.37396	0.01631
feb. 3.2	18.96907	26.43678	
feb. 3.3	18.9899	27.54098	
mar. 1.1	17.6	24.20168	0.007299
mar. 1.2	17.6	21.82469	
mar. 1.3	16.77215	22.9021	
mar. 2.1	16.60377	24.47552	0.0003385
mar. 2.2	17.46032	24.15631	
mar. 2.3	18.01471	25.72534	
mar.3.1	16.92308	26.26642	0.0006525
mar. 3.2	17.66917	24.91749	
mar. 3.2	17.71772	24.74438	

9.6 Chromatograms for the lipid profiles

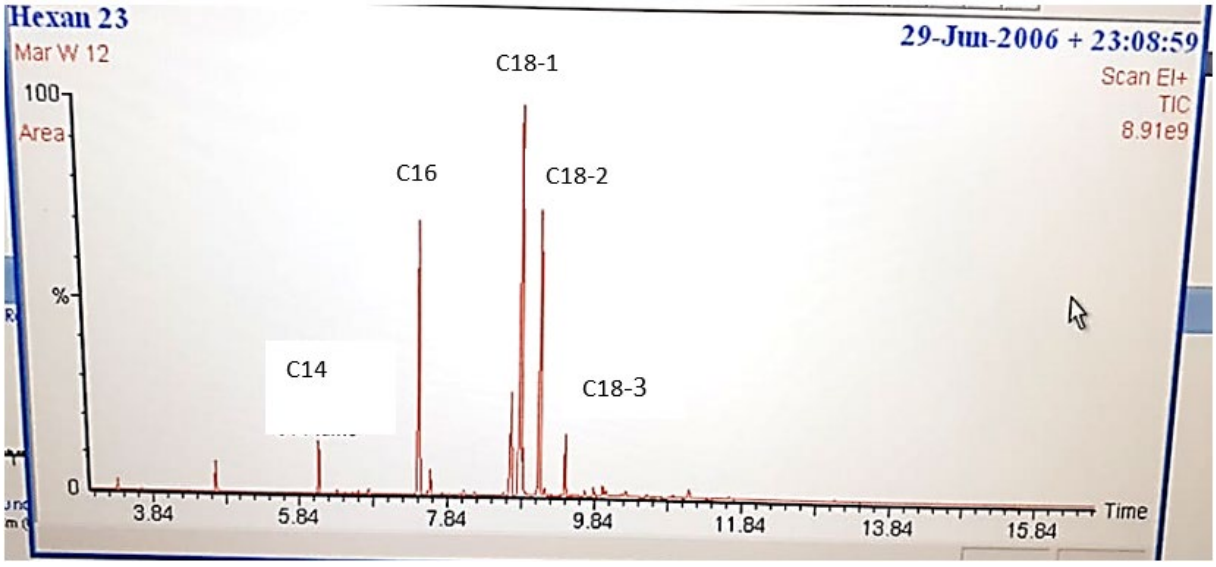

Figure 47. Chromatogram for the lipid profile to the lipid from the waste.

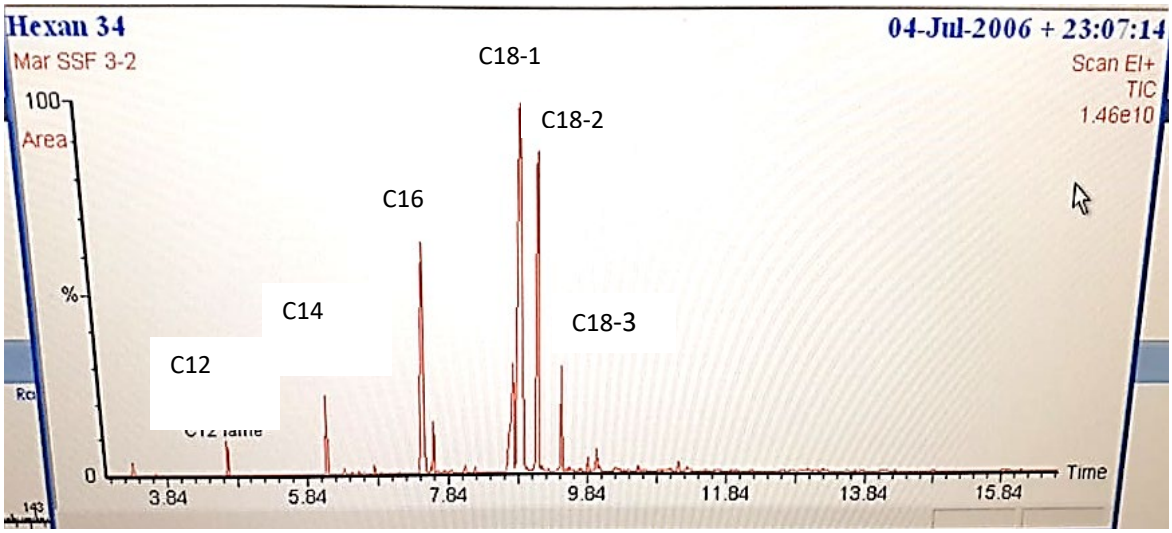

Figure 48. Chromatogram for the lipid profile to the lipids obtained from extracting the SSF dried broth.

9.7 Zoomed plots for section 6.8

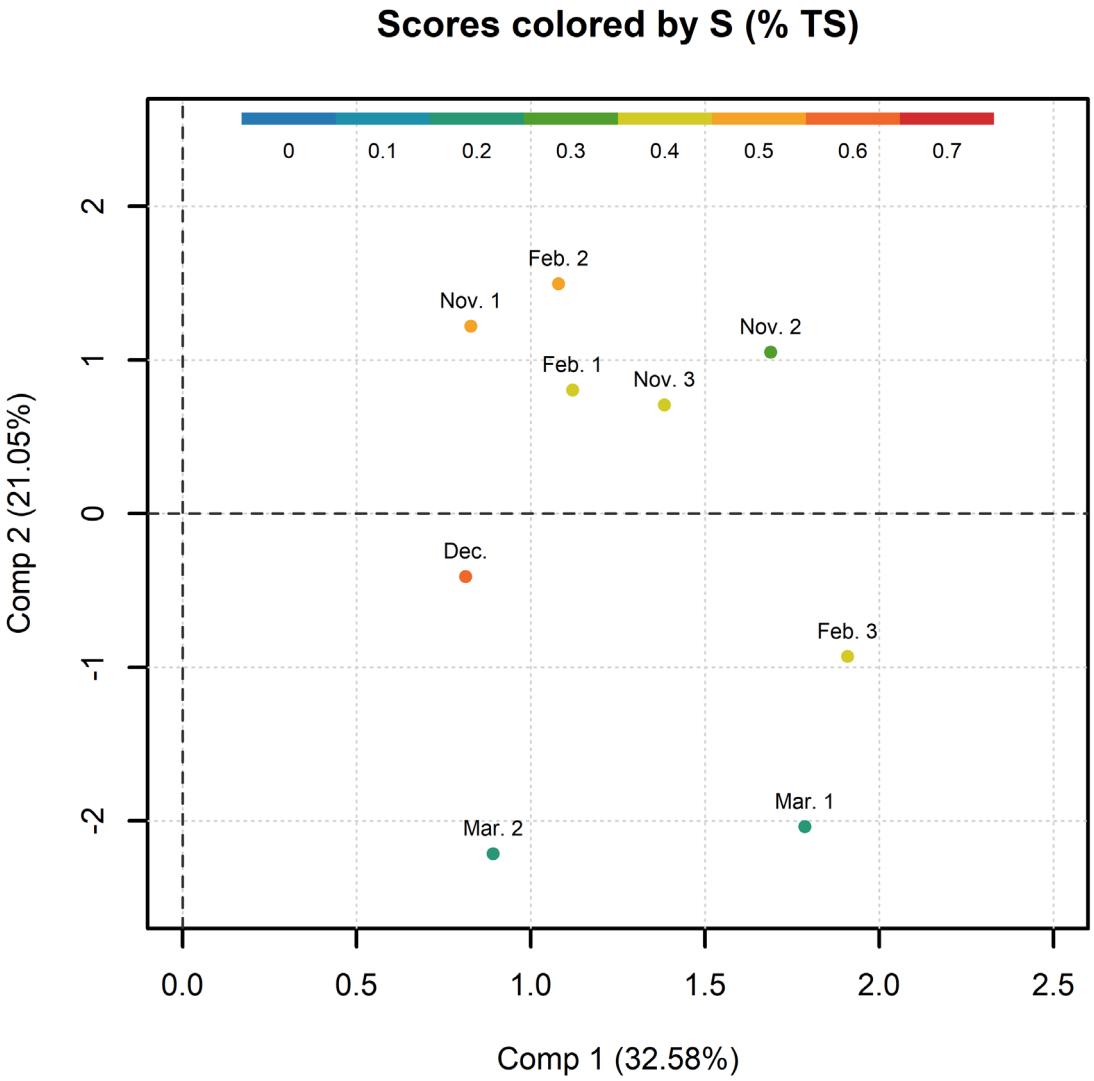

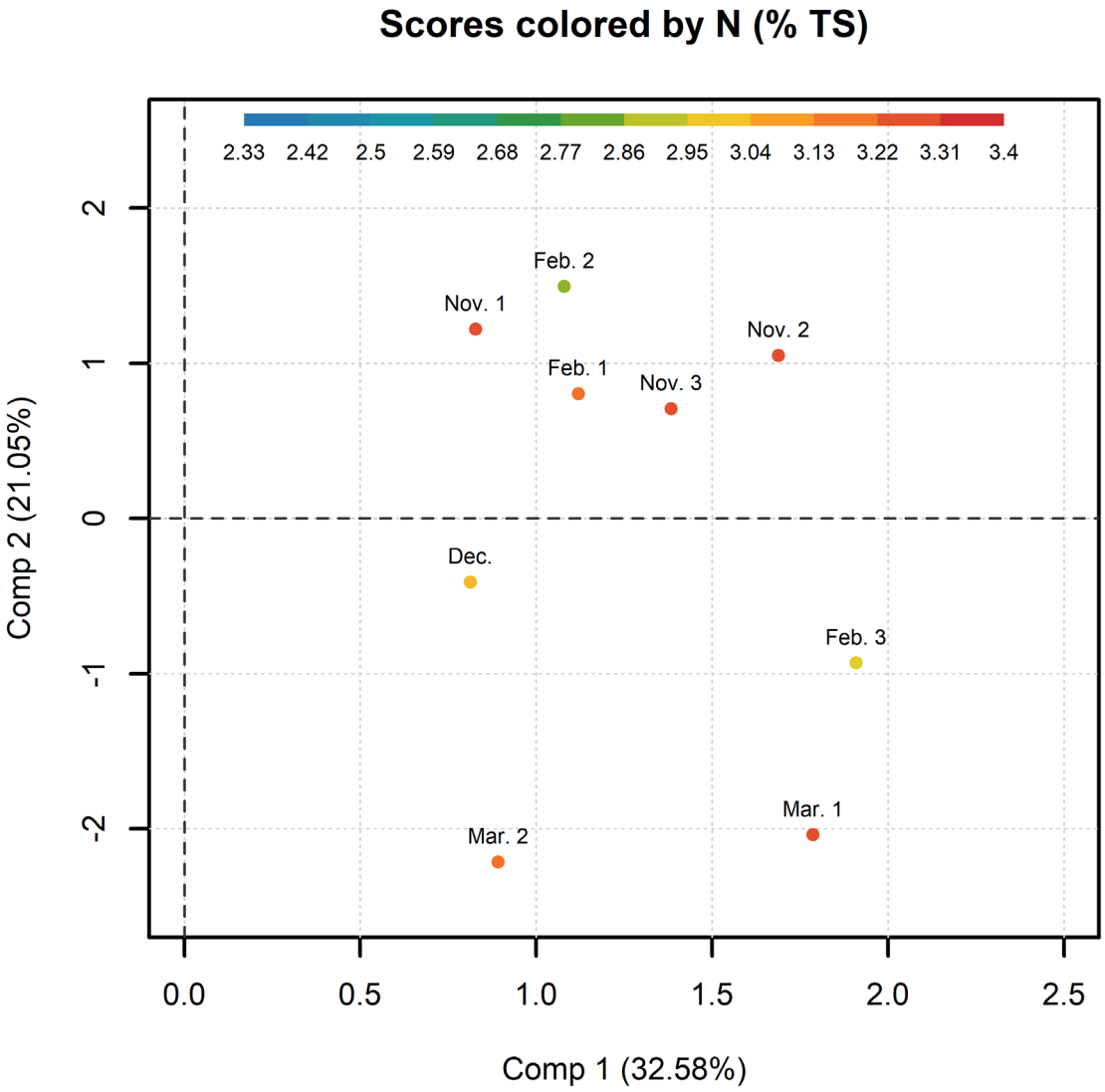
Scores colored by N (% TS)
2.33 2.42 2.5 2.59 2.68 2.77 2.86 2.95 3.04 3.13 3.22 3.31 3.4
Feb. 2
Nov. 1
Nov. 2
Feb. 1
Nov. 3
Dec.
Feb. 3
Mar. 1
Mar. 2
Comp 2 (21.05%)
Comp 1 (32.58%)
2
1
0
-1
-2
0.0
0.5
1.0
1.5
2.0
2.5

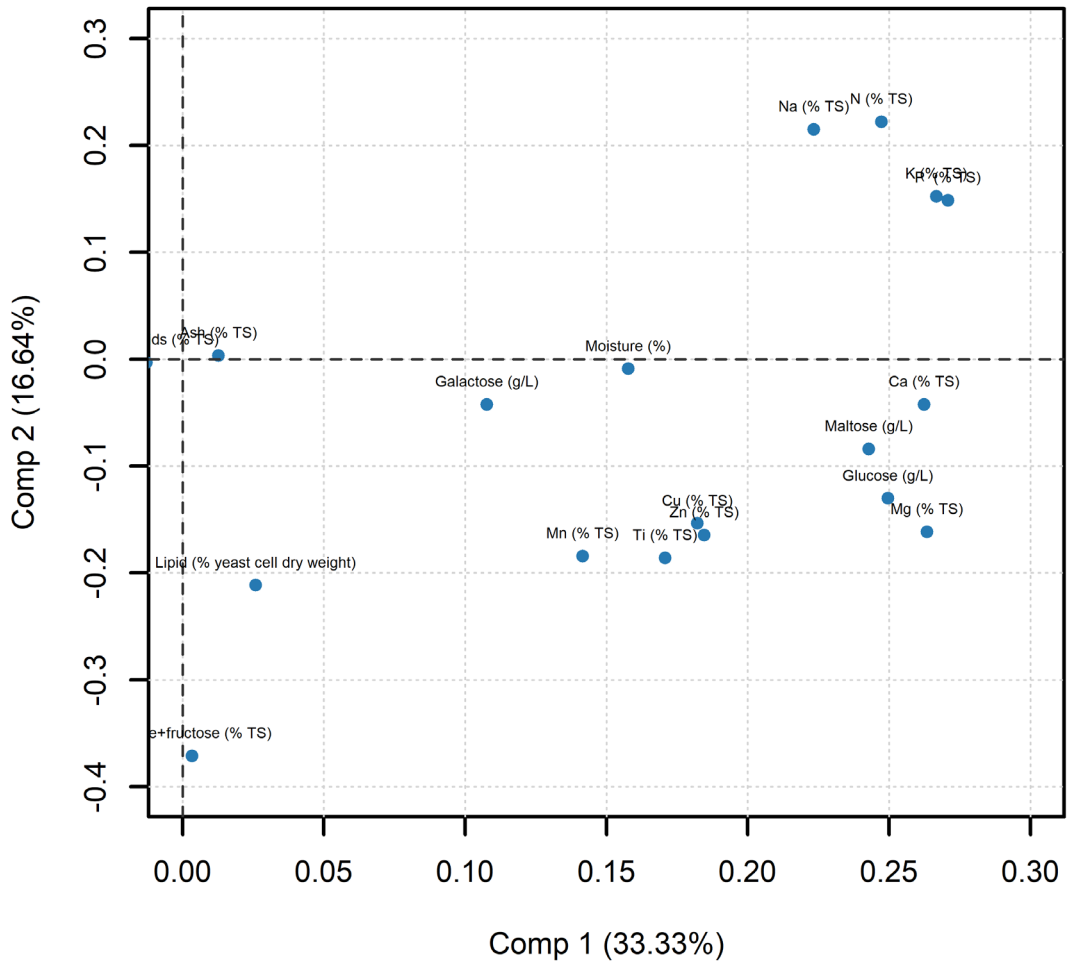

Figure 49. Zoomed loadings plot without E sample.

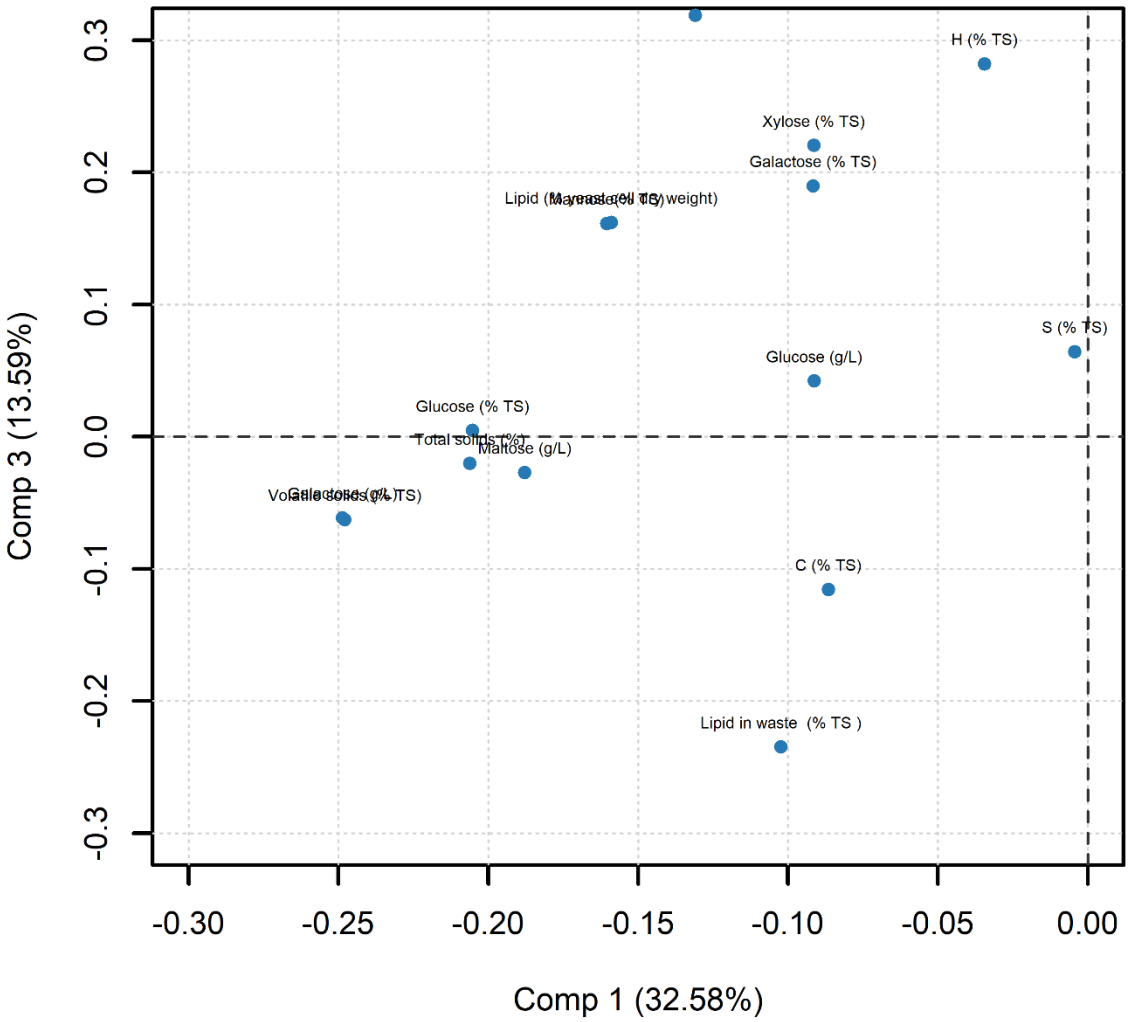

Figure 50. Zoomed Loadings plot for 1 and 3 components for all samples. Volatile solids and galactose are lying very close to each other. Lipids in yeast and mannose are also lying very close.

9.8 Residuals-plot explanation

The critical limits are given as 0.05 and 0.01, where objects placed after the first critical limit are detected as extreme values and objects placed after the second critical limit are outliers. Every object has a 5% chance to be detected as extreme and a 1% chance to be detected as an outlier.

[1] S. M. Andler and J. M. Goddard, “Transforming food waste: how immobilized enzymes can valorize waste streams into revenue streams,” *npj Science of Food 2018 2:1*, vol. 2, no. 1, pp. 1–11, Oct. 2018, doi: 10.1038/s41538-018-0028-2.

[2] “Worldwide food waste | ThinkEatSave.” https://www.unep.org/thinkeatsave/get-informed/worldwide-food-waste (accessed Jan. 08, 2022).

[3] “Global food waste statistics 2020 - CUBII.” https://cubii.co/en/global-food-waste-statistics-2020/ (accessed Jan. 08, 2022).

[4] “Food Loss and Food Waste | FAO | Food and Agriculture Organization of the United Nations.” https://www.fao.org/food-loss-and-food-waste/flw-data) (accessed Jan. 08, 2022).

[5] “2030 climate & energy framework | Climate Action.” https://ec.europa.eu/clima/policies/strategies/2030_en (accessed Mar. 25, 2021).

[6] L. Tao, A. Milbrandt, Y. Zhang, and W. C. Wang, “Techno-economic and resource analysis of hydroprocessed renewable jet fuel,” *Biotechnology for Biofuels*, vol. 10, no. 1, pp. 1–16, Nov. 2017, doi: 10.1186/S13068-017-0945-3/FIGURES/7.

[7] Mexico, “CONFERENCE ON AVIATION AND ALTERNATIVE FUELS”.

[8] M. Elkelawy, H. A.-E. Bastawissi, A. M. Radwan, M. T. Ismail, and M. El-Sheekh, “Biojet fuels production from algae: conversion technologies, characteristics, performance, and process simulation,” *Handbook of Algal Biofuels*, pp. 331–361, 2022, doi: 10.1016/B978-0-12-823764-9.00003-0.

[9] L. Starck, L. Pidol, N. Jeuland, T. Chapus, P. Bogers, and J. Bauldreay, “Second and Third Generation Biofuels: Towards Sustainability and Competitiveness Seconde et troisième génération de biocarburants : développement durable et compétitivité Production of Hydroprocessed Esters and Fatty Acids (HEFA)-Optimisation of Process Yield,” *Oil & Gas Science and Technology-Rev. IFP Energies nouvelles*, vol. 71, 2016, doi: 10.2516/ogst/2014007.

[10] A. Bauen, N. Bitossi, L. German, A. Harris, and K. Leow, “Sustainable aviation fuels status, challenges and prospects of drop-in liquid fuels, hydrogen and electrification in aviation,” *Johnson Matthey Technology Review*, vol. 64, no. 3, pp. 263–278, Jul. 2020, doi: 10.1595/205651320X15816756012040.

[11] M. Fredsgaard, L. S. S. Hulkko, T. Chaturvedi, and M. H. Thomsen, “Process simulation and techno-economic assessment of Salicornia sp. based jet fuel refinery through Hermetia illucens sugars-to-lipids conversion and HEFA route,” *Biomass and Bioenergy*, vol. 150, p. 106142, Jul. 2021, doi: 10.1016/J.BIOMBIOE.2021.106142.

[12] J. H. Gary, G. E. Handwerk, and M. J. Kaiser, “PETROLEUM REFINING Technology and Economics Fifth Edition,” 2007, Accessed: Apr. 09, 2022. [Online]. Available: http://www.copyright.com/

[13] D. Lamers *et al.*, “Selection of oleaginous yeasts for fatty acid production,” *BMC Biotechnology*, vol. 16, no. 1, pp. 1–10, May 2016, doi: 10.1186/S12896-016-0276-7/TABLES/3.

[14] Q. He *et al.*, “Oleaginicity of the yeast strain Saccharomyces cerevisiae D5A 06 Biological Sciences 0601 Biochemistry and Cell Biology,” *Biotechnology for Biofuels*, vol. 11, no. 1, pp. 1–20, Sep. 2018, doi: 10.1186/S13068-018-1256-Z/FIGURES/6.

[15] P. Shaigani *et al.*, “Oleaginous yeasts- substrate preference and lipid productivity: a view on the performance of microbial lipid producers,” *Microbial Cell Factories*, vol. 20, no. 1, pp. 1–18, Dec. 2021, doi: 10.1186/S12934-021-01710-3/FIGURES/5.

[16] F. Abeln and C. J. Chuck, “The history, state of the art and future prospects for oleaginous yeast research,” *Microbial Cell Factories*, vol. 20, no. 1, pp. 1–31, Dec. 2021, doi: 10.1186/S12934-021-01712-1/FIGURES/7.

[17] “The Yeast Handbook”.

[18] L. A. Garay *et al.*, “Eighteen new oleaginous yeast species,” *Journal of Industrial Microbiology and Biotechnology*, vol. 43, no. 7, pp. 887–900, Jul. 2016, doi: 10.1007/S10295-016-1765-3.

[19] L. A. Sargeant, C. J. Chuck, J. Donnelly, C. D. Bannister, and R. J. Scott, “Optimizing the lipid profile, to produce either a palm oil or biodiesel substitute, by manipulation of the culture conditions for Rhodotorula glutinis,” *Biofuels*, vol. 5, no. 1, pp. 33–43, Jan. 2014, doi: 10.4155/BFS.13.64.

[20] S. Shi and H. Zhao, “Metabolic engineering of oleaginous yeasts for production of fuels and chemicals,” *Frontiers in Microbiology*, vol. 8, no. NOV, p. 2185, Nov. 2017, doi: 10.3389/FMICB.2017.02185/BIBTEX.

[21] M. Rakicka, Z. Lazar, T. Dulermo, P. Fickers, and J. M. Nicaud, “Lipid production by the oleaginous yeast Yarrowia lipolytica using industrial by-products under different culture conditions,” *Biotechnology for Biofuels 2015 8:1*, vol. 8, no. 1, pp. 1–10, Jul. 2015, doi: 10.1186/S13068-015-0286-Z.

[22] A. L. Demain, “Microbial production of primary metabolites,” *Naturwissenschaften*, vol. 67, no. 12, pp. 582–587, Dec. 1980, doi: 10.1007/BF00396537.

[23] R. Saini, K. Hegde, C. S. Osorio-Gonzalez, S. K. Brar, and P. Vezina, “Evaluating the Potential of Rhodosporidium toruloides-1588 for High Lipid Production Using Undetoxified Wood Hydrolysate as a Carbon Source,” *Energies (Basel)*, vol. 13, no. 22, p. 5960, 2020, doi: 10.3390/en13225960.

[24] Z. Gong, H. Shen, W. Zhou, Y. Wang, X. Yang, and Z. K. Zhao, “Efficient conversion of acetate into lipids by the oleaginous yeast Cryptococcus curvatus,” *Biotechnology for Biofuels*, vol. 8, no. 1, pp. 1–9, 2015, doi: 10.1186/s13068-015-0371-3.

[25] S. H. Yoon and J. S. Rhee, “Lipid from yeast fermentation: Effects of cultural conditions on lipid production and its characteristics of rhodotorula glutinis,” *J Am Oil Chem Soc*, vol. 60, no. 7, pp. 1281–1286, 1983, doi: 10.1007/BF02702101.

[26] A. Chattopadhyay, M. Mitra, and M. K. Maiti, “Recent advances in lipid metabolic engineering of oleaginous yeasts,” *Biotechnology Advances*, vol. 53, p. 107722, Dec. 2021, doi: 10.1016/J.BIOTECHADV.2021.107722.

[27] M. I. Santek, S. Beluhan, and B. Santek, “Production of Microbial Lipids from Lignocellulosic Biomass,” *Advances in Biofuels and Bioenergy*, Jul. 2018, doi: 10.5772/INTECHOPEN.74013.

[28] H. Takaku, T. Matsuzawa, K. Yaoi, and H. Yamazaki, “Lipid metabolism of the oleaginous yeast Lipomyces starkeyi”, doi: 10.1007/s00253-020-10695-9/Published.

[29] Y.-K. Park and J.-M. Nicaud, “microorganisms Metabolic Engineering for Unusual Lipid Production in Yarrowia lipolytica”, doi: 10.3390/microorganisms8121937.

[30] S. Papanikolaou and G. Aggelis, “Lipids of oleaginous yeasts. Part I: Biochemistry of single cell oil production,” *European Journal of Lipid Science and Technology*, vol. 113, no. 8, pp. 1031–1051, Aug. 2011, doi: 10.1002/EJLT.201100014.

[31] “Lipid accumulation by oleaginous and non-oleaginous yeast strains in nitrogen and phosphate limitation | Enhanced Reader.”

[32] “Glycolysis | Cellular respiration | Biology (article) | Khan Academy.” https://www.khanacademy.org/science/biology/cellular-respiration-and-fermentation/glycolysis/a/glycolysis (accessed Jan. 04, 2022).

[33] “The Citric Acid (Krebs) Cycle | Boundless Microbiology.” https://courses.lumenlearning.com/boundless-microbiology/chapter/the-citric-acid-krebs-cycle/ (accessed Jan. 04, 2022).

[34] P. A. Botham and C. Ratledge, “A biochemical explanation for lipid accumulation in Candida 107 and other oleaginous micro-organisms,” *Journal of General Microbiology*, vol. 114, no. 2, pp. 361–375, Oct. 1979, doi: 10.1099/00221287-114-2-361/CITE/REFWORKS.

[35] F. Bracharz, T. Beukhout, N. Mehlmer, and T. Brück, “Opportunities and challenges in the development of Cutaneotrichosporon oleaginosus ATCC 20509 as a new cell factory for custom tailored microbial oils,” *Microbial Cell Factories*, vol. 16, no. 1, pp. 1–15, Oct. 2017, doi: 10.1186/S12934-017-0791-9/TABLES/3.

[36] Á. Fonseca, T. Boekhout, and J. W. Fell, “Cryptococcus Vuillemin (1901),” *The Yeasts*, vol. 3, pp. 1661–1737, Jan. 2011, doi: 10.1016/B978-0-444-52149-1.00138-5.

[37] D. Awad, F. Bohnen, N. Mehlmer, and T. Brueck, “Multi-factorial-guided media optimization for enhanced biomass and lipid formation by the oleaginous yeast Cutaneotrichosporon oleaginosus,” *Frontiers in Bioengineering and Biotechnology*, vol. 7, no. MAR, p. 54, 2019, doi: 10.3389/FBIOE.2019.00054/BIBTEX.

[38] P. Shaigani *et al.*, “Oleaginous yeasts- substrate preference and lipid productivity: a view on the performance of microbial lipid producers,” *Microbial Cell Factories 2021 20:1*, vol. 20, no. 1, pp. 1–18, Dec. 2021, doi: 10.1186/S12934-021-01710-3.

[39] N. di Fidio, F. Minonne, C. Antonetti, A. Maria, R. Galletti, and C. Antonetti, “Cutaneotrichosporon oleaginosus: A Versatile Whole-Cell Biocatalyst for the Production of Single-Cell Oil from Agro-Industrial Wastes Cutaneotrichosporon oleaginosus: A Versatile Whole-Cell Biocatalyst for the Production of Single-Cell Oil from,” 2021, doi: 10.3390/catal11111291.

[40] “Merck | Denmark.” https://www.sigmaaldrich.com/DK/en (accessed Apr. 12, 2022).

[41] T. Hofmeyer, S. Hackenschmidt, F. Nadler, A. Thürmer, R. Daniel, and J. Kabisch, “Draft Genome Sequence of Cutaneotrichosporon curvatus DSM 101032 (Formerly Cryptococcus curvatus), an Oleaginous Yeast Producing Polyunsaturated Fatty Acids,” *Genome Announcements*, vol. 4, no. 3, pp. 362–378, 2016, doi: 10.1128/GENOMEA.00362-16.

[42] T. Fuchs *et al.*, “Identifying carbohydrate-active enzymes of Cutaneotrichosporon oleaginosus using systems biology,” *Microbial Cell Factories*, vol. 20, no. 1, pp. 1–18, Dec. 2021, doi: 10.1186/S12934-021-01692-2/FIGURES/9.

[43] B. Technologies Office, “Sustainable Aviation Fuel: Review of Technical Pathways Report”.

[44] S. Yang *et al.*, “Comparison of Nitrogen Depletion and Repletion on Lipid Production in Yeast and Fungal Species,” 2016, doi: 10.3390/en9090685.

[45] “Food Loss and Food Waste | FAO | Food and Agriculture Organization of the United Nations.” https://www.fao.org/food-loss-and-food-waste/flw-data) (accessed Apr. 13, 2022).

[46] “Food waste is responsible for 6% of global greenhouse gas emissions - Our World in Data.” https://ourworldindata.org/food-waste-emissions (accessed Apr. 13, 2022).

[47] “Food Waste | The Nutrition Source | Harvard T.H. Chan School of Public Health.” https://www.hsph.harvard.edu/nutritionsource/sustainability/food-waste/ (accessed Apr. 13, 2022).

[48] “Food: Material-Specific Data | US EPA.” https://www.epa.gov/facts-and-figures-about-materials-waste-and-recycling/food-material-specific-data (accessed Apr. 13, 2022).

[49] “How is food waste recycled? | Recycle Now.” https://www.recyclenow.com/how-to-recycle/how-is-food-waste-recycled (accessed Apr. 13, 2022).

[50] “NYT: Vi sorterer fortsat mere affald til genanvendelse - Danmarks Statistik.” https://www.dst.dk/da/Statistik/nyheder-analyser-publ/nyt/NytHtml?cid=34686 (accessed Apr. 13, 2022).

[51] P. Wavrer, “Theory of Sampling (TOS) applied to characterisation of Municipal Solid Waste (MSW)-a case study from France a”, doi: 10.1255/tosf.101.

[52] K. Haro *et al.*, “Characterization and Potential Recovery of Household Solid Waste in the City of Ouagadougou (Burkina Faso),” *Journal of Environmental Protection*, vol. 9, no. 4, pp. 309–324, Apr. 2018, doi: 10.4236/JEP.2018.94021.

[53] P. Wavrer, “Theory of Sampling (TOS) applied to characterisation of Municipal Solid Waste (MSW)-a case study from France a”, doi: 10.1255/tosf.101.

[54] “(PDF) Compositional analysis of food waste entering the source segregation stream in four European regions and implications for valorisation via anaerobic digestion.” https://www.researchgate.net/publication/258148792_Compositional_analysis_of_food_waste_entering_the_source_segregation_stream_in_four_European_regions_and_implications_for_valorisation_via_anaerobic_digestion (accessed Sep. 22, 2021).

[55] Amaka NWOBI, “Techno-Economic Analysis of Biofuel Production from Organic Fraction of Municipal Solid Waste (OFMSW) Generated in Abu Dhabi, UAE,” pp. 68–70, 1377.

[56] K. S. Ho and L. M. Chu, “Characterization of food waste from different sources in Hong Kong,” *https://doi.org/10.1080/10962247.2018.1526138*, vol. 69, no. 3, pp. 277–288, Mar. 2018, doi: 10.1080/10962247.2018.1526138.

[57] P. Flyhammar, “HEAVY METALS IN MUNICIPAL SOLID WASTE DEPOSITS,” 1997.

[58] P. Flyhammar, “Estimation of heavy metal transformations in municipal solid waste,” 1997.

[59] P. Flyhammar, F. Tamaddon, and L. Bengtsson, “HEAVY METALS IN A MUNICIPAL SOLID WASTE DEPOSITION CELL.”

[60] H. U A Z H A N G , † P I N -J I N G H E , and † L I -M I N G S H A O , † A N D D U U -J O N G L E E, “Source Analysis of Heavy Metals and Arsenic in Organic Fractions of Municipal Solid Waste in a Mega-City (Shanghai)”, doi: 10.1021/es702303x.

[61] M. Zennaro, F. Cristofori, D. Formigoni, F. Frignani, and B. Pavoni, “Heavy metal contamination in compost. A possible solution.,” 2005.

[62] M. POLLAK, “HEAVY METALS AND ORGANIC COMPOUNDS FROM WASTES USED AS ORGANIC FERTILISERS Final Report,” Austria, 2004. Accessed: Nov. 29, 2021. [Online]. Available: moz-extension://2cd68a06-5e49-47da-93a7-a6f7d049b67e/enhanced-reader.html?openApp&pdf=https%3A%2F%2Fec.europa.eu%2Fenvironment%2Fpdf%2Fwaste%2Fcompost%2Fhm_finalreport.pdf

[63] S. Rajakumar, A. Abhishek, G. S. Selvam, and V. Nachiappan, “Effect of cadmium on essential metals and their impact on lipid metabolism in Saccharomyces cerevisiae,” *Cell Stress & Chaperones*, vol. 25, no. 1, p. 19, Jan. 2020, doi: 10.1007/S12192-019-01058-Z.

[64] G. Stewart and F. Priest, *Handbook of Brewing*, 2nd ed. 2006.

[65] B. S. P. Nuran Ercal, B. S. P. Hande Gurer-Orhan, and B. S. P. Nukhet Aykin-Burns, “Toxic metals and oxidative stress part I: mechanisms involved in metal-induced oxidative damage,” *Curr Top Med Chem*, vol. 1, no. 6, pp. 529–539, Mar. 2001, doi: 10.2174/1568026013394831.

[66] H. C. Yang and L. A. Pon, “Toxicity of Metal Ions Used in Dental Alloys: A Study in the Yeast Saccharomyces cerevisiae,” *http://dx.doi.org/10.1081/DCT-120020403*, vol. 26, no. 2, pp. 75–85, 2003, doi: 10.1081/DCT-120020403.

[67] “Regulation of Phospholipid Synthesis in Saccharomyces cerevisiae by Zinc* | Elsevier Enhanced Reader.” https://reader.elsevier.com/reader/sd/pii/S0021925820668065?token=ED04B75153F246332C338C1197EFF84CE5DA8BAA4E77D6766F8C7941C4DD492221B39CDBA26E2AF5C197B44E705935B1&originRegion=eu-west-1&originCreation=20220203131337 (accessed Feb. 06, 2022).

[68] H.-C. Yang and L. A. Pon, “Toxicity of Metal Ions Used in Dental Alloys: A Study in the Yeast Saccharomycesï¿¿cerevisiae,” *Drug and Chemical Toxicology*, vol. 26, no. 2, pp. 75–85, 2003, doi: 10.1081/DCT-120020403.

[69] M. F. Zainuddin, C. K. Fai, A. B. Ariff, L. Rios-Solis, and M. Halim, “Current pretreatment/cell disruption and extraction methods used to improve intracellular lipid recovery from oleaginous yeasts,” *Microorganisms*, vol. 9, no. 2, pp. 1–28, 2021, doi: 10.3390/microorganisms9020251.

[70] M. Athenaki *et al.*, “Lipids from yeasts and fungi: physiology, production and analytical considerations,” *Journal of Applied Microbiology*, vol. 124, no. 2, pp. 336–367, 2018, doi: 10.1111/jam.13633.

[71] P. J. Slininger *et al.*, “Comparative lipid production by oleaginous yeasts in hydrolyzates of lignocellulosic biomass and process strategy for high titers,” *Biotechnology and Bioengineering*, vol. 113, no. 8, pp. 1676–1690, Aug. 2016, doi: 10.1002/bit.25928.

[72] Q. Sha, “The Faculty of Natural Resources and Agricultural Sciences A comparative study on four oleaginous yeasts on their lipid accumulating capacity CORE View metadata, citation and similar papers at core.ac.uk provided by Epsilon Archive for Student Projects”, Accessed: Apr. 25, 2022. [Online]. Available: http://stud.epsilon.slu.se

[73] P. Shaigani *et al.*, “Oleaginous yeasts- substrate preference and lipid productivity: a view on the performance of microbial lipid producers,” *Microbial Cell Factories*, vol. 20, no. 1, pp. 1–18, Dec. 2021, doi: 10.1186/S12934-021-01710-3/FIGURES/5.

[74] H. J. S. Lopes, N. Bonturi, E. J. Kerkhoven, E. A. Miranda, and P. J. Lahtvee, “C/N ratio and carbon source-dependent lipid production profiling in Rhodotorula toruloides,” *Applied Microbiology and Biotechnology*, vol. 104, no. 6, pp. 2639–2649, Mar. 2020, doi: 10.1007/S00253-020-10386-5/FIGURES/5.

[75] Z. Ye *et al.*, “Optimising nutrients in the culture medium of Rhodosporidium toruloides enhances lipids production,” *AMB Express*, vol. 11, no. 1, Dec. 2021, doi: 10.1186/S13568-021-01313-6.

[76] V. Johnson, M. Singh, V. S. Saini, V. R. Sista, and N. K. Yadav, “Effect of pH on lipid accumulation by an oleaginous yeast:Rhodotorula glutinis IIP-30,” *World Journal of Microbiology & Biotechnology*, vol. 8, no. 4, pp. 382–384, Jul. 1992, doi: 10.1007/BF01198749.

[77] I. Gientka, M. Kieliszek, K. Jermacz, and S. Błazejak, “Identification and Characterization of Oleaginous Yeast Isolated from Kefir and Its Ability to Accumulate Intracellular Fats in Deproteinated Potato Wastewater with Different Carbon Sources,” *BioMed Research International*, vol. 2017, 2017, doi: 10.1155/2017/6061042.

[78] W. C. Lam, T. H. Kwan, C. Sze, and K. Lin, “Enzymes in Processing of Nutraceuticals,” *Enzymes in Food and Beverage Processing*, no. November, pp. 417–440, 2015, doi: 10.1201/b19408-25.

[79] D. Norouzian, A. Akbarzadeh, J. M. Scharer, and M. Moo Young, “Fungal glucoamylases,” *Biotechnol Adv*, vol. 24, no. 1, pp. 80–85, Jan. 2006, doi: 10.1016/J.BIOTECHADV.2005.06.003.

[80] J. Sauer *et al.*, “Glucoamylase: structure/function relationships, and protein engineering,” *Biochim Biophys Acta*, vol. 1543, no. 2, pp. 275–293, Dec. 2000, doi: 10.1016/S0167-4838(00)00232-6.

[81] W. Paper, T. View, and C. Lehmann, “Hydrolytic Enzymes : Amylases , Proteases , Lipases,” no. January 2001, pp. 0–4, 2016.

[82] P. Kumar and T. Satyanarayana, “A novel thermo-alkalistable xylanase for production of xylooligosaccharides View project Characteristics of recombinant phytase of the thermophilic mold Sporotrichum thermophile expressed in Pichia pastoris View project Microbial glucoamylases: characteristics and applications,” *Critical Reviews in Biotechnology*, vol. 29, no. 3, pp. 225–255, 2009, doi: 10.1080/07388550903136076.

[83] P. Kumar and T. Satyanarayana, “Microbial glucoamylases: characteristics and applications,” *Crit Rev Biotechnol*, vol. 29, no. 3, pp. 225–255, 2009, doi: 10.1080/07388550903136076.

[84] S. Negi, *Green Bio-processes*, no. December. Springer Singapore, 2019. doi: 10.1007/978-981-13-3263-0.

[85] R. C. Kuhad, R. Gupta, and A. Singh, “Microbial cellulases and their industrial applications,” *Enzyme Research*, vol. 2011, no. 1, 2011, doi: 10.4061/2011/280696.

[86] S. Sethi, A. Datta, B. L. Gupta, and S. Gupta, “Optimization of Cellulase Production from Bacteria Isolated from Soil,” *ISRN Biotechnology*, vol. 2013, pp. 1–7, Feb. 2013, doi: 10.5402/2013/985685.

[87] “(PDF) Microbial cellulases-Production, applications and challenges.” https://www.researchgate.net/publication/228635285_Microbial_cellulases-Production_applications_and_challenges (accessed Apr. 14, 2022).

[88] “Intracellular Proteolytic Systems.” https://pubs.niaaa.nih.gov/publications/arh27-4/317-324.htm (accessed Mar. 20, 2022).

[89] “Digestive Enzymes: Amylase, Protease, And Lipase | Integrative Therapeutics.” https://www.integrativepro.com/articles/digestive-enzymes-amylase-protease-lipase (accessed Mar. 20, 2022).

[90] “Proteases for biocatalysis for smarter chemical synthesis”.

[91] A. Razzaq *et al.*, “Microbial proteases applications,” *Frontiers in Bioengineering and Biotechnology*, vol. 7, no. JUN, p. 110, 2019, doi: 10.3389/FBIOE.2019.00110/BIBTEX.

[92] M. B. Rao, A. M. Tanksale, M. S. Ghatge, and V. v. Deshpande, “Molecular and Biotechnological Aspects of Microbial Proteases,” *Microbiology and Molecular Biology Reviews : MMBR*, vol. 62, no. 3, p. 597, Sep. 1998, doi: 10.1128/MMBR.62.3.597-635.1998.

[93] T. S. P. de Souza and H. Y. Kawaguti, “Cellulases, Hemicellulases, and Pectinases: Applications in the Food and Beverage Industry,” *Food and Bioprocess Technology 2021 14:8*, vol. 14, no. 8, pp. 1446–1477, Jun. 2021, doi: 10.1007/S11947-021-02678-Z.

[94] “Microbial degradation of hemicellulose (Enzymes, Steps, Mechanisms).” https://microbenotes.com/microbial-degradation-of-hemicellulose/ (accessed Mar. 21, 2022).

[95] D. Shallom and Y. Shoham, “Microbial hemicellulases,” *Current Opinion in Microbiology*, vol. 6, no. 3, pp. 219–228, 2003, doi: 10.1016/S1369-5274(03)00056-0.

[96] S. Singh, B. Pillay, V. Dilsook, and B. A. Prior, “Production and properties of hemicellulases by a Thermomyces lanuginosus strain,” *J Appl Microbiol*, vol. 88, no. 6, pp. 975–982, 2000, doi: 10.1046/J.1365-2672.2000.01063.X.

[97] Y. Yi, “Tiny bugs play big role,” *Advances in 2nd Generation of Bioethanol Production*, pp. 113–136, 2021, doi: 10.1016/B978-0-12-818862-0.00007-8.

[98] N. Hugouvieux-Cotte-Pattat, G. Condemine, and V. E. Shevchik, “Minireview Bacterial pectate lyases, structural and functional diversity,” 2014, doi: 10.1111/1758-2229.12166.

[99] S. Uluisik and G. B. Seymour, “Pectate lyases: Their role in plants and importance in fruit ripening,” *Food Chemistry*, vol. 309, p. 125559, Mar. 2020, doi: 10.1016/J.FOODCHEM.2019.125559.

[100] M. C. Marín-Rodríguez, J. Orchard, and G. B. Seymour, “Pectate lyases, cell wall degradation and fruit softening,” *Journal of Experimental Botany*, vol. 53, no. 377, pp. 2115–2119, Oct. 2002, doi: 10.1093/JXB/ERF089.

[101] E. Bonnin, M. C. Ralet, J. F. Thibault, and H. A. Schols, “Enzymes for the valorisation of fruit- and vegetable-based co-products,” *Handbook of Waste Management and Co-Product Recovery in Food Processing*, vol. 2, pp. 257–285, Oct. 2009, doi: 10.1533/9781845697051.3.257.

[102] Z. Kádár, Z. Szengyel, and K. Réczey, “Simultaneous saccharification and fermentation (SSF) of industrial wastes for the production of ethanol,” *Industrial Crops and Products*, vol. 20, pp. 103–110, 2004, doi: 10.1016/j.indcrop.2003.12.015.

[103] J. D. Wright, C. E. Wyman, and K. Grohmann, “Simultaneous saccharification and fermentation of lignocellulose - Process evaluation,” *Applied Biochemistry and Biotechnology*, vol. 18, no. 1, pp. 75–90, Aug. 1988, doi: 10.1007/BF02930818.

[104] A. Nwobi, I. Cybulska, W. Tesfai, Y. Shatilla, J. Rodríguez, and M. H. Thomsen, “ENVIRONMENTAL BIOTECHNOLOGY Simultaneous saccharification and fermentation of solid household waste following mild pretreatment using a mix of hydrolytic enzymes in combination with Saccharomyces cerevisiae”, doi: 10.1007/s00253-014-5977-z.

[105] K. Olofsson, M. Bertilsson, and G. Lidén, “Biotechnology for Biofuels A short review on SSF-an interesting process option for ethanol production from lignocellulosic feedstocks,” 2008, doi: 10.1186/1754-6834-1-7.

[106] Z. Gong, H. Shen, Q. Wang, X. Yang, H. Xie, and Z. K. Zhao, “Efficient conversion of biomass into lipids by using the simultaneous saccharification and enhanced lipid production process,” *Biotechnology for Biofuels*, vol. 6, no. 1, 2013, doi: 10.1186/1754-6834-6-36.

[107] M. Grubiši, K. Mihajlovski, and A. M. Gruiˇ, “Strategies for Improvement of Lipid Production by Yeast Trichosporon oleaginosus from Lignocellulosic Biomass,” 2021.

[108] “Madaffald.” https://www.ragnsells.dk/baredygtige-losninger/affaldstyper2/madaffald/ (accessed Nov. 30, 2021).

[109] F. Mariotti, D. Tomé, and P. Mirand, “Converting Nitrogen into Protein-Beyond 6.25 and Jones’ Factors,” *Critical Reviews in Food Science and Nutrition*, vol. 48, no. 2, pp. 177–184, 2008, doi: 10.1080/10408390701279749ï.

[110] E. S. Krul, “Calculation of Nitrogen-to-Protein Conversion Factors: A Review with a Focus on Soy Protein,” *J Am Oil Chem Soc*, vol. 96, no. 4, pp. 339–364, Apr. 2019, doi: 10.1002/AOCS.12196.

[111] “Fully Programmable Soxhlet Extraction System SOXTHERM.” https://www.analytica-world.com/en/products/59125/soxhlet-extraction-system-extractor-soxtherm.html (accessed Apr. 20, 2022).

[112] “Ultrasonic Extraction and its Working Principle - Hielscher Ultrasonics.” https://www.hielscher.com/ultrasonic-extraction-and-its-working-principle.htm (accessed Apr. 21, 2022).

[113] N. A. A. R. Zahari, G. H. Chong, L. C. Abdullah, and B. L. Chua, “Ultrasonic-Assisted Extraction (UAE) Process on Thymol Concentration from Plectranthus Amboinicus Leaves: Kinetic Modeling and Optimization,” *Processes 2020, Vol. 8, Page 322*, vol. 8, no. 3, p. 322, Mar. 2020, doi: 10.3390/PR8030322.

[114] H. C. Moon *et al.*, “Enzymatic hydrolysis of food waste and ethanol fermentation,” *International Journal of Energy Research*, vol. 33, no. 2, pp. 164–172, Feb. 2009, doi: 10.1002/ER.1432.

[115] W. Han, Y. Yan, Y. Shi, J. Gu, J. Tang, and H. Zhao, “Biohydrogen production from enzymatic hydrolysis of food waste in batch and continuous systems,” *Scientific Reports 2016 6:1*, vol. 6, no. 1, pp. 1–9, Dec. 2016, doi: 10.1038/srep38395.